

UNDERSTANDING PRIMATE MANDIBULAR
SYMPHYSEAL FUSION:
FUNCTION, INTEGRATION, AND ONTOGENY

A DISSERTATION
SUBMITTED TO THE FACULTY OF THE
UNIVERSITY OF MINNESOTA
BY

RYAN P. KNIGGE

IN PARTIAL FULFILLMENT OF THE REQUIREMENTS
FOR THE DEGREE OF
DOCTOR OF PHILOSOPHY

DR. KIERAN P. MCNULTY

December 2017

@ Ryan P. Knigge 2017

Acknowledgements

First, I am deeply indebted to my advisor and mentor, Kieran McNulty, for many years of patience and support. He opened my eyes to exciting and innovative areas of scientific research and has challenged me to become a better student of anthropology, biology, and statistical practices. I am also particularly grateful for my committee members, Martha Tappen, Michael Wilson, and Alan Love, for so many interesting discussions and insights over the years.

I thank the Department of Anthropology and my many friends and colleagues within for years of emotional and academic support. Many data collection and field work trips were funded through department block grants. Surely without these contributions, I would not have been able to succeed as a graduate student.

I would like thank the previous and current managers of the Evolutionary Anthropology Labs at the University of Minnesota, John Soderberg and Matt Edling, for access to the collections and technical support. Without their help and generosity, data collection and analysis would not have been possible.

I thank the University of Minnesota for supporting my research in many ways during my graduate school career. Portions of my data collection were funded through the University of Minnesota Graduate School Thesis Research Travel Grant. Dissertation writing support was provided through the Doctoral Dissertation Fellowship.

I thank the curators and staff of the many institutions that let me visit and research in their collections: Field Museum of Natural History, Chicago, Illinois; Smithsonian

National Museum of Natural History, Washington, D.C.; American Museum of Natural History, New York City, New York; Duke Lemur Center, Durham, North Carolina; National Museums of Kenya, Nairobi, Kenya; and Institut Catala de Paleontologia Miguel Crusafont, Sabadell, Spain. I would also like to thank Drs. Christopher J. Vinyard and Lauren Halenar and also Jason Massey for sharing their 3D models of primate skulls. I would also like to thank Dr. Christopher J. Vinyard for sharing EMG data that were collected with support from NSF. I thank the Smithsonian's Division of Mammals (Dr. Kristofer Helgen) and Human Origins Program (Dr. Matt Tocheri) for the scans of USNM specimens used in this research (<http://humanorigins.si.edu/evidence/3d-collection/primate>).

I am profoundly indebted to my friends and family, particularly my parents and partner, Allison. I could not have completed this journey without their unconditional personal support and patience over the years.

Abstract

Understanding the function-shape relationships of the primate masticatory apparatus has been a focus of anthropological research for many decades. One particular feature of the masticatory apparatus, mandibular symphyseal fusion, is investigated in this work because symphyseal fusion has the potential to provide important information on masticatory function and mandibular fragments are often preserved in the fossil record. Regardless of the attention this anatomical feature has received, a complete understanding of the underlying mechanisms driving the evolution of symphyseal fusion remains elusive. The research presented in this dissertation tackles this dilemma by investigating the functional, integrative, and ontogenetic elements of symphyseal fusion. Function and morphology are linked through innovative approaches using the burgeoning geometric morphometric toolkit to challenge previously held notions about mandibular symphyseal fusion and generate new hypotheses. Ultimately, this work acknowledges similar underlying mechanisms for symphyseal fusion in different primate lineages which were previously thought to be different, questions the utility of symphyseal fusion for reconstructing evolutionary relationships of primates, and finds potential evidence for the independent evolution of symphyseal fusion within the crown anthropoid clade.

Table of Contents

Acknowledgements	i
Abstract.....	iii
List of Tables	vii
List of Figures.....	ix
1 Introduction.....	1
1.1 Overview of the masticatory apparatus.....	2
1.1.1 Structure of the masticatory apparatus	2
1.1.2 Jaw kinematics and chewing cycle.....	5
1.2 Methods overview: Geometric morphometrics.....	9
1.2.1 Procrustes superimposition.....	10
1.2.2 Application of geometric morphometrics in this study	13
1.3 Importance of research on mandibular symphyseal fusion.....	17
2 Function and fusion of the mandibular symphysis in living and extinct primates	19
2.1 Introduction	19
2.1.1 Masticatory activity and loading regimes.....	22
2.1.2 The function of mandibular symphyseal fusion	26
2.1.3 Symphyseal fusion in fossil lineages.....	29
2.1.4 Study goals	33
2.2 Materials and methods	35
2.3 Results	50
2.3.1 Masticatory muscle activity and mandibular shape.....	50
2.3.2 Testing hypotheses of strength and stiffness for symphyseal fusion.....	58
2.3.3 Inferring masticatory function in fossil primates	64
2.4 Discussion	72
2.4.1 EMG patterns and mandibular shape.....	72
2.4.2 Strength vs. stiffness models for symphyseal fusion.....	78
2.4.3 Partial vs complete symphyseal fusion.....	81

2.4.4 Masticatory function and symphyseal fusion in fossil primates.....	82
2.5 Conclusions	88
3 Mandibular symphyseal fusion and the wishboning motor pattern	90
4 Morphological integration of the skull and the evolution of symphyseal fusion	93
4.1 Introduction	93
4.1.1 Mandibular symphyseal fusion in primates.....	93
4.1.2 The relationship between the wishboning motor pattern and loading regime..	96
4.1.3 Evolution of the wishboning motor pattern	97
4.1.4 Mandibular fusion and the WMP as an Evolutionary Stable Configuration..	103
4.1.5 Evolutionary impact of mandibular symphyseal fusion	105
4.1.6 Study goals	107
4.2 Materials and methods	110
4.3 Results	119
4.3.1 Analysis of the WMP and skull shape.....	119
4.3.2 Comparisons of skull shape between primates with and without the WMP ..	124
4.3.3 Patterns of craniomandibular integration associated with the WMP	129
4.4 Discussion	138
4.4.1 Wishboning motor pattern and skull morphology	138
4.4.2 Morphological integration of skull components as an ESC	143
4.4.3 Interpreting mandibular symphyseal fusion and the WMP	145
4.4.4 Masticatory patterns and morphology within anthropoids	148
4.4.5 Phylogenetic context of the WMP and symphyseal fusion	149
4.5 Conclusions	151
5 Insights into mandibular symphyseal fusion from an ontogenetic perspective	153
6 Mandibular ontogeny and the evolution of mandibular symphyseal fusion	155
6.1. Introduction	155
6.1.1 Ontogenetic timing of symphyseal fusion	156
6.1.2 Mandibular variation and function	159

6.1.3 Postnatal growth and development of the mandible.....	163
6.1.4 Study goals	166
6.2 Materials and methods	167
6.3 Results	173
6.3.1 Ontogenetic allometric patterns of mandibular shape in primates	173
6.3.2 Mandibular variation among age groups	181
6.3.3 Intraspecific mandibular shape and symphyseal fusion	183
6.4 Discussion	184
6.4.1 Comparison of ontogenetic allometric patterns of mandibular shape and function among primate species	184
6.4.2 Mandibular shape variation associated with early and late ontogenetic fusion	189
6.4.3 An ontogenetic perspective on the strength and stiffness hypotheses for symphyseal fusion	192
6.5 Conclusions	194
7 Summary.....	196
8 References.....	200

List of Tables

Table 2.1: Extant (a) and fossil (b) taxa used in this study. State of symphyseal fusion designated as fused, complex partial, simple partial, or unfused.....	39
Table 2.2: List of mandibular landmarks and semilandmarks. Landmarks begin with “M” and semilandmarks begin with “MS”. Landmark numbers noted with an asterisk (*) were used in the reduced dataset to include fossil specimens.....	42
Table 2.3: Loadings for the EMG variables from an F-PLS on all taxa with EMG data. Variables with the largest loadings for each singular vector are identified with an asterisk.	48
Table 2.4: Statistical results from an F-PLS on all taxa with EMG data.....	48
Table 2.5: Loadings for the EMG variables from an F-PLS on all taxa with some degree of symphyseal fusion. Variables with the largest loadings for each singular vector are identified with an asterisk.	53
Table 2.6: Statistical results from an F-PLS on only taxa with some degree of symphyseal fusion.....	53
Table 2.7: Loadings for the EMG variables from a P-PLS on all taxa with EMG data. Variables with the largest loadings for each singular vector are identified with an asterisk.	57
Table 2.8: Statistical results from a P-PLS on all taxa with EMG data.....	57
Table 2.9: Loadings for the EMG variables from an F-PLS on all taxa with EMG data using the reduced landmark dataset. Variables with the largest loadings for each singular vector are identified with an asterisk.	67
Table 2.10: Statistical results from an F-PLS on all taxa with EMG data using the reduced dataset.....	67
Table 2.11: Loadings for the EMG variables from an F-PLS on all anthropoid taxa with EMG data using the reduced landmark dataset. Variables with the largest loadings for each singular vector are identified with an asterisk.....	71
Table 2.12: Statistical results from an F-PLS on anthropoid taxa with EMG data using the reduced dataset.	71
Table 4.1: Sample size by taxon used in this study. State of symphyseal fusion designated as complete, partial, or unfused.	109
Table 4.2: Description of landmarks and semilandmarks used in this study.....	112

Table 4.3: Loadings for the EMG variables from an F-PLS on all taxa with EMG data. Variables with the largest loadings for each singular vector are identified with an asterisk.	121
Table 4.4: Statistical results from an F-PLS on all taxa with EMG data.....	121
Table 4.5: Statistical results from a P-PLS on all taxa with EMG data.....	131
Table 4.6: Statistical results from a pooled PLS on all taxa.	136
Table 6.1: Sample size by age group for each taxon.	167
Table 6.2: List of mandibular landmarks and semilandmarks. Landmarks begin with “M” and semilandmarks begin with “MS”.	168

List of Figures

Figure 1.1: Features of the mandible demonstrated on a specimen of *Pan troglodytes*: posterior view (left), lateral view (right).2

Figure 1.2 Diagram of a chimpanzee skull depicting the attachment sites of the temporalis (a), superficial (b: dashed line) and deep masseters (b: dotted line), lateral pterygoid (c: dotted line), and medial pterygoid muscles (c: dashed line). Arrows indicate the direction of muscle activity.....3

Figure 1.3: Diagram of the triplet organization of muscles and their force directions during the closing and power stroke stages of mastication. Black arrows represent the line of action for various masticatory muscles. Gray arrows represent movement of the mandible during each triplet. bs=balancing-side, ws=working-side, SM=superficial masseter, MP=medial pterygoid, PT=posterior temporalis (Modified from Ross and Iriarte-Diaz, 2014).....6

Figure 1.4: Depiction of symphyseal orientation of *Cebus apella* (left) and *Propithecus verreauxi* (right). Lateral views of the skulls are oriented based on the plane of the palate (black line). The symphyses for both specimens are outlined in black with the measurements of symphyseal height (dashed arrow) and symphyseal thickness (dotted arrow) as described by Ravosa (1991).13

Figure 2.1: Phylogeny of extant primates showing the status of mandibular fusion in adult forms: unfused or simple partial fusion=open circles, complex partial fusion=gray circles, complete fusion=closed circles. Branch lengths are not to scale.....21

Figure 2.2: Expected stress patterns at the symphysis due to dorsoventral shear (a), coronal bending associated with twisting of the corpora (b), and lateral transverse bending or wishboning (c). Muscle (m) and bite (b) forces are demonstrated with solid black arrows and predicted symphyseal stresses are shown by white arrows. Modified from Hylander, (1988).23

Figure 2.3: Two models for the evolution of complete symphyseal fusion (noted by gray stars) in anthropoids. Modified from Ravosa (1999).....30

Figure 2.4: Mandibular (a-rostral, b-dorsal, c-lateral) landmarks and semilandmark curves (blue line) used in this analysis. Both sides of the mandible were digitized for the analysis, but this figure only displays landmarks on the left side and midline.43

Figure 2.5: Plot of the first pair of axes from the F-PLS of mandibular shape and EMG data including all nine species with EMG data. Visualization shows mandibular shape change along the first F-PLS shape axis from negative (left) to positive (right) values.	47
Figure 2.6: Plot of the second pair of axes from the F-PLS of mandibular shape and EMG muscle activity data. Visualization shows mandibular shape change along the second F-PLS shape axis from negative (left) to positive (right) values.	49
Figure 2.7: Plot of the first pair of axes from the F-PLS including only species with fusion (except <i>Homo</i>). Visualization shows mandibular shape change along the first F-PLS shape axis from negative (left) to positive (right) values.	52
Figure 2.8: BGPCA to separate primates with complete fusion and partial fusion. Visualization shows mandibular shape change along BGPCA1 from negative (left) to positive (right) values.	54
Figure 2.9: Plot of the first pair of axes a phylogenetic PLS of the nine species with EMG data. Visualization shows mandibular shape change along the first P-PLS shape axis from negative (left) to positive (right) values.	56
Figure 2.10: Plot of symphyseal log(centroid size) against log(centroid size) of the entire mandible.	59
Figure 2.11: Multivariate regression of mandibular shape coordinates on log(centroid size) of the mandible for anthropoids (top) and strepsirrhines (bottom). Visualizations to the right depict the vector of shape change from negative (left) to positive (right).	60
Figure 2.12: Multivariate regression of the mandibular shape coordinates on log(symphyseal curvature) for anthropoids (top) and strepsirrhines (bottom). Visualizations to the right depict vector of shape change from negative (left) to positive (right).	61
Figure 2.13. Visualization of differences between mean configurations of select species with and without symphyseal fusion by warping a three-dimensional model of <i>Pan troglodytes</i> using a thin plate spline deformation. Species were chosen that have similar mandibular centroid size to mitigate confounding allometric effects.	63
Figure 2.14: plot of the first pair of axes from the functional PLS including all taxa with EMG data using the reduced landmark set. A boxplot is included showing all extant and fossil specimens projected onto the first F-PLS axis.	

Visualization shows mandibular shape change along the first F-PLS shape axis.....	66
Figure 2.15: Fossil specimens projected onto the BGPCA eigenvector calculated from the difference between mean configurations of primates with complete and partial fusion.....	68
Figure 2.16: Plot of the first pair of axes of the F-PLS on the reduced landmark set including only anthropoid taxa. The boxplot shows the projection of all extant and fossil anthropoid specimens onto the first shape axis. Visualization shows mandibular shape change along the first F-PLS shape axis.....	70
Figure 2.17: Plot of the log (centroid size) of the mandibular symphysis to log(mandibular length) including all extant species and fossil specimens.	73
Figure 2.18: Visualization of select specimen landmark configurations that by warping a three-dimensional model of <i>Pan troglodytes</i> using a thin plate spline deformation. Each set of comparisons includes fossil specimens and the mean configuration of a strepsirrhine species with no symphyseal fusion and similar mandibular length.	74
Figure 4.1: Diagram of the differences in structural configuration of the temporomandibular joint (TMJ), gonial angle, and zygomatic arches between anthropoids and strepsirrhines (modified from Ravosa et al., 2000). The line between the zygomatic arch and gonial angle represents the masseter muscle. The distance between the zygomatic arch and TMJ does not differ between anthropoids and strepsirrhines, so a deeper gonial angle in anthropoids results in a more vertical masseter muscle.	102
Figure 4.2: Two models for the evolution of complete symphyseal fusion (noted by gray stars) in anthropoids.....	105
Figure 4.3: Three-dimensional landmarks and semilandmark curves used in the study. Landmarks=black dots, semilandmarks=blue curves	114
Figure 4.4: Plot of the first pair of F-PLS axes and the visualization along the shape axis. Lateral view: dotted line= orbital plane, black line= basion-hormion, dashed line= staphylion-incision, white line=m1-m3 alveolar plane. Frontal view: black line= orientation of masseter muscle from zygomatic arch to inferior ramus.....	120
Figure 4.5: Plot of the second pair of F-PLS axes and the visualization along the shape axis. Lateral view: dotted line= orbital plane, black line= basion-hormion, dashed line= staphylion-incision, white line=m1-m3 alveolar plane.	

Frontal view: black line= orientation of masseter muscle from zygomatic arch to inferior ramus.....	122
Figure 4.6: Plot of BGPCA of catarrhines and strepsirrhines without the WMP and the visualization of shape change along this axis. Lateral view: dotted line= orbital plane, black line= basion-hormion, dashed line= staphylion-incision, white line=m1-m3 alveolar plane. Frontal view: black line= orientation of masseter muscle from zygomatic arch to inferior ramus.	126
Figure 4.7: Plot of BGPCA of platyrrhines and strepsirrhines without the WMP and the visualization of shape change along this axis. Lateral view: dotted line= orbital plane, black line= basion-hormion, dashed line= staphylion-incision, white line=m1-m3 alveolar plane. Frontal view: black line= orientation of masseter muscle from zygomatic arch to inferior ramus.	127
Figure 4.8: Plot of BGPCA of strepsirrhines with and without the WMP and the visualization of shape change along this axis. Lateral view: dotted line= orbital plane, black line= basion-hormion, dashed line= staphylion-incision, white line=m1-m3 alveolar plane. Frontal view: black line= orientation of masseter muscle from zygomatic arch to inferior ramus.	128
Figure 4.9: Plot of the first pair of P-PLS axes on all taxa with EMG data and the visualization along each axis. Lateral view: dotted line= orbital plane, black line= basion-hormion, dashed line= staphylion-incision, white line=m1-m3 alveolar plane. Frontal view: black line= orientation of masseter muscle from zygomatic arch to inferior ramus.	131
Figure 4.10: Plot of the second pair of P-PLS axes and the visualization along each axis. Lateral view: dotted line= orbital plane, black line= basion-hormion, dashed line= staphylion-incision, white line=m1-m3 alveolar plane. Frontal view: black line= orientation of masseter muscle from zygomatic arch to inferior ramus.....	132
Figure 4.11: Plot of the third pair of P-PLS axes and the visualization along each axis. Lateral view: dotted line= orbital plane, black line= basion-hormion, dashed line= staphylion-incision, white line=m1-m3 alveolar plane. Frontal view: black line= orientation of masseter muscle from zygomatic arch to inferior ramus.....	133
Figure 4.12: Plot of the first pair of axes from a pooled within species PLS and the visualization along each axis. Lateral view: dotted line= orbital plane, black line= basion-hormion, dashed line= staphylion-incision, white line=m1-m3 alveolar plane. Frontal view: black line= orientation of masseter muscle from zygomatic arch to inferior ramus.	136

Figure 4.13: Plot of the second pair of axes from the pooled within species PLS and the visualization along each axis. Lateral view: dotted line= orbital plane, black line= basion-hormion, dashed line= staphylion-incision, white line=m1-m3 alveolar plane. Frontal view: black line= orientation of masseter muscle from zygomatic arch to inferior ramus.	137
Figure 4.14: Boxplot showing the variation in the angle of facial kyphosis for each species.....	140
Figure 4.15: Plot the multivariate regression of skull landmark coordinates on the angle of facial kyphosis. The distinct platyrrhine group in the upper right corner is <i>Alouatta seniculus</i> . Lateral view: dotted line= orbital plane, black line= basion-hormion, dashed line= staphylion-incision, white line=m1-m3 alveolar plane. Frontal view: black line= orientation of masseter muscle from zygomatic arch to inferior ramus.	141
Figure 6.1: Mandibular (a-rostral, b-dorsal, c-lateral) landmarks and semilandmark curves (blue lines) used in this analysis. Both sides of the mandible were digitized, but only landmarks on the left side and midline are displayed.	169
Figure 6.2: Multivariate regression of the Procrustes landmark coordinates on log centroid size for the ontogenetic series of (a) <i>Macaca fascicularis</i> , (b) <i>Colobus guereza</i> , (c) <i>Pan troglodytes</i> , (d) <i>Cebus apella</i> , (e) <i>Propithecus verreauxi</i> , and (f) <i>Lemur catta</i> . The ontogenetic allometric vector of shape change is visualized to the right of each plot from negative end (left column) to positive end (right column) of the axis.	171
Figure 6.3: Results from a between-group PCA and canonical variates analysis of all anthropoid specimens using age group as the classifying variable. The shape vectors described by the BGPC and CV axes are similar, so only the shape vectors for the first two BGPC axes are visualized.	175
Figure 6.4: Results from a between-group PCA on the mean configurations of the different age groups of <i>Propithecus verreauxi</i> . The shape vectors for the first two BGPC axes are visualized.....	176
Figure 6.5: Results from a between-group PCA on the mean configurations of the different age groups of <i>Lemur catta</i> . The shape vectors for the first two BGPC axes are visualized.	177
Figure 6.6: Visualization of the shape change between specimens with and without symphyseal fusion in <i>Macaca fascicularis</i> and <i>Propithecus verreauxi</i>	180

1 Introduction

Primate craniofacial functional morphology has been a fruitful area of research for students of biological anthropology for many decades (e.g., Beecher, 1977; Bouvier, 1986a,b; Cachel, 1984; DuBrul, 1977; DuBrul and Sicher, 1954; Hiiemae and Kay, 1972; Hylander, 1979b; Ravosa et al, 2000; Smith, 1978; Terhune et al., 2015; Vinyard et al., 2008a; Walker and Murray, 1975). In particular, a significant focus has been placed on understanding how the function of the masticatory apparatus is reflected in cranial and mandibular form. Experimental research using electromyography and strain gauges in conjunction with theoretical hypotheses rooted in physics and Newtonian mechanics have provided a foundational understanding of how the skull, specifically the mandible, changes in size and shape in response to different loading regimes during food processing. The studies presented in this dissertation build on previous comparative analyses of functional morphology in unique and insightful ways by testing old hypotheses of craniomandibular form and generating new ones through the application of complex phenotypic descriptors of form and multivariate statistical methods. In particular, this work focuses on the appearance of an important feature in primate evolutionary history: the fusion or ossification of the mandibular symphysis. A brief overview of the general structure and function of the primate masticatory apparatus is pertinent for setting the stage for these analyses.

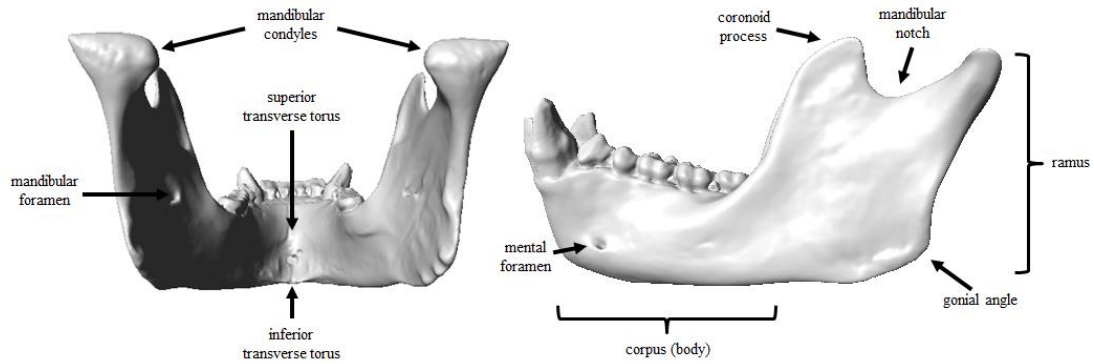


Figure 1.1: Features of the mandible demonstrated on a specimen of *Pan troglodytes*: posterior view (left), lateral view (right).

1.1 OVERVIEW OF THE MASTICATORY APPARATUS

1.1.1 Structure of the masticatory apparatus

The primate head is comprised of multiple components that work together to process and ingest food. While the maxilla and mandible form the bony scaffolding of the masticatory apparatus due to the location of the dentition, other aspects of the cranium are important for the attachment of masticatory muscles and articulation of the mandible with the cranium. The mandible is composed of two main regions, the ramus and the corpus (Figure 1.1). Together these components make up the hemimandibles on each side of the jaw. The left and right corpora articulate anteriorly at the mandibular symphysis. Technically, the mandibular symphysis refers to the surfaces of the hemimandibles at the midline when they are unfused; however, it is commonly used to refer to the anterior region of the mandible beneath the lower central incisors (White et al., 2011). The shape, orientation, and structure of the symphysis vary by primate taxon or clade and are generally determined by masticatory function along with other factors (see Daegling,

2001). Typically, the most prominent features of the symphysis are two projections on the posterior surface, the superior and inferior transverse tori. Additionally, humans have a mental prominent on the inferior portion of the anterior surface. Primates exhibit variability in the degree of ossification of this joint, which is the main topic of this research.

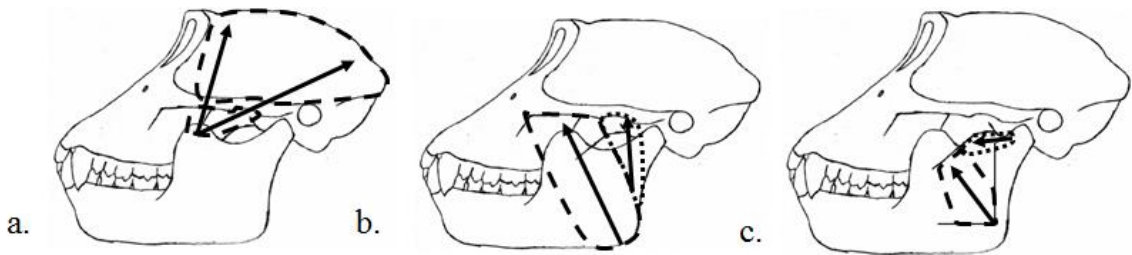


Figure 1.2 Diagram of a chimpanzee skull depicting the attachment sites of the temporalis (a), superficial (b: dashed line) and deep masseters (b: dotted line), lateral pterygoid (c: dotted line), and medial pterygoid muscles (c: dashed line). Arrows indicate the direction of muscle activity.

Five muscles cause the primary movements of the mandible during mastication: temporalis, masseter, medial pterygoid, lateral pterygoid, and digastric. The temporalis, masseter, and medial pterygoid muscles create the largest forces during mastication. The temporalis muscle (Figure 1.2a) originates on the side of the neurocranium and inserts onto the coronoid process of the mandible. The fibers of the temporalis muscle are variably oriented with the anterior portion having vertical fibers anterior to the temporomandibular joint (TMJ) and the posterior portion having horizontal fibers behind the TMJ. The variability in fiber orientation allows the temporalis muscle to move the mandible in different directions. The entire muscle works to elevate (adduct) the mandible, whereas the anterior portion slightly protrudes and posterior portion retracts it.

The attachment of the temporalis muscle on the sides of the cranium can leave raised bony ridges called temporal lines, and when these converge at the midline of the cranium form a single, sagittal crest.

The masseter muscle originates on the inferior aspect of the zygomatic bone and zygomatic arch and inserts onto the lateral aspect of the mandibular ramus and gonial angle. This muscle has both deep and superficial portions with differently oriented fibers (Figure 1.2b). The deep masseter, with transversely oriented muscle fibers, originates on the internal surface of the zygomatic arch and inserts on the lateral aspect of the ascending ramus. The superficial masseter has a more vertical and anterior orientation with an origination on the anteroinferior border of the zygomatic and insertion on the gonial angle. Together, these muscle parts work to elevate the mandible, but the deep portion also causes mediolateral translation (side-to-side) and superficial portion causes protrusion.

The medial pterygoid muscle originates on the medial aspect of the lateral pterygoid plate and inserts on the medial aspect of the ramus and gonial angle to elevate the mandible and cause some mediolateral translation (Figure 1.2c). Together the medial pterygoid and masseter muscles form a sling around the gonial angle that, when fired together, strongly adduct the mandible with little mediolateral movement.

The lateral pterygoid muscle originates from two locations but both insert onto the anterior surface of the condylar neck and fibrous capsule of the TMJ (Figure 1.2c). The inferior head is larger and originates on the lateral surface of the lateral pterygoid plate, and the superior head has an origin on the infratemporal surface and greater wing of the sphenoid. This muscle acts to protrude the mandible and stabilize the condyle in the TMJ.

The digastric muscle has two bodies connected by a tendon that runs through a connective tissue loop attached to the hyoid. The posterior body originates just medial to the mastoid process on the basicranium, and the anterior body inserts into the digastric fossa at the inferior, lingual aspect of the mandibular symphysis. When contracted, the digastric muscle is generally thought to depress and slightly retract the mandible if the infrahyoid muscles hold the hyoid bone in place. In addition, this muscle also raises the hyoid when the teeth are fixed in occlusion and the infrahyoid muscles are relaxed. Two other muscles, the geniohyoid and mylohyoid, similarly run from the base of the mandible to the hyoid and can potentially depress the mandible if the hyoid is stationary, but likely play a larger role in stabilizing the hyoid bone. For more detailed descriptions of the skeletal and muscular components of the masticatory apparatus, see White et al. (2011) and Hylander (2006).

1.1.2 Jaw kinematics and chewing cycle

Primates perform two main types of chewing: bilateral incision primarily with the anterior dentition (although canines and premolars can be used for this purpose) and unilateral mastication with the postcanine dentition. Both of these activities utilize different combinations of mandibular movements and muscle contractions that work to generate considerable forces at precise locations along the dental arcade; slight deviations from the intended chewing trajectory can be problematic. The left and right sides of the jaw mirror each other in activity for incision but act asymmetrically during unilateral

mastication. For the latter, it is important to consider the halves of the jaw separately, as either the working-side (chewing side) or balancing-side (non-chewing side).

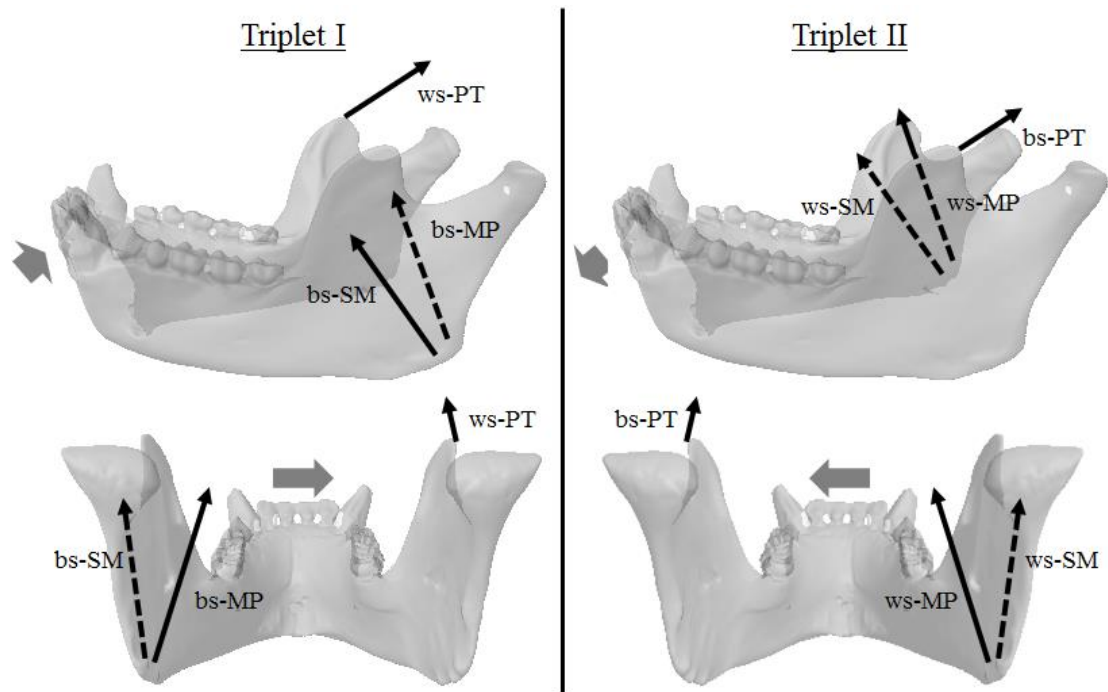


Figure 1.3: Diagram of the triplet organization of muscles and their force directions during the closing and power stroke stages of mastication. Black arrows represent the line of action for various masticatory muscles. Gray arrows represent movement of the mandible during each triplet. bs=balancing-side, ws=working-side, SM=superficial masseter, MP=medial pterygoid, PT=posterior temporalis (Modified from Ross and Iriarte-Diaz, 2014)

Incision: Jaw movement during incision can be divided into three actions: opening, closing, and the power stroke (Hylander, 2006; Jankelson et al., 1953; Sheppard, 1964). Opening occurs through the depression of the mandible by the digastric muscles (and possibly mylohyoid and geniohyoid muscles) and anterior translation of the condyles by contractions of the inferior heads of the lateral pterygoid muscles. The closing stroke follows and is initiated bilaterally by the contraction of the jaw adductor muscles,

terminating when the anterior dentition contacts the food object. During the power stroke of incision, the mandibular incisors are elevated, through the food object, until they approach the apex of the maxillary incisors. At this point, the mandible is retracted to move the mandibular incisors along the lingual aspect of the maxillary incisors as they are elevated. All of the jaw adductor muscles contract more or less simultaneously and bilaterally during the incision power stroke (Hannam et al., 1977; Hylander and Johnson, 1985; Moller, 1966). The lateral pterygoid muscles are also thought to be active during the power stroke to stabilize the TMJ (Hylander, 2006).

Mastication: The jaw movements during mastication are partitioned into the same three stages as incision (Hiemae and Kay, 1973; Hylander, 2006; Kay and Hiemae, 1974; Weijs, 1994). The combination of these three stages (opening, closing, and power stroke) constitutes a single chewing cycle during mastication. The number of chewing cycles in a sequence depends on the size and material properties of the food object. The opening stroke (or recovery stroke) abducts the jaw, brings the midline slightly to the balancing-side, and subsequently swings it back towards the working-side (Hiemae and Kay, 1972; Weijs, 1994). This is achieved through the bilateral contraction of abductor jaw muscles and asymmetric contraction of the lateral pterygoid muscles with the activity of the working-side preceding the balancing-side (Hylander, 2006; Ross and Iriarte-Diaz, 2014; Weijs, 1994).

The closing stroke (or preparatory stroke) adducts the mandible, accompanied by anterior translation, and moves the working-side of the jaw first laterally then medially until the dentition contacts the food object. The adduction of the jaw into occlusion occurs in two steps. In the first step (triplet or diagonal I) the balancing-side superficial

masseter, balancing-side medial pterygoid, and working-side temporalis move the working-side of the jaw upward and laterally (Figure 1.3) (Hylander et al., 2005; Weijs, 1994). The second step (triplet or diagonal II) activates the balancing-side temporalis, working-side superficial masseter, and working-side medial pterygoid muscles to bring the working-side jaw upward and medially until the teeth are in occlusion (Figure 1.3) (Hylander et al., 2005; Ross and Iriarte-Diaz, 2014; Weijs, 1994).

The power stroke is divided into two phases and begins when the upper and lower dentition contact each other. During Phase I, the working-side dentition is moved upward, medially, and slightly anteriorly into centric occlusion. Conversely, the balancing-side dentition is moved upward, laterally, and slightly posteriorly (Hiemae and Kay, 1972; 1973; Hylander, 2006; Kay and Hiemae, 1974). The working-side dentition is moved out of occlusion during Phase II in a downward, medial, and anterior motion while maintaining occlusal contact (Hiemae and Kay, 1972; 1973; Kay and Hiemae, 1974; Ross and Iriarte-Diaz, 2014). Alternatively, sometimes after Phase I, the jaw can abduct, and the dentition falls out of occlusion without the additional medial translation of Phase II (Hiemae and Kay, 1972; 1973; Hylander, 2006). The adduction of the jaw until occlusion produces the highest amounts of muscle force during the chew cycle. The movements of the jaw and resulting muscle forces create stress and strain on certain aspects of the mandible during specific periods throughout the cycle.

While incisal activity certainly has an important role in food processing in primates, the analyses in this dissertation will focus on the relationship between unilateral mastication and mandibular symphyseal fusion. Greaves (1988; 1993) suggested that incision, particularly of small objects like seeds, may have played a role in the evolution

of mandibular symphyseal fusion in primates, but others have provided compelling arguments against this hypothesis (Ravosa and Hogue, 2004; Ravosa and Hylander, 1993; 1994). Behavioral data indicate that the majority of primates with fused symphyses do not consume seeds or other small objects as a major part of their diet (see Fleagle, 1988; Richard, 1985), and those that do often process small objects with the postcanine dentition (Happel, 1988; Hylander, 1975; Jolly, 1970). Additionally, there is little evidence from the fossil record to indicate that early anthropoids used incision to crush small seeds or objects (e.g., Kirk and Simons, 2001; Rosenberger, 1986; Simons and Rasmussen, 1996). Lastly, the presence of partial symphyseal fusion in primates with a tooth comb is problematic for hypotheses linking symphyseal fusion to incisal preparation of small, hard food objects (Ravosa and Hylander, 1994). Therefore, the following analyses will focus on the loading regimes and masticatory patterns employed during unilateral mastication to understand the evolution of mandibular symphyseal fusion in primates.

1.2 METHODS OVERVIEW: GEOMETRIC MORPHOMETRICS

Analyzing the size and shape of the mandible, and its associated components, is important for understanding the function of the masticatory apparatus. In the late 1980s and early 1990s, new methods for quantifying and analyzing shape were developed which helped to remedy some of the issues with traditional morphometrics. These new landmark-based methods (generally referred to as geometric morphometrics) relied on the use of two or three-dimensional landmarks quantified using Cartesian coordinates that

can be located at homologous locations across the data sample (see Bookstein, 1991; Rohlf and Marcus, 1993). The utilization of landmark coordinates, rather than linear distances or angles, as variables provides certain advantages including the preservation of the geometric properties of each specimen during statistical operations. This allows for the visualization of the shape change between two configurations through thin-plate splines and deformation grids. A visual representation of shape makes it possible to determine changes in spatial relationships among multiple variables rather than that having multiple linear measurements with no spatial orientation relative to one another.

1.2.1 Procrustes superimposition

The fundamental data used in a geometric morphometric analysis are a set of landmark configurations, one for each specimen or observation in the analysis. A landmark configuration consists of all of the coordinates of all of the landmarks measured. For example, a landmark configuration of 50 three-dimensional landmarks consists of 150 total coordinates. If the goal of geometric morphometric analyses is the study of shape, then all of the variance contained within raw landmark configurations that is unrelated to shape must first be removed. Kendall (1977) recognized shape as the information left over once variation due to location, scale, and rotational effects are removed. The most commonly used method to orient landmark configurations and remove extraneous information is a least-squares approach called Procrustes superimposition which minimizes the differences between configurations while maintaining their geometric properties (Gower, 1975; Rohlf and Slice, 1990). For most

analyses, including those presented here, the specific type of superimposition used is a generalized Procrustes analysis (GPA), which iteratively aligns more than two landmark configurations with the mean configuration (Gower, 1975; Rohlf and Slice, 1990; Slice, 1996; 2001). There are three basic procedures for aligning configurations and generating shape variables. First, the centroids of each landmark configuration are translated to the origin to remove differences in location. The configurations are then scaled to a common unit size (a centroid size of one). At this point, each of the landmark configurations resides as a single point in preshape space (Rohlf, 1999; Slice et al., 1996). Lastly, the configurations are rotated iteratively based on a least-squares approximation to minimize the sum of squared Euclidean distances between homologous landmarks (Gower, 1975; Rohlf and Slice, 1990; Slice, 2001). The superimposed landmark configurations are now defined by shape coordinates, and the deviations of a specimen's coordinates from the mean configuration (the average of all landmark configurations) are referred to as the Procrustes residuals (Slice et al., 1996). Lastly, the shortest distance between two landmark configurations (square root of the summed squared coordinate-wise differences) is typically called Procrustes distance (see Dryden and Mardia, 1998), and reflects the difference in shape of the landmark configurations (Kendall, 1984; Slice et al., 1996).

After aligning the landmark configurations by GPA, the points representing each landmark configuration occupy the surface of a hyperhemisphere that approximates Kendall's shape space (Rohlf, 1999; Slice, 2001). This space takes the form of a Riemannian manifold with $kp-7$ degrees of freedom for 3D landmarks, or $kp-4$ degrees of freedom for 2D landmarks, where k is the number of dimensions (2 or 3) and p is the

number of landmarks (Bookstein, 1991; Kendall, 1981; 1984; 1985; Mitteroecker and Huttegger, 2009; Slice, 2001). When the landmark configurations are not scaled to a common unit size in the Procrustes superimposition, the resulting space is referred to as form space (Dryden and Mardia, 1992; Goodall, 1991; Kendall, 1989; Rohlf, 1996). Statistical analyses can be carried out in form space or a variation of form space when both size and shape are important in the analysis (see Klingenberg, 2016; Mitteroecker et al., 2004a; 2005).

Statistical analyses are often performed on the landmark configurations in shape space or in a linear Euclidean space tangent to the hyperhemisphere (typically constructed at the point of the mean configuration) (Rohlf, 1996; 1998; Slice, 2001). The Euclidean geometry of tangent space allows for meaningful interpretations of configurations or trajectories within the space (Huttegger and Mitteroecker, 2011; Mitteroecker and Gunz, 2009; Rohlf, 1996). However, when the variation in shape among configurations is small, it is possible to make a good linear approximation of the space for which standard multivariate methods are applicable (Kent, 1994; Rohlf, 1999). Marcus et al. (2000) demonstrated that the linear approximation of shape space by a Euclidean tangent space was sufficient for a variety of mammalian taxa. Therefore, it may be practical to determine whether the shape variation in one's sample is sufficiently small for such an approximation, and this can be done by plotting Euclidean distances between all pairs of points in the tangent space against their Procrustes distances in shape space (Rohlf, 1999; 2002). An approximately linear relationship with a slope near 1 demonstrates that shape variation is sufficiently small. When the variation among configurations is small, many prefer to apply the standard multivariate statistical analyses

to shape variables, ignoring the curvature of Kendall's shape space since the relevant space closely approximates the linear tangent space (Rohlf, 1999; 2002).

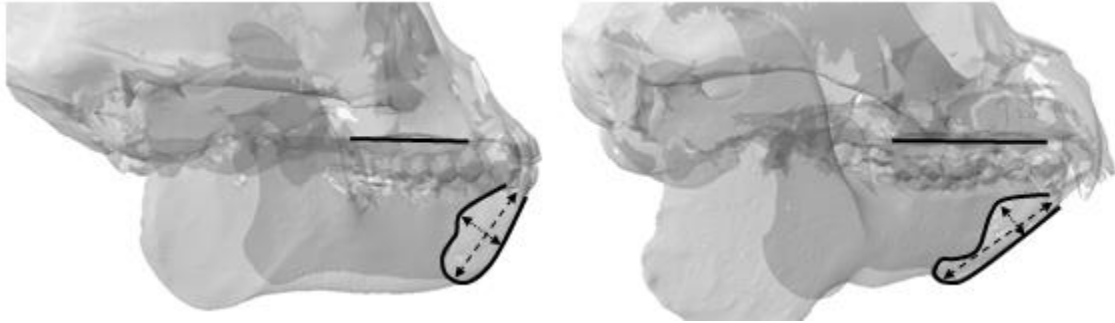


Figure 1.4: Depiction of symphyseal orientation of *Cebus apella* (left) and *Propithecus verreauxi* (right). Lateral views of the skulls are oriented based on the plane of the palate (black line). The symphyses for both specimens are outlined in black with the measurements of symphyseal height (dashed arrow) and symphyseal thickness (dotted arrow) as described by Ravosa (1991).

1.2.2 Application of geometric morphometrics in this study

Geometric morphometric methods were chosen for this study because of the benefits provided through retention of geometric relationships among variables throughout the analysis. The vast majority of previous studies have relied on scaling relationships of linear measurements that have a theoretical functional relevance for interpreting mandibular functional morphology. Although these works are of fundamental importance, linear measurements are often unable to detect nuanced yet important changes in the shape or orientation of structures that might be functionally significant. One relevant example of this limitation is demonstrated by the shape and orientation of the mandibular symphysis in primates. Experimental studies have identified significant lateral transverse bending (or wishboning) during unilateral mastication where the

posterior aspects of the hemimandibles are pulled apart generating labial compression and lingual tension at the symphysis (Hylander, 1979a,b). The most efficient way to counter the stresses generated by this action is to increase the labiolingual thickness of the mandibular symphysis (Hylander, 1984; 1985; Vinyard and Ravosa, 1998). This is dependent in part, however, on the orientation of the mandibular symphysis. Anthropoids are generally known to have a more vertically oriented mandibular symphysis whereas strepsirrhines often have a more anteriorly inclined symphysis -- noting significant variation within each clade. Figure 1.4 demonstrates the orientation of the mandibular symphysis for an anthropoid (*Cebus apella*) and a strepsirrhine (*Propithecus verreauxi*). Many studies investigating the functional significance of the mandibular symphysis have used the measure of labiolingual thickness, described by Ravosa (1991) as the “greatest width measured orthogonal to symphyseal height,” as a proxy for the ability to resist wishboning stress generated at the symphysis (Figure 1.4). However, measuring labiolingual thickness could approximate resistance to different stresses depending on the orientation of the symphysis. If the symphysis is more vertically oriented (as in *Cebus apella*), labiolingual thickness would give an appropriate measure for resisting wishboning stress since labiolingual thickness is oriented more so in the anteroposterior plane. Conversely, the anteriorly inclined symphysis of *Propithecus verreauxi* aligns symphyseal height closer to the anteroposterior plane than labiolingual thickness. This would suggest that Ravosa’s (1991) measure of symphyseal height might provide a better indication of wishboning stress resistance than labiolingual thickness in *Propithecus verreauxi*. The application of geometric morphometric techniques remedies these

limitations by retaining the geometric shape and orientation of structures like the symphysis throughout the analysis.

There has been considerable debate concerning the appropriate metrics for studying interspecific scaling of biomechanical features of the masticatory apparatus. Some researchers have criticized the use of body mass or measures of overall size as “inappropriate” or “misleading” (e.g., Bouvier, 1986a; Hylander, 1985; 1988; Langenback and Weijs, 1990; Ravosa, 1990) for functional comparisons of craniofacial dimensions. Hylander (1985: 325) acknowledges the utility of body mass in allometric studies of limb morphology, but argues that “primates do not routinely transmit body weight or locomotor stress through their faces,” and suggests the use of moment arm approximations relative to bending moments on the mandible (e.g., mandibular arch length) as being more suitable for scaling analyses. However some researchers who have made this argument discuss their results in the context of body size when only comparing scaling dimensions within a functional complex and do not scale their metrics against an appropriate measure of overall size (e.g., Bouvier, 1986a,b; Ravosa, 1991, 1996). For example, in describing the scaling relationship of corpus height below M_2 to palate length, Ravosa (1991) states that “larger-skulled” prosimians converge on the mandibular proportions of “similar-sized” anthropoids. Whereas palate length may be an appropriate dimension for interpreting biomechanical properties of the masticatory apparatus, it has not been shown in this analysis to appropriately reflect overall skull or body size, therefore making references to overall size inappropriate and contradictory to previous arguments. Smith (1993) clearly demonstrates the importance and utility of scaling measurements to both an overall size measure and another dimension within the same

functional system, but notes that interpretations must appropriately reflect what variables are scaled against. Whereas the latter may provide specific information on biomechanical adaptations, the former might provide information on how variables change with respect to the organism as a whole.

Some functional morphologists (see McNulty and Vinyard, 2015; Terhune et al., 2015) have voiced concern about the application of geometric morphometrics for biomechanical analyses of the masticatory apparatus. These concerns stem primarily from the aggrandizement by practitioners of geometric morphometric methods of size removal accomplished through Procrustes superimposition; given the critical importance of “size” to analyses of function and adaptation, the removal of size from one’s data would seem to be contraindicated in biomechanical study. In fact, these types of questions can be addressed using geometric morphometric methods through multivariate regressions on centroid size or other variables (Klingenberg, 2016; Monteiro, 1999), utilizing the underappreciated Procrustes form space, or through a variety of other methods (e.g., Bookstein, 2015; Klingenberg, 1996; Mitteroecker et al., 2004). Likewise, the usage of centroid size in functional analyses has been scrutinized much the same way that body size was (McNulty and Vinyard, 2015; Vinyard, 2008). However, as argued by Smith (1993), functional analyses that utilize different scaling or size dimensions are necessary to understand the full adaptive context of morphology. The catch is that one needs to be mindful of the appropriate interpretations that can be made within each analysis. Since primates transmit masticatory stress through the mandible from forces generated by muscles attached to the mandibular ramus and through tooth-tooth or tooth-food interactions, centroid size of the mandible (or the natural logarithm of centroid size)

is an appropriate surrogate for the size of the masticatory apparatus, and used in the analyses presented here.

1.3 IMPORTANCE OF RESEARCH ON MANDIBULAR SYMPHYSEAL FUSION

Fusion of the mandibular symphysis has occurred numerous times throughout the evolutionary history of primates, although many clades that have independently evolved this feature have no living descendants. In the current distribution extant primates, symphyseal fusion is demonstrated by all anthropoids and some groups of strepsirrhines (e.g., indriids, *Prolemur*, and *Hapalemur*) while all other primate species retain the primitive configuration of two separate, unfused hemimandibles. As a confounding factor, the degree of symphyseal fusion varies in different clades: anthropoids have complete fusion whereas strepsirrhines only exhibit partial fusion. Additionally, anthropoids fuse early in ontogeny while strepsirrhines fuse during later stages of growth and development. These factors have led researchers to suggest that different mechanisms lead to symphyseal fusion in anthropoids in comparison to strepsirrhines (Ravosa, 1999; Ravosa and Hogue, 2004; Ravosa and Hylander, 1994). Nevertheless, symphyseal fusion is believed to be a response to adaptive shifts in masticatory loading regimes, and therefore provides information on masticatory adaptations in living and extinct primates. Additionally, some researchers have proposed that mandibular symphyseal fusion is a phylogenetically important feature in anthropoids and has been used to interpret evolutionary relationships of extinct stem and crown anthropoid taxa (Lockwood, 2007; Ravosa, 1999; Ravosa and Hogue, 2004; Scott et al., 2012a).

The research presented in this dissertation challenges previous ideas related to symphyseal fusion in primates by investigating the functional, integrative, and ontogenetic elements of fusion. In the first study, biomechanical data reflecting the loading regimes thought to underlie symphyseal fusion are leveraged to extract functional signals from mandibular landmark data with the goal of identifying the shape patterns associated with symphyseal fusion. This approach is particularly innovative for geometric morphometric studies, for which researchers typically try to append functional significance to distributions of shape variation, rather than exploiting functional data to extract directly relevant shape patterns. The second study evaluates previously untested hypotheses that purport to explain symphyseal fusion through broad, integrated changes in skull morphology. The last study presents the first comparative assessment of morphological variation associated with the ontogenetic timing of symphyseal fusion. Collectively, the results from these analyses contribute to new understandings of the functional underpinnings of symphyseal fusion in different primate lineages, and challenge the utility of symphyseal fusion for phylogenetic inference, thereby impacting how paleoanthropologists reconstruct the evolutionary relationships of extinct primates.

2 Function and fusion of the mandibular symphysis in living and extinct primates

2.1 INTRODUCTION

Mandibular symphyseal fusion is the ossification of the midline joint between the left and right halves of the mandible. Research on mammalian jaw morphology over the last century has acknowledged the variability of symphyseal structure and fusion in primates and across the mammalian clade (e.g., Beecher 1977; 1979; Geibel 1874-1883; Lonneberg, 1902; Martin, 1990; Scapino, 1965; 1981; Scott et al., 2012a,b; Szalazy and Delson, 1979; Tullberg, 1889; Weber, 1928). Although the degree of mandibular symphyseal fusion can change throughout the lifetime of an individual, the characterization of symphyseal fusion for a species is generally discussed in relation to the terminal state reached in adult forms: unfused, partially fused, and completely fused. In some cases, partial fusion has been divided into “simple partial fusion” and “complex partial fusion” which serves to demonstrate the continuous nature of this feature (Scapino, 1981; Scott et al., 2012b). Simple partial fusion is characterized by some ossification and simple rugosities while symphyses with complex fusion tend to have a greater degree of ossification and interlocking rugosities (Scapino, 1981; Scott et al., 2012b). Mandibular symphyseal fusion is functionally significant because it is understood to be an adaptive response to changes in masticatory structure and function; however, researchers have attributed varying degrees of importance to symphyseal fusion for resolving phylogenetic relationships based on the clade in question and the degree of

ossification. Additionally, partial or complete fusion has evolved independently at least 14 times throughout primate evolution and many more times across the mammalian clade (e.g., Crompton et al., 2010; Herring and Scapino, 1973; Ravosa and Hogue, 2004; Scapino, 1981; Scott et al., 2012a,b; Weijs and Dantuma, 1981; Weijs et al., 1989; Williams et al., 2007; 2008; 2009), calling into question its phylogenetic utility. In order to appropriately evaluate this feature in a phylogenetic context, it is important to understand the underlying mechanisms associated with fusion in different primate lineages.

Two separate, unfused hemimandibles is the ancestral condition for primates and all mammals (see Ravosa and Hogue, 2004). Among living primates, all anthropoids exhibit complete fusion of the mandibular symphysis while most extant strepsirrhines and tarsiers retain a primitive, unfused mandibular symphysis (Figure 2.1). However, some extant strepsirrhines do exhibit a complex partial fusion (e.g., indriids and *Prolemur*) while others (primarily *Hapalemur*) have a simple form of partial fusion (Beecher, 1977; Scott et al., 2012b). Partial or complete symphyseal fusion has also evolved within a number of extinct primate groups including the omomyoids, adapoids, Malagasy subfossil lemurs, and stem anthropoids. The evolution of symphyseal fusion in anthropoids has been of particular interest over the last few decades in determining whether complete fusion is a homologous trait shared among platyrrhines and catarrhines or if it evolved independently in each lineage. The phylogenetic reconstructions of two extinct anthropoid taxa (i.e., oligopithecids and parapithecids) depend in part on the resolution of this question.

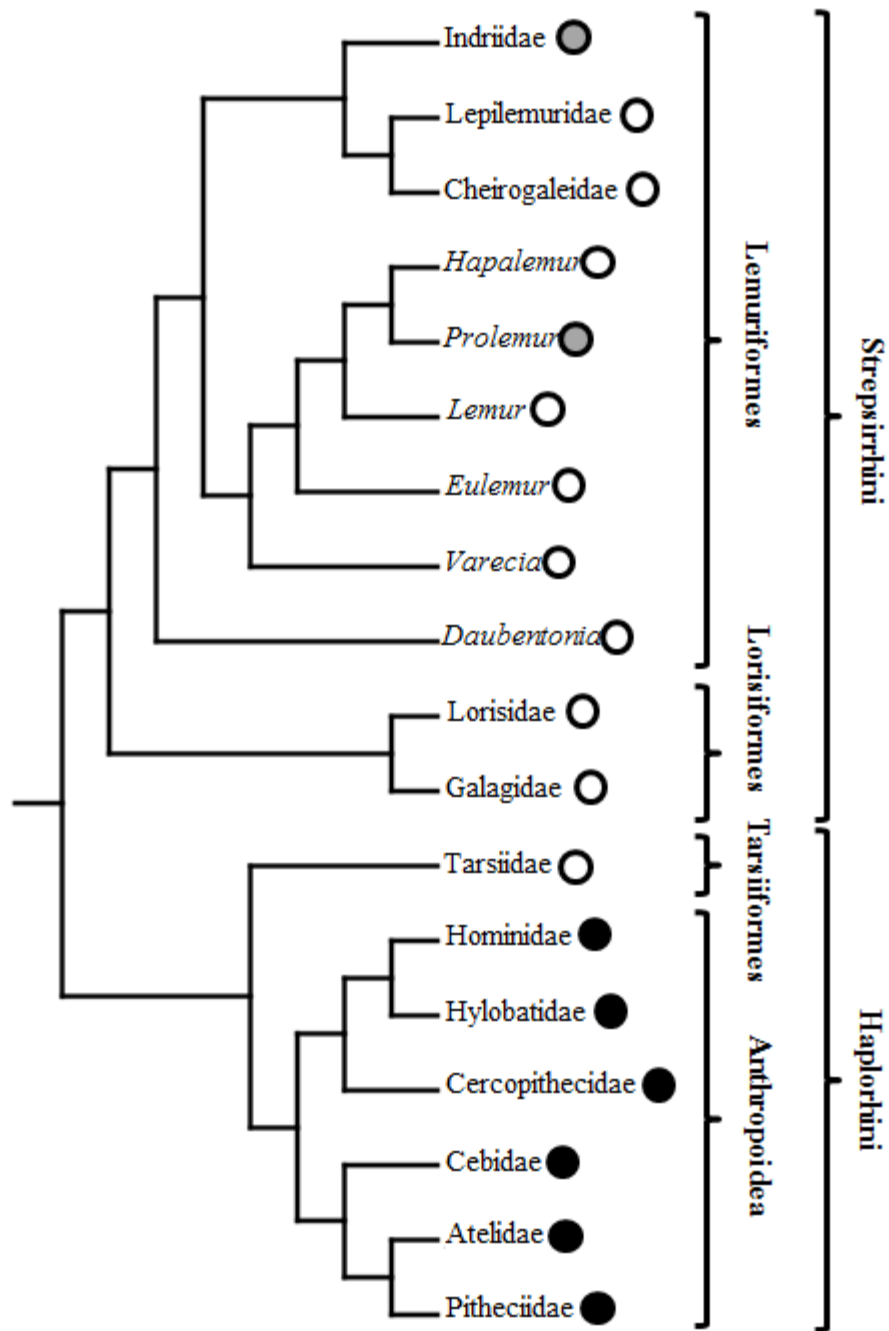


Figure 2.1: Phylogeny of extant primates showing the status of mandibular fusion in adult forms: unfused or simple partial fusion=open circles, complex partial fusion=gray circles, complete fusion=closed circles. Branch lengths are not to scale.

2.1.1 Masticatory activity and loading regimes

Over the last few decades, Hylander and colleagues have constructed a body of experimental work to understand the basic functional underpinnings of primate mastication and the biomechanical factors driving mandibular symphyseal fusion in primates. Early work by Hylander (1977; 1979a; 1986) found that macaques and galagos exhibit similar amounts of peak working-side corpus strain during unilateral mastication, but only macaques have comparable amounts of balancing-side (BS) corpus strain. Therefore, macaques recruit greater balancing-side adductor muscle force than galagos, and as a result, different loading patterns are generated at the corpus and symphysis (Hylander, 1984). Since then, researchers have investigated the link between balancing-side adductor muscle force recruitment and symphyseal fusion in primates, finding that all observed primates with complex partial and complete fusion recruit greater amounts of balancing-side muscle force (Hylander et al., 1992; 1998; 2000; 2004; 2005; 2011; Ross and Hylander, 2000; Vinyard et al., 2006; 2007; 2008), regardless of body size (Hylander et al., 1998). However, it is unclear whether the balancing-side muscle recruitment increases masticatory forces vertically, transversely (mediolateral), or both. Each muscle force direction would generate different stresses at the corpus and symphysis, and thus potentially affect mandibular morphology in different ways.

A greater recruitment of vertically oriented balancing-side muscle force would generate increased dorsoventral shear at the symphysis (Figure 2.2a) (Hylander, 1979a,b). During the power stroke of mastication, balancing-side jaw adductor activity elevates the balancing-side of the jaw while the working-side is held relatively stationary due to tooth-tooth or tooth-food contact which would create a shearing effect at the symphysis.

Dorsoventral shear is best countered by increasing the cross-sectional area of the symphysis, which is not dependent on the shape of the symphysis, or potentially by mandibular fusion (Hylander, 1984). Greater balancing-side vertical muscle force also increases parasagittal bending of the balancing-side corpus, which is best resisted by increasing corpus height. However, greater bite force on the working-side of the mandible generates direct dorsoventral shear of the working-side corpus posterior to the bite point (Hylander, 1984) which may confound interpretations of increased corpus height. However, corresponding changes in symphyseal dimensions would not be expected simply from larger working-side bite forces since forces are not transferred across the symphysis.

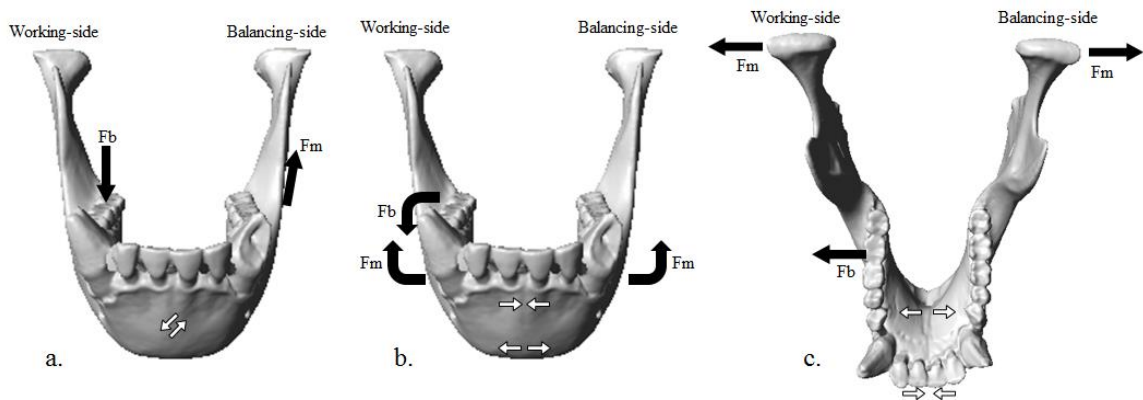


Figure 2.2: Expected stress patterns at the symphysis due to dorsoventral shear (a), coronal bending associated with twisting of the corpora (b), and lateral transverse bending or wishboning (c). Muscle (m) and bite (b) forces are demonstrated with solid black arrows and predicted symphyseal stresses are shown by white arrows. Modified from Hylander, (1988).

The corpora are twisted about the long axis during unilateral mastication (and incision) where the inferior corpus is everted and alveolar bone is inverted primarily from the muscle force resultant of the masseter muscle lateral to the mandible. This effect is exacerbated on the working-side of the jaw as the bite force has the opposite effect (Figure 2.2,b) (Hylander, 1979a,b; 1984). The resulting axial torsion of the mandibular corpora also causes coronal bending of the symphysis with inferior tension and superior compression. The torsional loads experienced by the corpora are best countered by increasing buccolingual thickness, and coronal bending is most efficiently resisted through increasing the vertical depth of the symphysis (Hylander, 1979a,b; 1985).

Recruitment of balancing-side muscle force that is transversely directed would generate greater wishboning (lateral transverse bending) stress at the symphysis by pulling the balancing-side of the jaw laterally while the bite force acts in the opposite direction causing labial compression and lingual tension at the symphysis (Figure 2.2c) (Hylander, 1979a,b). Increased labiolingual thickness of the symphysis, or possibly symphyseal fusion of the lingual portion of the symphysis, would best counteract increased wishboning (Hylander, 1984). Wishboning may also cause buccal compression and lingual tension along the corpus, resulting in a transversely thick mandibular corpus.

Historically, researchers have argued that only crown anthropoids generate significant mediolateral jaw movement through the recruitment of balancing-side muscle force. This muscle activity would create significant wishboning stress and result in complete symphyseal fusion in this clade (Ravosa, 1999; Ravosa and Hogue, 2004). The partial or complete fusion of strepsirrhines and extinct primates outside of the crown anthropoid clade was instead attributed to recruiting vertically oriented balancing-side

muscle force to either maintain or increase bite force as a result of allometric constraints on muscle activity or dietary adaptations. Partial and complete fusion in non-anthropoid taxa has been seen as a response to dorsoventral shear created from recruiting vertically oriented balancing-side muscle force (Ravosa, 1999; Ravosa and Hogue, 2004).

Electromyography studies have additionally shown that extant primates with partial or complete fusion share peak muscle activity patterns during mastication that differ from primates with unfused symphyses (Hylander et al., 2000; 2002; 2004; 2005; 2011; Ross and Hylander, 2000; Vinyard et al., 2006; 2007; 2008). During the closing stroke of the chew cycle, the masticatory muscles generally fire in two clusters: triplet I and triplet II (Hiimae and Kay, 1972; 1973). The muscles in the first triplet (balancing-side superficial masseter, balancing-side medial pterygoid, and working-side temporalis) work together to move the WS of the jaw laterally. Triplet II (working-side superficial masseter, working-side medial pterygoid, and balancing-side temporalis) brings the working-side of the jaw medially until the upper and lower dentition are in occlusion (Hiimae and Kay, 1972; 1973). In this general model, studies have shown that primates with fused and unfused symphyses vary drastically in the peak activity timing of the balancing-side deep masseter muscle (and possibly balancing-side posterior temporalis muscle) (Hylander and Crompton 1986; Hylander and Johnson, 1994; Hylander et al., 1987; 1992; 2000; 2002; 2004; Vinyard et al., 2006; 2008). The balancing-side deep masseter fires near the timing of triplet I in primates with unfused symphyses but at the end of triplet II in extant anthropoids and *Propithecus* (and presumably other indriids) as other muscle activity declines (Hylander et al., 2002; 2004; 2011; Vinyard et al., 2006; 2008). Since the deep masseter muscle has a vertical and transverse orientation, the

delayed activity of the balancing-side component has been interpreted as creating transverse or mediolateral occlusal forces during the power stroke by pulling the balancing-side of the jaw laterally and generating wishboning stress at the symphysis. The delayed activity of the balancing-side deep masseter to create mediolateral movement of the jaw is referred to as the wishboning motor pattern (WMP) (Hylander and Johnson, 1994). This stress is not present (or at least not significant) in primates with unfused symphyses since the force of the balancing-side deep masseter is offset by other muscles firing around the same time (Hylander et al., 2000). Although only previously associated with anthropoids, the presence of the WMP in *Propithecus* suggests that this masticatory pattern is not confined to the crown anthropoid clade and has evolved convergently in other primate lineages.

2.1.2 The function of mandibular symphyseal fusion

Some researchers have argued that the degree of mandibular fusion is a proportional response to the stresses experienced at the mandibular symphysis during mastication (e.g., Ravosa and Hylander 1993; 1994). Hence, fusion has been considered an adaptation to strengthen the symphyseal region to prevent structural failure as forces are applied during different activities (Currey, 1984). Previous studies have supported this idea by demonstrating that mammals with fused symphyses recruit greater amounts of balancing-side muscle force and experience greater amounts of stress during mastication (Herring and Scapino, 1973; Huang et al., 1994; Hylander et al., 1992; 1998;

2000; 2004; 2005; 2011; Ross and Hylander, 2000; Vinyard et al., 2006; 2007; 2008; Weijs and Dantuma, 1981; Weijs et al., 1989).

An alternative model proposes that the mandible fuses to stiffen the symphysis to resist deformation in response to applied forces, enabling the transfer of force across the bone. Studies that emphasize stiffness imply that the main function of bone is to remain rigid and not deform under load, with strength being of secondary importance (Currey, 1984; Lieberman and Crompton, 2000). Some researchers initially argued that symphyseal fusion would provide stiffness to the mandible to transfer vertically oriented muscle force across the symphysis (Greaves, 1988; 1993; Scapino, 1981). However, Dessem (1985) showed that fused and unfused mandibles transfer vertically oriented forces equally well from balancing-side to working-side as fused mandibles. The ligamentous articulations in unfused strepsirrhine symphyses provide support for this interpretation, considering that the joint consists mostly of cruciate ligaments with a dorsoventral orientation that would provide stiffness in this plane (Beecher, 1977; but see Scapino, 1965). Other researchers subsequently emphasized the importance of symphyseal fusion for transferring muscle force from the balancing-side to working-side to aid in the transverse movement of the mandible (Crompton et al., 2008; Herring et al., 2011; Lieberman and Crompton, 2000). Fused symphyses are more effective in transferring force in the transverse plane while an unfused symphysis allows for some independence of the hemimandibles and experiences less strain during mastication as stress dissipates in the symphyseal ligaments (Crompton et al., 2008; Herring and Mucci, 1991; Lieberman and Crompton, 2000). Fusion would benefit mammals whose diets require a strong and efficient transverse component of intercuspal movement during

occlusion, but would not be necessary, or would be less advantageous, for mammals with primarily dorsally-oriented occlusal trajectories or teeth that require some degree of rotation during occlusion (Lieberman and Crompton, 2000). Consequently, bone would be deposited to resist the stresses generated at the symphysis due to the stiffness caused by fusion of the hemimandibles (Lieberman and Crompton, 2000).

Lieberman and Crompton (2000) argue that this model is supported by comparative analyses of symphyseal fusion and occlusal orientation across several mammalian taxa. Generally, mammals with fused symphyses tend to have flatter occlusal surfaces which reflect the mediolateral direction of jaw movements during occlusion (Lieberman and Crompton, 2000). Additionally, goats and opossums, with unfused mandibles, have predominantly vertically-oriented tooth movements and maintain a nearly 1:1 working-side/balancing-side adductor muscle force ratio — similar to macaques (Hylander et al., 1998; Lieberman and Crompton, 2000). This supports the idea that unfused symphyses transfer vertically-oriented muscle force as well as fused symphyses (Lieberman and Crompton, 2000).

Ravosa and Hogue (2004), however, provide multiple arguments against the transverse stiffness model. In particular, they dismiss the assumptions that stiffness and rigidity are the primary function of bone, and that transverse muscle force can only be transferred adequately through a completely fused symphysis. However, Beecher's (1977) analysis of symphyseal ligaments in strepsirrhines demonstrates that the ligaments present in unfused symphyses are oriented to transfer vertical rather than mediolateral muscle force. Cruciate ligaments oriented in the dorsoventral plane, commonly found in the unfused symphyses of strepsirrhines, reflect vertically oriented muscle force, whereas

transverse ligaments are associated with mediolateral muscle force and jaw movements but are only observed in indriids with partial fusion (Beecher, 1997). Lastly, Ravosa and Hogue (2004) additionally point to the lack of an explanation for partial fusion in the transverse stiffness model.

These competing models for mandibular symphyseal fusion generate different predictions for symphyseal dimensions in fused and unfused mandibles. The stiffness model argues that fusion occurs primarily to create a rigid bony structure to transfer muscle force across the symphysis (Lieberman and Crompton, 2000). The lack of flexibility of the symphysis in transverse plane increases the wishboning stress produced at the lingual aspect of the symphysis, requiring a labiolingually thicker symphysis to accompany fusion (Lieberman and Crompton, 2000). In contrast, the strength model does not require correlated changes in the ossification and robusticity of the symphysis as fusion provides a strengthening of the symphysis against increased wishboning stress (Ravosa and Hogue, 2004).

2.1.3 Symphyseal fusion in fossil lineages

Although mandibular symphyseal fusion has evolved independently in multiple primate lineages, some researchers have noted its importance in phylogenetic reconstruction, particularly near the base of the crown anthropoid clade (Kay et al., 1997; Lockwood, 2007; Ravosa, 1999; Ravosa and Hogue, 2004). The earliest basal anthropoids, including the eosimiids, exhibit the ancestral condition of having two separate, unfused hemimandibles (Beard et al., 1994; Fleagle, 1999; Kay et al., 1997;

Simons, 1992). A derived partially fused symphysis is present in some fossil taxa referred to Anthropoidea, including *Catopithecus* and *Arsinoea*, while others (e.g., parapihceids including *Simonsius* and *Apidium*) exhibit a state of complete symphyseal ossification with no sutural remnants (Kay et al., 1997; Ravosa, 1999; Simons, 1992). Putative fossil catarrhines (e.g., *Aegyptopithecus* and *Propliopithecus*) and platyrrhines (e.g., *Branisella*) also have completely fused symphyses along with all extant catarrhines and platyrrhines (Kay et al., 1997; Fleagle, 1999; Ravosa, 1999).

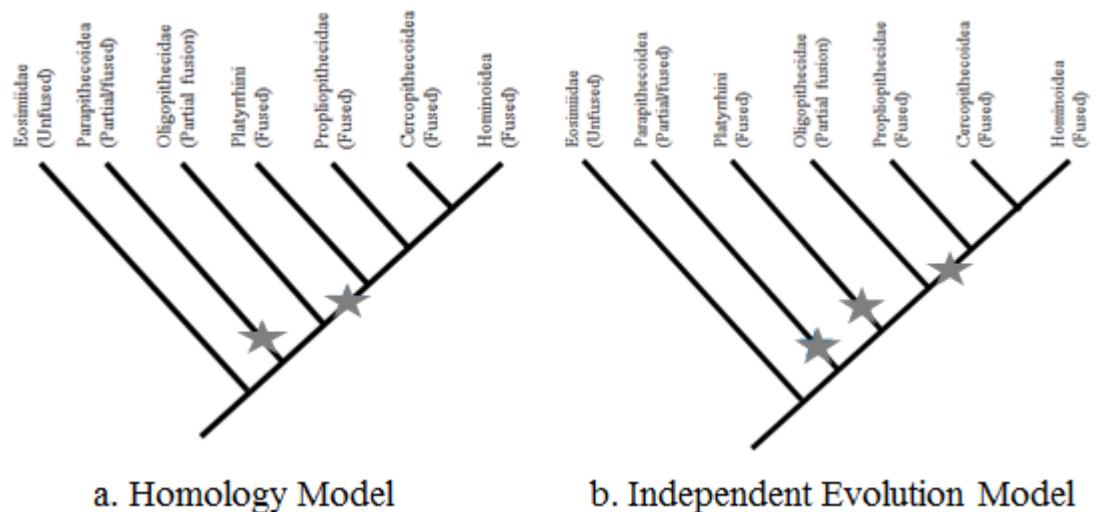


Figure 2.3: Two models for the evolution of complete symphyseal fusion (noted by gray stars) in anthropoids. Modified from Ravosa (1999)

Those who support the use of symphyseal fusion as an important character in phylogenetic reconstruction have argued that fusion in crown anthropoids is distinct and more complex relative to other instances of fusion, noting the underlying mechanisms rather than the final configuration as significant (Ravosa, 1999). As such, fusion in crown anthropoids (caused by significant wishboning stress) has been tied to a restructuring the

skull rather than an adaptation to a more mechanically demanding diet, which has historically been interpreted as the primary cause of fusion in other primate lineages (Ravosa, 1996; 1999; Ravosa et al., 2000). The presumed complexity of this feature in anthropoids has been used as supporting evidence for the singular evolution of an anthropoid-type symphyseal evolution prior to the common ancestor of catarrhines and platyrrhines, as it would be unlikely to evolve multiple times independently (Beard et al., 1996; Kay et al., 1997; Ravosa, 1999). Note, however, that this interpretation excludes *Catopithecus* and other oligopithecids from the crown anthropoid clade (Figure 2.3a) and implies that the independent evolution of partial or complete fusion present in these stem anthropoids results primarily to resist increased dorsoventral shear stress as a possible dietary response rather than to resist wishboning stress (Ravosa, 1999).

Alternatively, other researchers regard symphyseal fusion in crown anthropoids as no different from that found in other primate lineages (Seiffert and Simons, 2001; Simons and Rasmussen, 1996; Simons et al., 2001). From this perspective, *Catopithecus* and other oligopithecids are considered basal catarrhines due to the loss of the second premolar and shared postcranial features with other living and fossil catarrhines (Seiffert and Simons, 2001; Simons and Rasmussen, 1996; Simons et al., 2001). This phylogenetic reconstruction suggests that the last common ancestor of catarrhines and platyrrhines did not exhibit complete symphyseal fusion, implying that it evolved independently in each lineage (Figure 2.3b). These conflicting interpretations highlight the importance of understanding the mechanisms underlying symphyseal fusion in different primate lineages.

Outside of Anthroidea, complete symphyseal fusion is believed to have evolved independently three times among the recently extinct subfossil lemurs within the Archaeolemuridae, Palaeopropithecidae, and Megaladapidae. All archaeolemurids and megaladapids have complete symphyseal fusion while only *Palaeopropithecus* and *Archaeoindris* of the palaeopropithecid clade have evolved complete fusion. *Babakotia* and *Mesopropithecus* retain complex partial fusion of the mandibular symphysis (Ravosa and Simons, 1994; Ravosa et al., 2007; Scott et al., 2012b). As sister taxa, indriids and palaeopropithecids would have likely shared a common ancestor with a partially fused symphysis. Due to the correlation of symphyseal fusion and dietary mechanical properties, the prevailing expectation is that fusion is a response to increased dorsoventral shear from the recruitment of vertical balancing-side adductor muscle to forcefully chew tougher or harder food items (Scott et al., 2012b).

Complete and partial symphyseal fusion seen in certain adapoid and omomyoid lineages have also been attributed to resisting greater amounts of dorsoventral shear stress rather than wishboning, albeit based on different functional underpinnings (Ravosa, 1996). Each family of adapoids (Adapidae, Notharctidae, and Sivaladapidae) has examples of taxa with unfused, partially fused, and completely fused symphyses (Gebo, 2002; Ravosa, 1996). Most omomyoids retain unfused mandibular symphyses with some instances of partial fusion within the Omomyinae (Gebo, 2002; Ravosa, 1996). Unlike extant strepsirrhines and the recently extinct subfossil lemurs, symphyseal fusion does not appear to correlate with dietary mechanical demands in adapoids and omomyoids, but instead has been attributed to allometric effects on symphyseal stresses (Ravosa, 1996). The primary stress affecting symphyseal fusion is assumed to be dorsoventral shear rather

than wishboning due to the late ontogenetic timing of fusion observed in select adapoid and omomyoid species (Ravosa, 1996) and the notion that a partially ossified symphysis is poorly adapted to resisting wishboning stress (Ravosa, 1996).

2.1.4 Study goals

The first goal of this study is to provide a comparative assessment of masticatory function and mandibular shape across primates with fused, partially fused, and unfused mandibular symphyses, and to interpret these relationships in the context of strength and stiffness models for symphyseal fusion. These models provide specific predictions that are tested along with other confounding factors impacting mandibular and symphyseal morphology:

Electromyography (EMG) activity and mandibular shape: Rather than simply interpreting differences in mandibular shape in a functional context, EMG variables describing masticatory activity patterns are used to extract shape variations related directly to function among extant primates with fused, partially fused, and unfused mandibular symphyses.

Strength vs. stiffness hypotheses: If symphyseal fusion serves to strengthen the symphysis against increased stress levels, additional changes in symphyseal shape are not expected (Lieberman and Crompton, 2000). Therefore, similar-sized primates with fused and unfused symphyses are not expected to differ in symphyseal form. If symphyseal fusion serves to primarily stiffen the symphysis to transfer mediolaterally oriented forces from the balancing-side to the working-side of the mandible, symphyseal shape is

predicted to change in response to accompanying increases in stress levels at the symphysis (Lieberman and Crompton, 2000). Specifically, primates exhibiting greater dorsoventral shear stress are expected to have a greater symphyseal cross-sectional area and taller mandibular corpora resulting from parasagittal bending (Hylander, 1984); increased wishboning stress should result in labiolingually thicker symphyses and possibly buccolingually thicker corpora (Hylander, 1984).

Additionally, other factors are expected to impact masticatory loading regimes that may provide insight into the strength and stiffness debate. Larger individuals have proportionately smaller cross-sectional areas of their masticatory muscles due to the negative allometric relationship between cranial size and jaw muscle size (Cachel, 1984) and therefore, are expected to recruit more vertically oriented balancing-side muscle force to generate equivalent bite forces (Ravosa, 1991; 1996). Greater balancing-side adductor recruitment should result in greater dorsoventral shear stress at the symphysis and parasagittal bending of the corpus, resulting in a relatively larger symphyseal area and deeper corpora in larger individuals. If an unfused symphysis transfers vertically oriented forces as efficiently as a fused symphysis (Dessem, 1985), this pattern would be expected in both anthropoids and strepsirrhines. However, if this pattern is observed in anthropoids but not unfused strepsirrhines, then a fused symphysis may provide the stiffness necessary to transfer vertically oriented muscle force across the symphysis whereas an unfused symphysis does not (Greaves, 1988; 1993; Scapino, 1981).

Since the mandible is modeled as a curved beam, symphyseal curvature is an important factor in the production of wishboning stress at the symphysis. A symphysis that is more curved in the transverse plane would result in elevated stress concentrations

along the lingual aspect of the symphysis during mediolateral mandibular movements (Hylander, 1984; 1985; 1988; Ravosa and Vinyard, 2002; Vinyard and Ravosa, 1998). In anthropoids (and other primates with symphyseal fusion), greater symphyseal curvature is expected to correlate with a labiolingually thicker symphysis (or more horizontal symphyseal orientation) to resist increased wishboning stress. Increased symphyseal curvature is not expected to result better wishboning resistance in strepsirrhines lacking mandibular fusion due to the inefficient transfer of mediolateral force across an unfused symphysis (Lieberman and Crompton, 2000).

The second goal of this study is to make inferences about masticatory function in fossil primates based on the comparative assessment of extant primates. If significant shape-function relationships are demonstrated in extant primates, the extracted shape vectors can be used to estimate masticatory function based on mandibular shape in extinct taxa. Additionally, this has the potential to help identify the functional factors driving symphyseal fusion in different extinct primate lineages.

2.2 MATERIALS AND METHODS

The specimens for this study included mandibles from 35 extant and 10 extinct primate species sampling widely across the primate clade. Table 2.1 provides sample sizes for each taxon. Most specimens were scanned using a Breuckmann SmartSCAN white light scanner to collect a series of surface scans for each specimen. Geomagic Design X software was used to clean, align, and merge the resulting scans to create 3D models. Other specimens were acquired as 3D models from the Smithsonian 3D primate

collection or as .tiff stack images output from μ CT scans generously contributed by Dr. CJ Vinyard. Final 3D surface models of the .tiff stacks were generated using Checkpoint software (Stratovan Corporation, Davis, CA).

The fossil specimens from both anthropoid and strepsirrhine clades included in this analysis all exhibit partial or complete mandibular fusion. The fossil anthropoids consist of putative stem catarrhines (*Aegyptopithecus zeuxis* and *Epipliopithecus vindobonensis*), stem anthropoids (*Simonsius grangeri* and *Apidium phiomense*), as well as *Catopithecus browni* with uncertain affinities to the crown anthropoid clade. Of these specimens, all have complete symphyseal fusion except the partially fused mandible of *Catopithecus*. Four subfossil lemur species were sampled for this analysis, two with complete fusion (*Megaladapis edwardsi* and *Archaeolemur majori*) and two with complex partial fusion (*Mesopropithecus dolichobrachion* and *Babakotia radolfilai*). Lastly, two specimens of *Notharctus tenebrosus* with complete symphyseal fusion were included in the analysis to represent the notharctine clade of adapoids.

A total of 196 three-dimensional landmarks and semilandmarks (Table 2.2, Figure 2.4) were collected for each extant primate mandible using Checkpoint software (Stratovan Corporation, Davis, CA). A reduced set of 51 three-dimensional landmarks and semilandmarks were collected on the fossil primate mandibles to represent the aspects of morphology shared among all specimens (i.e., the mandibular condyle, corpus, and symphysis). Fossil specimens preserving only the left side of the mandible were reflected to create all right-sided specimens. The landmark configurations for extant taxa were reduced to match those collected for fossil specimens. Missing landmarks for extant

specimens were estimated in the Geomorph package in R (Adams and Otarola-Castillo, 2013) using a thin plate spline approximation for each taxon separately.

The raw landmark configurations contain information other than shape (i.e., size, orientation, and location) that must be removed before they can be analyzed. This variation was removed using a generalized Procrustes analysis (Gower, 1975; Rohlf and Slice, 1990) performed with the Geomorph package in R (Adams and Otarola-Castillo, 2013), separately for both the full and reduced landmark sets. During superimposition, semilandmarks were allowed to slide along tangents to the curves in order to minimize bending energy (Bookstein, 1997; Gunz et al., 2005). The alternative method of minimizing Procrustes distance across all specimens (see Gunz and Mitteroecker, 2013) was not used as it resulted in semilandmarks sliding past each other. Semilandmarks were placed in relatively high density to best approximate the local curvature as the semilandmarks are slid along tangents to the curves.

Additional linear measurements were calculated from landmark coordinates to specifically address factors driving variation in symphyseal form. Mandibular length (ML) was calculated as the distance between the posterior condyle and infradentale (Table 2.2, Figure 2.4: M4-M20). Mandibular width (MW) was calculated as the bilateral distance between left and right M₁ (Table 2.2, Figure 2.4: M10-M10). The curvature of the symphysis (SC) was calculated by dividing mandibular length by mandibular width ($SC=ML/MW$), where symphyseal curvature increases as the value increases. Centroid size (CS) was calculated for all of the mandibular landmarks and again for only the landmarks of the symphyseal outline. The centroid size of the whole mandible was used

as a proxy for overall size of the masticatory apparatus while the centroid size of the symphysis was calculated specifically as a measure of symphyseal size.

Table 2.1: Extant (a) and fossil (b) taxa used in this study. State of symphyseal fusion designated as fused, complex partial, simple partial, or unfused.

a.	Taxon	Sample size (N)	Fusion
Cercopitheciidae	<i>Macaca fascicularis</i>	25	fused
	<i>Papio anubis</i>	10	fused
	<i>Cercopithecus nictitans</i>	3	fused
	<i>Allenopithecus nigroviridis</i>	2	fused
	<i>Colobus guereza</i>	25	fused
	<i>Nasalis larvatus</i>	3	fused
	<i>Trachypithecus cristatus</i>	4	fused
	<i>Presbytis potenziani</i>	4	fused
Hominidae	<i>Pan troglodytes</i>	25	fused
	<i>Homo sapiens</i>	10	fused
Hylotidae	<i>Hylotates lar</i>	27	fused
Atelidae	<i>Alouatta seniculus</i>	28	fused
	<i>Ateles geoffroyi</i>	25	fused
Cebidae	<i>Cebus apella</i>	25	fused
	<i>Aotus trivirgatus</i>	25	fused
	<i>Callithrix jacchus</i>	5	fused
	<i>Leontideus rosalia</i>	2	fused
Pitheciidae	<i>Chiropotes satanas</i>	5	fused
	<i>Cacajao calvus</i>	2	fused
Lemuridae	<i>Lemur catta</i>	23	unfused
	<i>Haplemur griseus</i>	10	simple partial
	<i>Eulemur rufus</i>	2	unfused
	<i>Eulemur fulvus</i>	2	unfused
	<i>Eulemur mongoz</i>	2	unfused
	<i>Eulemur macaco</i>	2	unfused
	<i>Varecia variegata</i>	4	unfused
	<i>Lepilemur mustelinus</i>	2	unfused
	<i>Propithecus verreauxi</i>	23	complex partial
	<i>Avahi laniger</i>	2	complex partial
Galagidae	<i>Otolemur crassicaudatus</i>	10	unfused
Lorisidae	<i>Perodicticus potto</i>	4	unfused
	<i>Arctocebus aureus</i>	2	unfused
	<i>Arctocebus calabarensis</i>	2	unfused
	<i>Nycticebus coucang</i>	4	unfused
	<i>Loris lydekkerianus</i>	2	unfused
Total: 351			
b.	Taxon	Sample size (N)	Fusion
Anthropoidea	<i>Catopithecus browni</i> †	1	partial
	<i>Simonsius grangeri</i> †	1	fused
	<i>Apidium phiomense</i> †	1	fused
	<i>Aegyptopithecus zeuxis</i> †	1	fused
	<i>Epipliopithecus vindobonensis</i> †	1	fused
Strepsirrhini	<i>Notharctus tenebrosus</i> †	2	fused
	<i>Megaladapis edwardsi</i> †	1	fused
	<i>Archaeolemur majori</i> †	1	fused
	<i>Mesopropithecus dolichobrachion</i> †	1	complex partial
	<i>Babakotia radolfilai</i> †	1	complex partial
Total: 11			

The first goal of this study was to analyze the relationship between mandibular morphology and variation in masticatory muscle activity. To accomplish this, a 2-block partial least squares analysis was employed to find patterns of covariation between the mandibular landmark configurations and experimentally derived electromyography data (Hylander et al., 2000; 2002; 2004; 2005; 2011; Ross and Hylander, 2000; Vinyard et al., 2006; 2007; 2008), including working-side/balancing-side muscle force ratios and peak timing of masticatory muscle activity. The EMG data reflect measures that are direct indicators of the WMP and other aspects of masticatory muscle activity, and thus provides a direct link between the WMP and variation in mandible shape. This analysis is referred to here as a functional partial least squares (F-PLS) and was performed on taxa with varying degrees of symphyseal fusion to determine mandibular shape vectors that covary with loading regimes associated with fusion. Pairs of singular vectors or axes were constructed for the two blocks of multivariate data (**X** and **Y**) that maximally covary with each other (Rohlf and Corti, 2000). The newly formed axes were calculated using a singular value decomposition of the interblock variance-covariance matrix (**R_{xy}**), meaning that the analysis excluded the covariances *within* each block of data (**R_{xx}** and **R_{yy}**). In the context of a standard variance-covariance matrix, with the two blocks of data arranged sequentially, the interblock variance-covariance matrix can be visualized in the formula:

$$R = \begin{pmatrix} R_{xx} & R_{xy} \\ R_{yx} & R_{yy} \end{pmatrix}.$$

Singular values represent the covariance between each pair of singular vectors and are ordinated from greatest to least.

EMG data were available for nine primate species: *Macaca fascicularis*, *Papio hamadryas*, *Aotus trivirgatus*, *Callithrix jacchus*, *Lemur catta*, *Otolemur crassicaudatus*, *Propithecus verreauxi*, *Homo sapiens*, and *Cebus apella*. EMG data for *Homo sapiens* and *Cebus apella* were obtained from Dr. CJ Vinyard. Data for the remaining seven species were collected from previous publications (Hylander et al., 2000; 2002; 2004; 2005; 2011; Ross and Hylander, 2000; Vinyard et al., 2006; 2007; 2008). Timing of peak activity was calculated for each masticatory muscle as milliseconds before or after the peak activity of the working-side superficial masseter muscle. Since larger primates have absolutely longer chewing cycles, the peak times were scaled by an estimation of the length of the power stroke that was calculated as the time between the peaks of the first and last muscles to fire (Ross et al., 2008). The resulting firing times and muscle force ratios were standardized by the standard deviation of each variable. The F-PLS was performed using species averages since morphometric and EMG data were not collected on the same specimens, only the same species.

Table 2.2: List of mandibular landmarks and semilandmarks. Landmarks begin with “M” and semilandmarks begin with “MS”. Landmark numbers noted with an asterisk (*) were used in the reduced dataset to include fossil specimens.

Element	Landmark number	Landmark description	Bilateral/Midline/Symmetric
<u>Mandible</u>	M1*	Most medial point on the articular surface of the mandibular condyle	Bilateral
	M2*	Most lateral point on the articular surface of the mandibular condyle	Bilateral
	M3*	Most anterior point on the mandibular condyle at the midpoint of the mediolateral curve	Bilateral
	M4	Most posterior point on the mandibular condyle at the midpoint of the mediolateral curve	Bilateral
	M5	Coronion	Bilateral
	M6	Attachment of the anterior ascending ramus on the mandibular corpus	Bilateral
	M7	Gonion	Bilateral
	M8	Inferior border of the mandibular foramen	Bilateral
	M9*	Most distal molar point projected on the alveolar margin	Bilateral
	M10*	Point on the lingual alveolar margin at the midpoint of m1	Bilateral
	M11*	Most inferior point on mandibular corpus under m1	Bilateral
	M12*	Point on the buccal alveolar margin at the midpoint of m1	Bilateral
	M13*	Premolar-molar contact projected on the buccal alveolar margin	Bilateral
	M14*	Premolar-molar contact projected on the lingual alveolar margin	Bilateral
	M15*	Canine-premolar contact projected on the buccal alveolar margin	Bilateral
	M16*	Canine-premolar contact projected on the lingual alveolar margin	Bilateral
	M17*	Most inferior point on the mental foramen	Bilateral
	M18	Most mesial point on the midline of m1	Bilateral
	M19	Contact at the apex of the central incisor	Midline
	M20*	Infradentale	Midline
	M21*	Gnathion	Midline
	M22*	Mandibular orale	Midline
MS1	Mandibular border curve (p=63)	Symmetric	
MS2	Coronoid process curve (p=21)	Bilateral	
MS3*	Mandibular corpus outline under m1 (p=15)	Bilateral	
MS4*	Mandibular symphysis outline (p=21)	Midline	

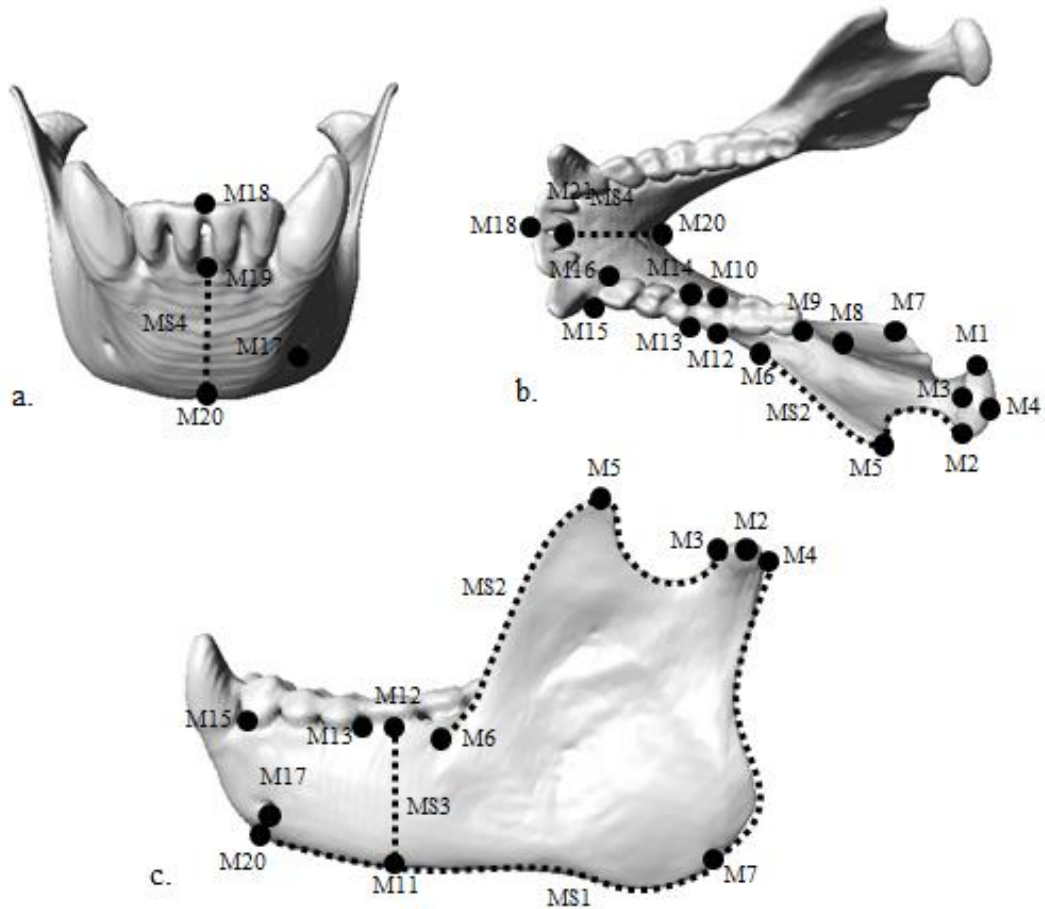


Figure 2.4: Mandibular (a-rostral, b-dorsal, c-lateral) landmarks and semilandmark curves (blue line) used in this analysis. Both sides of the mandible were digitized for the analysis, but this figure only displays landmarks on the left side and midline.

A note of caution is needed for interpreting the p-values reported in analyses utilizing EMG data. The sample sizes for these analyses are small and therefore lack the power to detect significant relationships, increasing the likelihood of type II error. However even with the paucity of available experimental data, the results nevertheless meaningful relationships between shape and function for the species in the analyses.

A second F-PLS analysis was performed including only taxa that have complete or partial fusion to determine if degree of fusion manifests different shape-function

relationships. A separate F-PLS analysis was run rather than interpreting subsequent axes of the original analysis so that the potential differences between primates with partial and complete fusion were not constrained by the correlations described on previous pairs of axes. Additionally, a between-group principal component analysis (BGPCA) was used as a multivariate ordination method to summarize shape differences between primates with completely and partially fused symphyses to determine if these shape differences can provide insight into variation in degree of fusion. In this analysis, the full dataset of specimens is projected onto the eigenvectors of the group mean configurations of all specimens that exhibit complete and partial fusion (Boulesteix, 2005; Mitteroecker and Bookstein, 2011). This approach has the benefit of summarizing group differences, similar to a canonical variates or discriminant function analysis, but employs a rigid rotation of the data rather than warping the shape space.

Since the primate species used in this study have a shared evolutionary history, they should not be thought of as independent observations. Shared evolutionary history generally manifests in a proportional degree of phenotypic similarity. Therefore, analyses of evolutionary correlations or covariances of traits need a phylogenetic context to account for the lack of independence among taxa. Therefore, an additional phylogenetic PLS or P-PLS (Adams and Felice, 2014) was performed between the landmark coordinate and EMG data to identify patterns of covariation between mandibular shape and masticatory function while accounting for phylogenetic relationships. This method calculates a singular value decomposition of the interblock portion of the evolutionary covariance matrix (Adams and Felice, 2014). The phylogeny used in this analysis was based off the molecular phylogeny generated by Perelman et al., (2011). In essence, the

phylogenetic PLS finds axes that maximally covary between the two blocks of data based on the estimated changes from nodes to tips rather than the measured values for each species. This method allows for analysis of how masticatory function and mandibular shape covary along the evolutionary tree rather than simply comparing overall patterns among terminal taxa that might reflect similarities due to phylogenetic history.

Additional analyses were performed to investigate how different factors impact symphyseal morphology in primates with both fused and unfused symphyses, and to incorporate a larger number of species for which no experimental data are available. First, allometric effects were tested using linear regression analysis of the log(symphyseal CS) on log(mandibular CS) to determine how symphyseal size scales with overall mandibular size in primates with and without symphyseal fusion. Multivariate regressions (Klingenberg, 2016; Monteiro, 1999) of the landmark coordinates on log(mandibular CS) were performed separately for anthropoids and strepsirrhines to investigate the shape variation associated with changes in size of the masticatory apparatus. Additional multivariate regressions were performed to determine the relationship of symphyseal shape to changes in symphyseal curvature in anthropoids and strepsirrhines. Additional visual comparisons are provided between primates with different degrees of symphyseal fusion of a similar mandibular size to illustrate actual differences in mandibular and symphyseal shape between species. To create these, mean configurations were calculated for each species and a three-dimensional model (a specimen of *Pan troglodytes*) was warped to each configuration using Landmark Editor.

The second goal of this study was to use form-function relationships in extant taxa to make inferences about masticatory function and the evolution of symphyseal

fusion in extinct primates. For this aim, the set of landmarks and semilandmarks was reduced to 51 and only includes the right hemimandible so as to incorporate as many fossil primate specimens as possible. An F-PLS was again performed on the extant taxa using the reduced landmark set and the functional EMG variables. The landmark coordinate data for the fossil specimens were then projected onto the resulting singular vectors corresponding to mandibular shape. Fossil specimens were also projected onto the single shape vector separating primates with complete symphyseal fusion and partial fusion as computed using a BGPCA. Since morphology is expected to reflect masticatory loading regimes, inferences of masticatory function are made for fossil specimens based on morphological similarity to extant primate species.

Lastly, similar to the analysis of extant primates, visual comparisons were made between fossil specimens and mean configurations of extant species with unfused symphyses of similar mandibular size. The landmark configurations from fossil specimens and mean configurations of extant species were visualized by warping a hemimandible of *Pan troglodytes*. Comparisons were made only for fossil specimens that had extant taxa with similar mandibular sizes to mitigate any confounding allometric effects.

Functional PLS 1

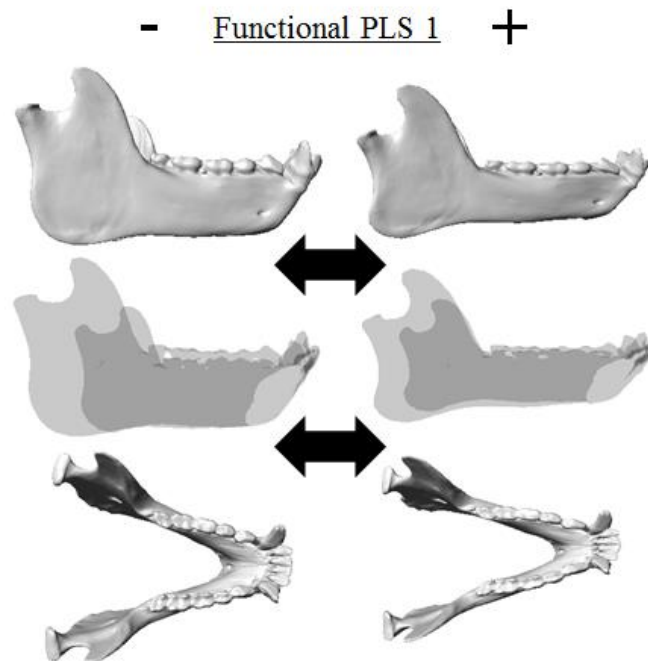
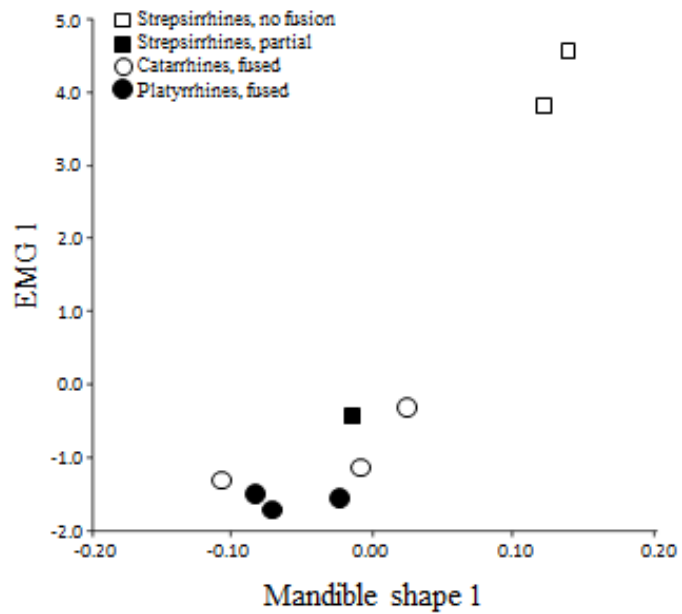


Figure 2.5: Plot of the first pair of axes from the F-PLS of mandibular shape and EMG data including all nine species with EMG data. Visualization shows mandibular shape change along the first F-PLS shape axis from negative (left) to positive (right) values.

Table 2.3: Loadings for the EMG variables from an F-PLS on all taxa with EMG data. Variables with the largest loadings for each singular vector are identified with an asterisk.

<u>EMG variables</u>	<u>Data type</u>	<u>F-PLS 1</u>	<u>F-PLS 2</u>
Superficial masseter	W/B ratio	-0.158	*0.393
Deep masseter	W/B ratio	*-0.352	0.044
Anterior temporalis	W/B ratio	-0.283	0.009
Posterior temporalis	W/B ratio	*-0.377	-0.154
WS deep masseter	Peak muscle timing	-0.189	-0.137
BS superficial masseter	Peak muscle timing	-0.213	*0.490
BS deep masseter	Peak muscle timing	*-0.371	0.189
WS anterior temporalis	Peak muscle timing	-0.341	-0.296
BS anterior temporalis	Peak muscle timing	-0.227	0.275
WS posterior temporalis	Peak muscle timing	-0.292	*-0.591
BS posterior temporalis	Peak muscle timing	*-0.393	0.101

Table 2.4: Statistical results from an F-PLS on all taxa with EMG data.

	<u>F-PLS 1</u>	<u>F-PLS2</u>
Singular value	0.187	0.077
p-value	0.029	0.047
correlation	0.933	0.884
% covariation	75.03%	12.77%

Functional PLS 2

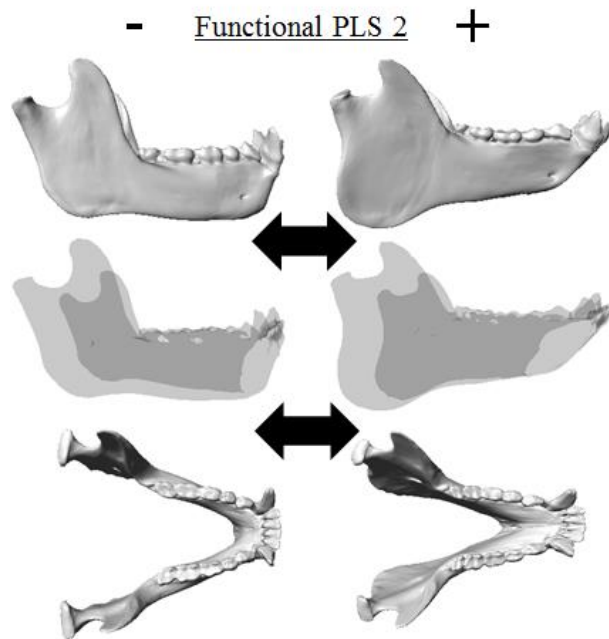
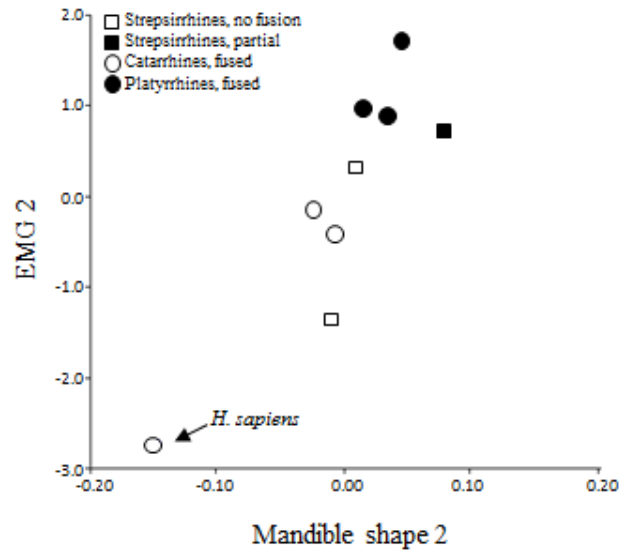


Figure 2.6: Plot of the second pair of axes from the F-PLS of mandibular shape and EMG muscle activity data. Visualization shows mandibular shape change along the second F-PLS shape axis from negative (left) to positive (right) values.

2.3 RESULTS

2.3.1 Masticatory muscle activity and mandibular shape

The F-PLS of mandibular shape and EMG muscle data with all 9 extant species (Tables 2.3-2.4) resulted in a primary set of axes that differentiate unfused strepsirrhines (i.e., *Lemur* and *Otolemur*) from primates with some degree of fusion (i.e., *Aotus*, *Callithrix*, *Cebus*, *Homo*, *Macaca*, *Papio*, and *Propithecus*) at the other end (Figure 2.5). Importantly, the close association of *Propithecus* with anthropoids confirms that this analysis elucidates shape-function relationships associated with symphyseal fusion rather than basic phenetic differences reflecting phylogeny. Along the first pair of axes, a deeper gonial region, taller mandibular condyle, deeper corpus, and taller, labiolingually thicker symphysis correlate with delayed activity and increased recruitment of the balancing-side deep masseter and posterior temporalis muscles (Figure 2.5).

The second pair of F-PLS axes provides evidence that *Homo* exhibits a unique relationship between mandibular shape and masticatory function among primates (Figure 2.6). Interestingly, the timing of the balancing-side superficial masseter and working-side posterior temporalis and a reduction in balancing-side superficial masseter recruitment contribute most to the variation along the second axis. The balancing-side superficial masseter muscle fires earlier in the chewing cycle and is the first to reach peak activity. In this sample, this pattern is unique to *Homo* and *Otolemur* with the working-side deep masseter reaching peak activity first in all other primates. The working-side posterior temporalis is delayed in the *Homo* chew cycle and reaches peak activity near the same time as the working-side superficial masseter. These changes in masticatory function

correlate with a wider mandibular arch, reduced gonial region, and shorter, more vertical symphysis (Figure 2.6).

A second F-PLS not including unfused strepsirrhines (Tables 2.5-2.6) was used to determine if a shape-function relationship could identify differences between complete and partial fusion. *Homo* was also excluded from this analysis to prevent its unique shape-function relationship from being a significant driver of covariation between the two blocks of data. Unexpectedly, catarrhines and platyrrhines are separated along the first axis with *Propithecus* plotting in the middle (Figure 2.7). Along this axis, an early firing working-side deep masseter correlates with a less vertically oriented ramus, wider condyles, deeper corpus, narrower mandibular arch, and the development of an inferior transverse torus (Figure 2.7).

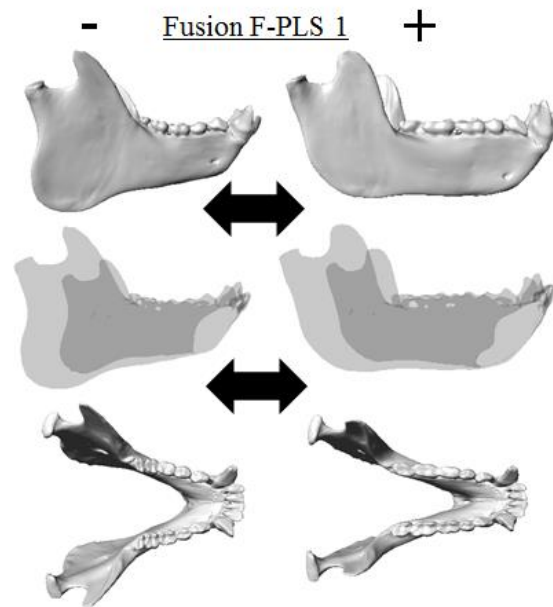
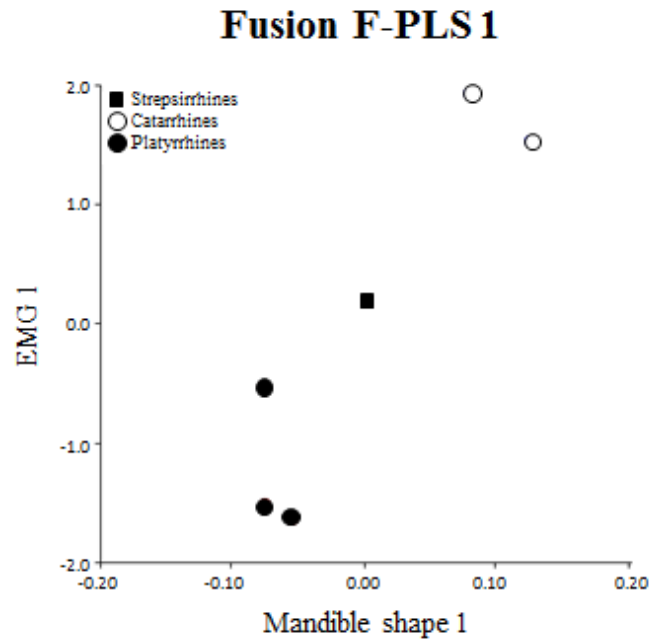


Figure 2.7: Plot of the first pair of axes from the F-PLS including only species with fusion (except *Homo*). Visualization shows mandibular shape change along the first F-PLS shape axis from negative (left) to positive (right) values.

Table 2.5: Loadings for the EMG variables from an F-PLS on all taxa with some degree of symphyseal fusion. Variables with the largest loadings for each singular vector are identified with an asterisk.

<u>EMG variables</u>	<u>Data type</u>	<u>F-PLS 1</u>
Superficial masseter	W/B ratio	0.234
Deep masseter	W/B ratio	-0.069
Anterior temporalis	W/B ratio	-0.018
Posterior temporalis	W/B ratio	-0.106
WS deep masseter	Peak muscle timing	*0.615
BS superficial masseter	Peak muscle timing	*0.557
BS deep masseter	Peak muscle timing	0.081
WS anterior temporalis	Peak muscle timing	0.012
BS anterior temporalis	Peak muscle timing	*0.444
WS posterior temporalis	Peak muscle timing	-0.107
BS posterior temporalis	Peak muscle timing	0.158

Table 2.6: Statistical results from an F-PLS on only taxa with some degree of symphyseal fusion.

	<u>F-PLS 1</u>
Singular value	0.118
p-value	0.132
correlation	0.915
% covariation	85.95%

BGPCA: Complete vs Partial fusion

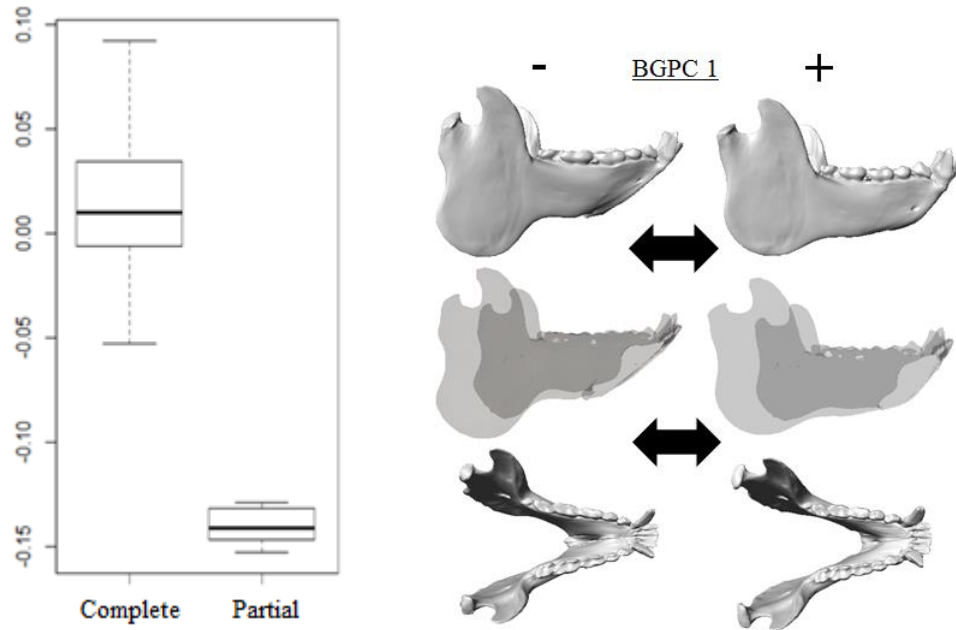


Figure 2.8: BGPCA to separate primates with complete fusion and partial fusion. Visualization shows mandibular shape change along BGPCA1 from negative (left) to positive (right) values.

A BGPCA distinguishing primates with complete and partial symphyseal fusion resulted in a single axis that separates these groups with no overlap (Figure 2.8). However, there is a much broader distribution of primates with complete fusion compared to those with partial fusion, likely reflecting the greater diversity of anthropoids in comparison to indriids. The results from this analysis indicate that primates with complete fusion (or specifically anthropoids when compared to indriids) have a more vertically oriented symphysis, an everted inferior mandibular corpus, wider mandibular condyles, and a less projecting gonial region (Figure 2.8). Overall ramus height increases toward the indriid end of the axis but condylar height above the occlusal surface is greater moving toward the anthropoid end of the axis. Additionally, the long axis of the mandibular symphysis is elongated in extant primates with partial fusion.

When accounting for the shared evolutionary history among taxa, the covariation demonstrated by the first pair of P-PLS axes generally separates primates with complete and partial fusion from those without symphyseal fusion, except *Papio* plots with unfused strepsirrhines (Figure 2.9, Table 2.7-2.8). This is likely because, in comparison to *Macaca*, *Papio* has an earlier peak firing time of the balancing-side deep masseter, working-side anterior temporalis, and working-side posterior temporalis, all of which load most heavily on the first pair of P-PLS axes. These masticatory patterns correlate with a posteriorly angled ramus that has a shorter condylar height, shorter corpus height, narrower mandibular arch, and a more circular symphyseal cross-section. The second pair of P-PLS axes is similar to the initial F-PLS that distinguishes *Homo* from the other taxa which has similar shape changes associated with early activity of the balancing-side superficial masseter and delayed activity of the working-side posterior temporalis and deep masseter muscles, and is therefore not displayed here.

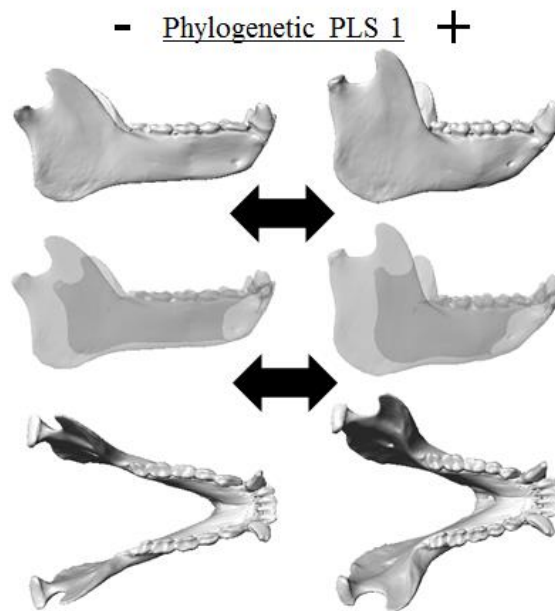
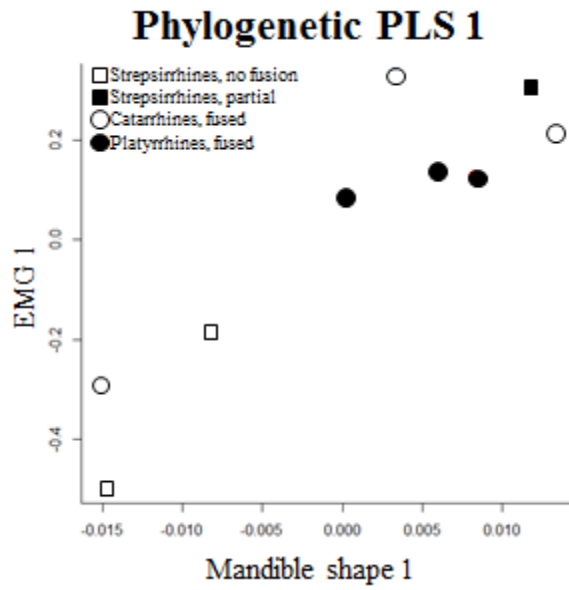


Figure 2.9: Plot of the first pair of axes a phylogenetic PLS of the nine species with EMG data. Visualization shows mandibular shape change along the first P-PLS shape axis from negative (left) to positive (right) values.

Table 2.7: Loadings for the EMG variables from a P-PLS on all taxa with EMG data. Variables with the largest loadings for each singular vector are identified with an asterisk.

<u>EMG variables</u>	<u>Data type</u>	<u>P-PLS 1</u>	<u>P-PLS 2</u>
Superficial masseter	W/B ratio	*-0.329	-0.284
Deep masseter	W/B ratio	-0.216	-0.185
Anterior temporalis	W/B ratio	-0.141	-0.045
Posterior temporalis	W/B ratio	-0.151	-0.029
WS deep masseter	Peak muscle timing	-0.179	*0.413
BS superficial masseter	Peak muscle timing	-0.09	*-0.415
BS deep masseter	Peak muscle timing	*-0.414	-0.321
WS anterior temporalis	Peak muscle timing	*-0.431	0.152
BS anterior temporalis	Peak muscle timing	-0.232	-0.276
WS posterior temporalis	Peak muscle timing	*-0.550	*0.528
BS posterior temporalis	Peak muscle timing	-0.218	-0.237

Table 2.8: Statistical results from a P-PLS on all taxa with EMG data.

	<u>P-PLS 1</u>
p-value	0.248
correlation	0.914

2.3.2 Testing hypotheses of strength and stiffness for symphyseal fusion

For a given size, anthropoids have relatively larger symphyses compared to strepsirrhines that lack symphyseal fusion. Figure 2.10 shows that in a bivariate plot of symphyseal size to overall mandibular size, the anthropoid distribution ($p=0.0001$, $R^2=0.933$) is positioned above the strepsirrhine distribution ($p=0.0001$, $R^2=0.834$). Indriids are the exception in that both *Avahi* and *Propithecus* plot within or above the anthropoid distribution. A multivariate regression of the mandible coordinates on mandible size across anthropoids ($p=0.001$, $R^2=0.215$) shows that the symphysis is taller, more vertically oriented, and has a slight or no increase in relative size as overall mandibular size increases (Figure 2.11). Interestingly, smaller anthropoids have symphyses thicker in the labiolingual dimension whereas their larger counterparts emphasize a thicker dorsoventral dimension. Comparatively, in strepsirrhines ($p=0.001$, $R^2=0.452$) the symphysis becomes anteriorly inclined and decreases in relative size with an increase in overall mandibular size (Figure 2.11). Indriids with partial fusion (*Propithecus verreauxi* and *Avahi laniger*) do not follow the allometric patterns demonstrated by unfused strepsirrhines (Figure 2.11).

Multivariate regressions of the mandibular landmark coordinates on the degree of symphyseal curvature (Figure 2.12) identify a significant relationship across anthropoids ($p=0.0009$, $R^2=0.227$) but not strepsirrhines ($p=0.253$, $R^2=0.096$). As the curvature of the symphysis increases in anthropoids, the symphyseal region becomes more anteriorly inclined and elongated through the long axis which would provide better resistance to increased wishboning stress. Additionally, symphyseal curvature is associated with the development of a more prominent inferior transverse torus and a reduction in

anteroposterior thickness of the mandibular ramus. Mandibular shape does not change in a significant way with symphyseal curvature in unfused strepsirrhines. However, when indriids are included in the multivariate regression (Figure 2.12), it is clear that they have a different relationship between mandibular shape and symphyseal curvature likely reflecting the importance of the wishboning motor pattern and transverse jaw movement during mastication in indriids.

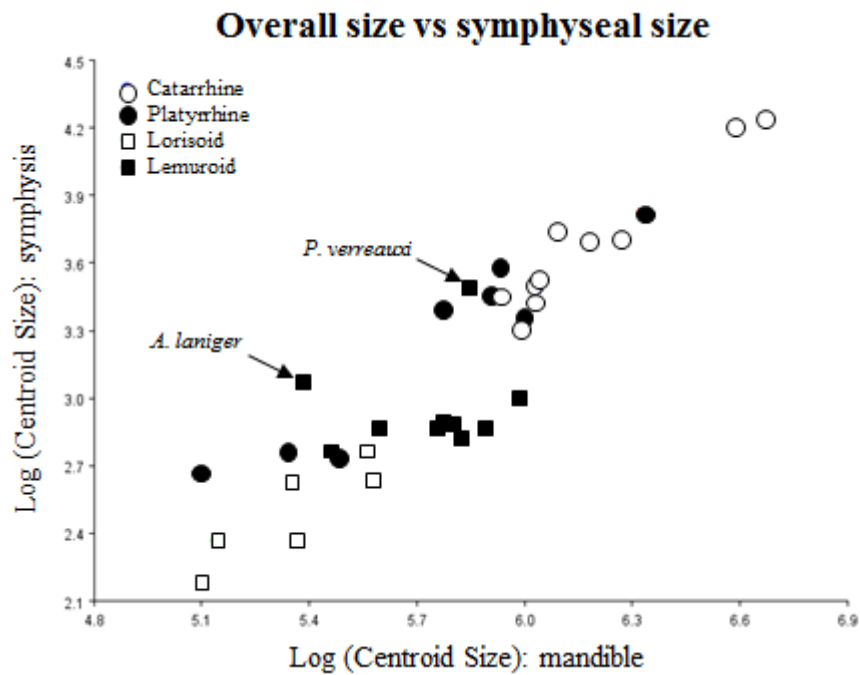


Figure 2.10: Plot of symphyseal log(centroid size) against log(centroid size) of the entire mandible.

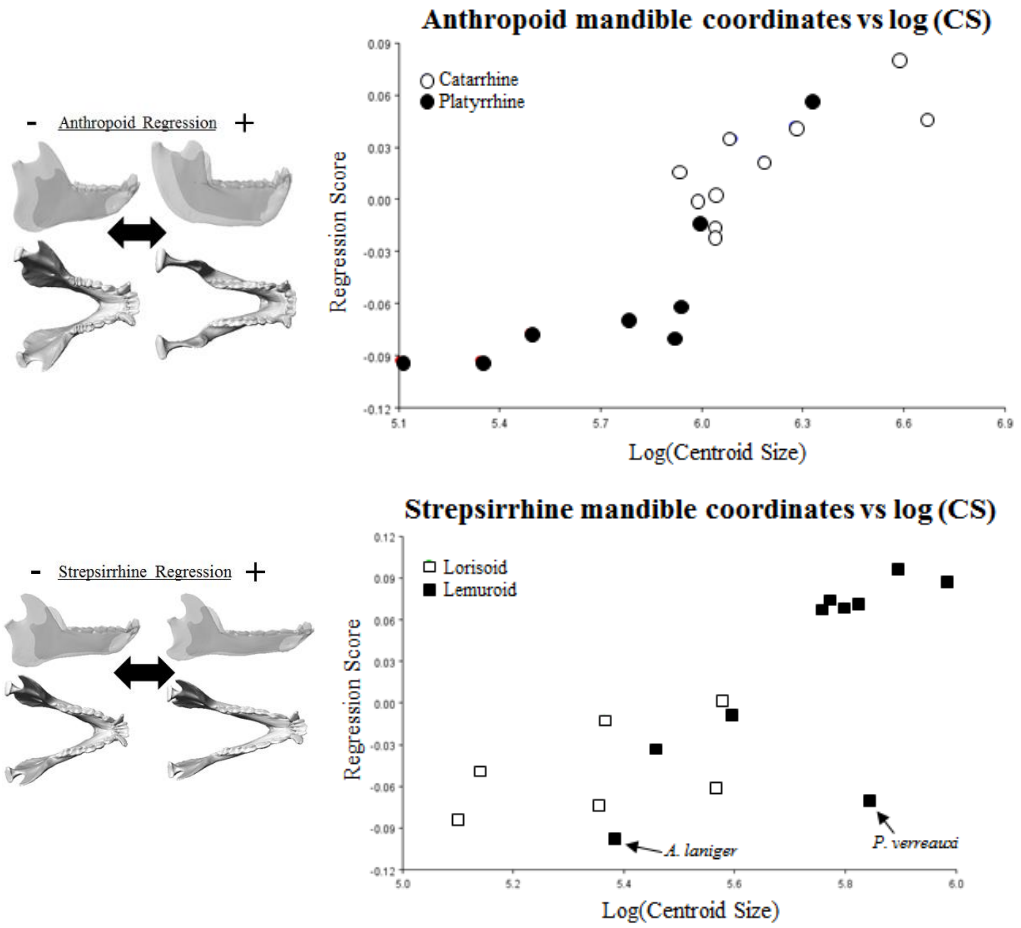


Figure 2.11: Multivariate regression of mandibular shape coordinates on log (centroid size) of the mandible for anthropoids (top) and strepsirrhines (bottom). Visualizations to the right depict the vector of shape change from negative (left) to positive (right).

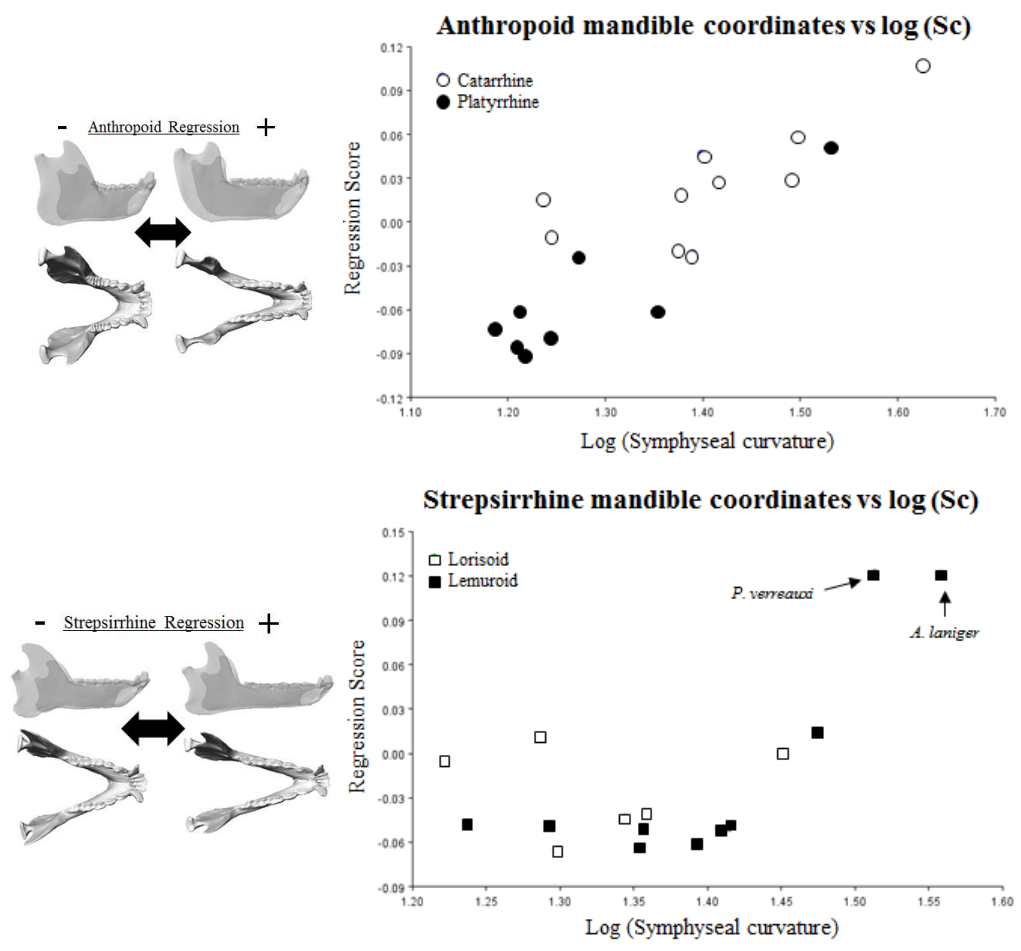


Figure 2.12: Multivariate regression of the mandibular shape coordinates on log(symphyseal curvature) for anthropoids (top) and strepsirrhines (bottom). Visualizations to the right depict vector of shape change from negative (left) to positive (right).

By visualizing shape differences between mean configurations of primates with similar mandibular lengths but differing in degree of symphyseal fusion allow for direct comparisons without confounding and different allometric effects. The clearly distinct allometric patterns in anthropoids and strepsirrhines complicate the removal of allometric effects across taxa. In each comparison, the species with complete or partial fusion possess relatively larger symphyseal regions compared to the species with no symphyseal fusion (Figure 2.13). In most of the anthropoid-strepsirrhine comparisons, the anthropoids have more vertically-oriented symphises (except for *Callithrix* and *Leontopithecus*) but maintain a labiolingually robust symphysis by the extension of a superior transverse torus (Figure 2.13a,b) or additional development of an inferior transverse torus (Figure 2.13c-e). Similarly, *Propithecus verreauxi* exhibits an inferolingual projection of the symphysis that could be described as an inferior transverse torus while maintaining a similar symphyseal orientation to *Lemur catta* (Figure 2.13f). Additionally, all primates with completely or partially fused symphises also have taller mandibular rami through both a deeper gonial region and increased height of the mandibular condyle, deeper corpora, and a wider mandibular arch compared to unfused strepsirrhines.

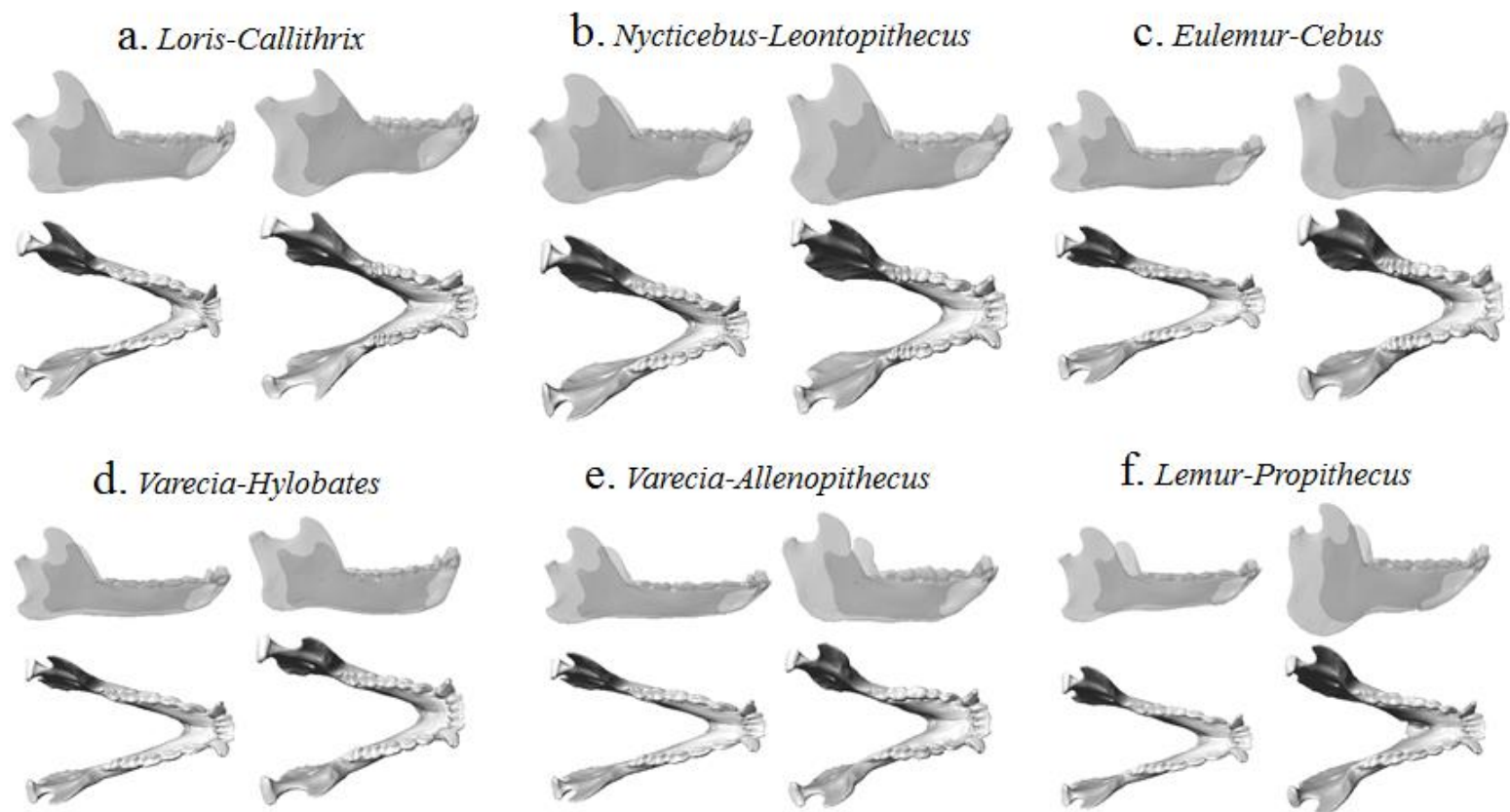


Figure 2.13. Visualization of differences between mean configurations of select species with and without symphyseal fusion by warping a three-dimensional model of *Pan troglodytes* using a thin plate spline deformation. Species were chosen that have similar mandibular centroid size to mitigate confounding allometric effects.

2.3.3 Inferring masticatory function in fossil primates

The plot of the first pair of axes for the F-PLS of the reduced landmark set and masticatory muscle activity patterns (Figure 2.14, Tables 2.9-10) is similar to the plot of the original F-PLS using the full mandible landmark configurations. F-PLS1 separates anthropoids and *Propithecus* from strepsirrhines with unfused symphyses. The EMG variables that load most heavily on this axis are the W/B ratios and peak timing of the posterior temporalis and deep masseter muscles which correlate primarily with a taller and thicker mandibular symphysis and a taller mandibular corpus (Figure 2.14). When the fossil specimens are projected onto this singular shape vector, each specimen plots either within the range or in close proximity to the distribution of primates with complete or partial fusion (Figure 2.14). *Apidium* plots farthest from the range of extant primates with complete or partial fusion but is still closer to this group than to primates with unfused symphyses.

The BGPCA calculated from the mean differences between primates with complete and partial fusion separates extant anthropoids from indriids, *Propithecus* and *Avahi* (Figure 2.15). When plotted on this axis, the subfossil lemurs *Babakotia*, *Mesopropithecus*, and *Megaladapis*, fall in the range of primates with partial fusion. The remaining fossil specimens (*Archaeolemur*, *Notharctus*, *Apidium*, *Simonsius*, *Catopithecus*, *Aegyptopithecus*, and *Epipliopithecus*) plot closer to anthropoids with complete fusion indicating mandibular shapes more similar to extant anthropoids than to indriids. The cases of *Archaeolemur* and *Notharctus* are interesting in that while more closely related to indriids, they plot closer to living anthropoids along this axis.

Since the initial F-PLS of primates with mandibular fusion identified differences between catarrhines and platyrrhines in their shape-function relationships, the fossil specimens were projected onto the shape singular vector constructed from an F-PLS using only anthropoids (Figure 2.16, Tables 2.11-12). Interestingly, only the specimen of *Aegyptopithecus* falls in the cercopithecoid range while *Catopithecus* and *Apidium* plot in the platyrrhine range. *Simonsius* and *Epipliopithecus* fall in the overlapping range between catarrhines and platyrrhines. When other extant species are projected onto this axis, there is an overlap with larger-bodied platyrrhines and colobines. Hominoids plot more closely with platyrrhines but also overlap with cercopithecoids.

In the scaling of symphyseal size to mandibular size, fossil specimens generally plot with anthropoids and indriids and have overall larger symphyseal sizes relative to mandibular size than unfused strepsirrhines (Figure 2.17). *Apidium* falls between the anthropoid and strepsirrhine distributions. When visualizing shape change between fossil specimens and unfused strepsirrhines, *Catopithecus* and *Apidium* both have more pronounced lingual projections of the superior transverse torus compared to *Perodicticus*, but still maintain anteriorly inclined symphyseal orientations (Figure 2.18a).

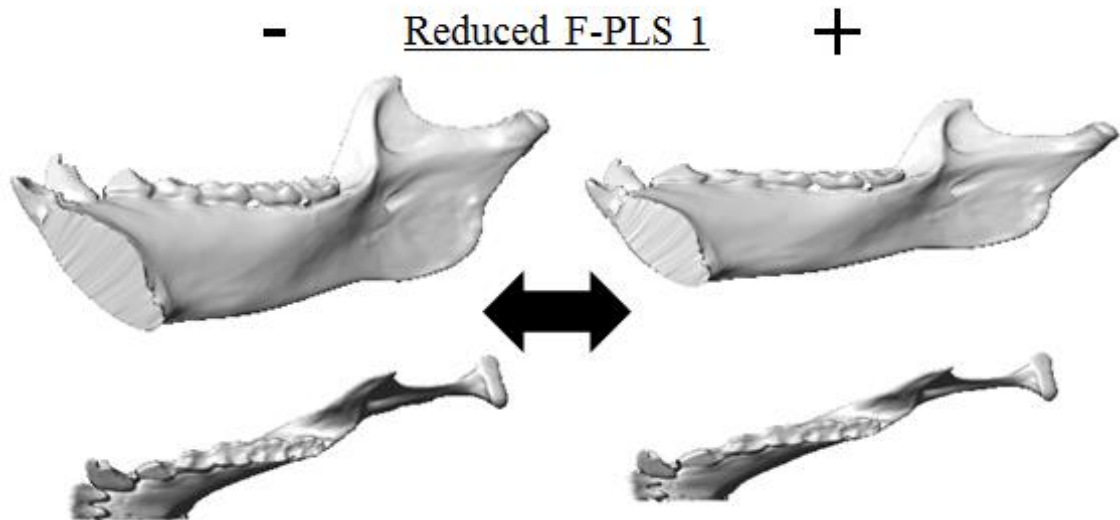
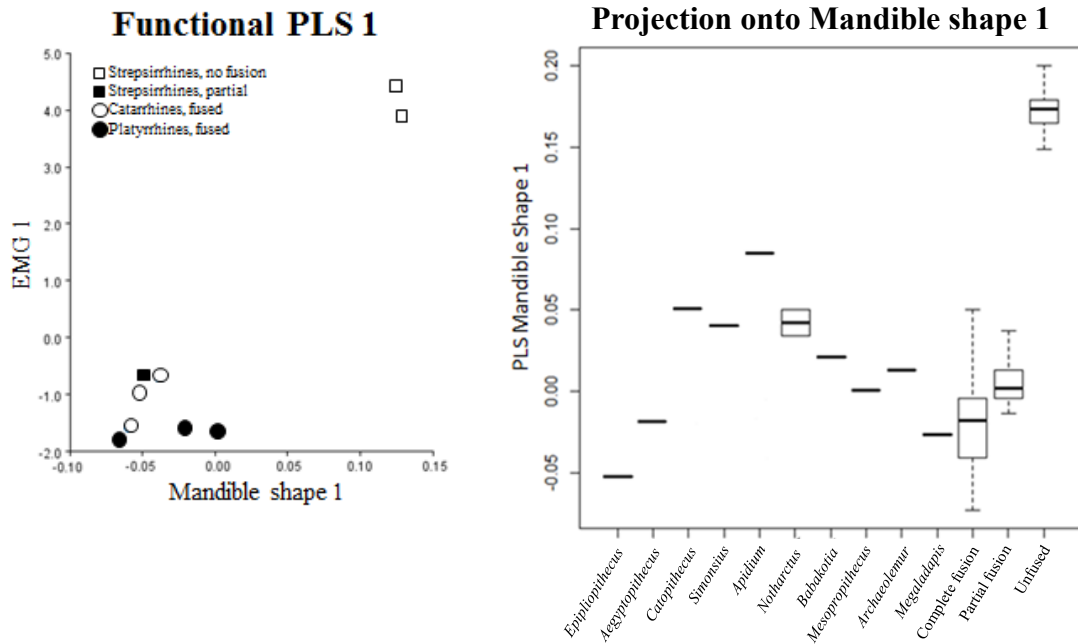


Figure 2.14: plot of the first pair of axes from the functional PLS including all taxa with EMG data using the reduced landmark set. A boxplot is included showing all extant and fossil specimens projected onto the first F-PLS axis. Visualization shows mandibular shape change along the first F-PLS shape axis.

Table 2.9: Loadings for the EMG variables from an F-PLS on all taxa with EMG data using the reduced landmark dataset. Variables with the largest loadings for each singular vector are identified with an asterisk.

<u>EMG variables</u>	<u>Data type</u>	<u>F-PLS 1</u>
Superficial masseter	W/B ratio	0.208
Deep masseter	W/B ratio	*0.403
Anterior temporalis	W/B ratio	0.314
Posterior temporalis	W/B ratio	*0.411
WS deep masseter	Peak muscle timing	0.027
BS superficial masseter	Peak muscle timing	0.173
BS deep masseter	Peak muscle timing	*0.401
WS anterior temporalis	Peak muscle timing	0.303
BS anterior temporalis	Peak muscle timing	0.169
WS posterior temporalis	Peak muscle timing	0.224
BS posterior temporalis	Peak muscle timing	*0.404

Table 2.10: Statistical results from an F-PLS on all taxa with EMG data using the reduced dataset.

	<u>F-PLS 1</u>
Singular value	0.181
p-value	0.018
correlation	0.949
% covariation	71.26%

Between-Group PCA: Complete Fusion vs. Partial Fusion

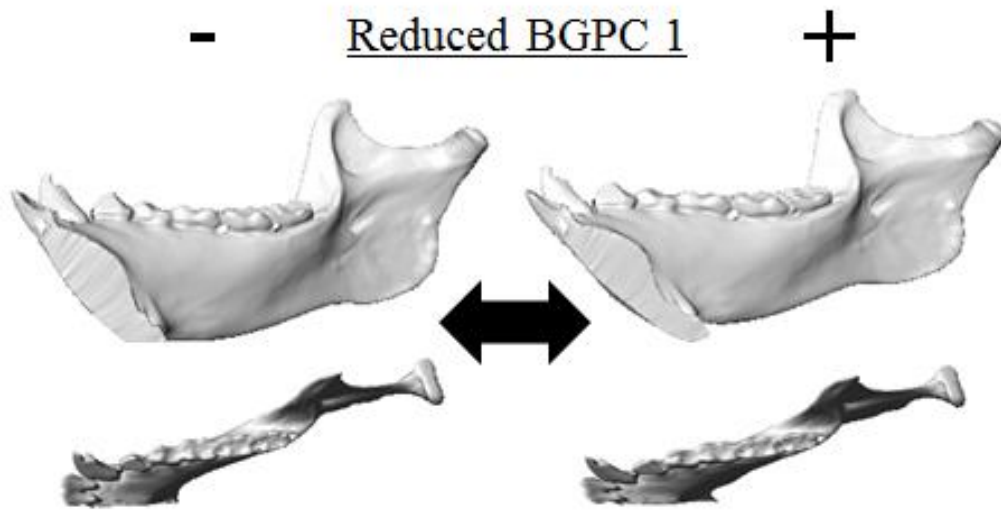
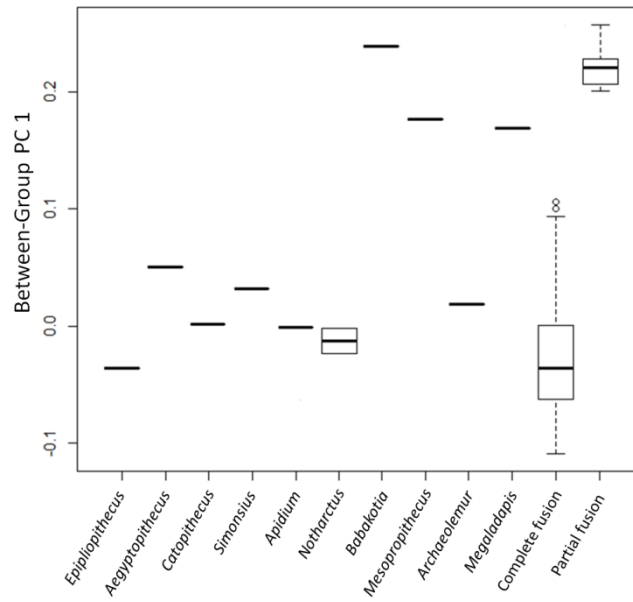


Figure 2.15: Fossil specimens projected onto the BGPCA eigenvector calculated from the difference between mean configurations of primates with complete and partial fusion.

Catopithecus also has a mandibular condyle that is higher above the occlusal surface of the dentition than in *Perodicticus*, but is less noticeable the elevated condyle in *Apidium*. The symphysis of *Simonsius* has a distinctly vertical orientation compared to *Otolemur* in addition to more robust dorsoventral and labiolingual dimensions (Figure 2.18b). The putative stem catarrhines, *Aegyptopithecus* and *Epipliopithecus*, both have overall robust and vertically oriented symphyses compared to *Varecia* (Figure 2.18c). *Aegyptopithecus* has a distinctly projecting superior transverse torus while *Epipliopithecus* has a sloping lingual surface and a labial surface that appears to project anteriorly. The subfossil lemurs *Babakotia* and *Mesopropithecus* resemble extant indriids in their symphyseal morphology by retaining an inclined orientation of the symphysis but elongating through the long axis (Figure 2.18c). The superior transverse torus is also thicker and an inferior lingual projection is present that could be described as an inferior transverse torus. These distinctions from *Varecia* result in an overall increase in surface area of the symphysis but also provide increased labiolingual thickness. Similar to the other extinct strepsirrhines in this sample, *Notharctus* retains an inclined orientation of the symphysis that is elongated compared to extant, unfused strepsirrhines (Figure 2.18c). The symphysis of *Notharctus* has a sloping lingual surface that terminates as a shelf with a short but steep drop to the inferior margin.

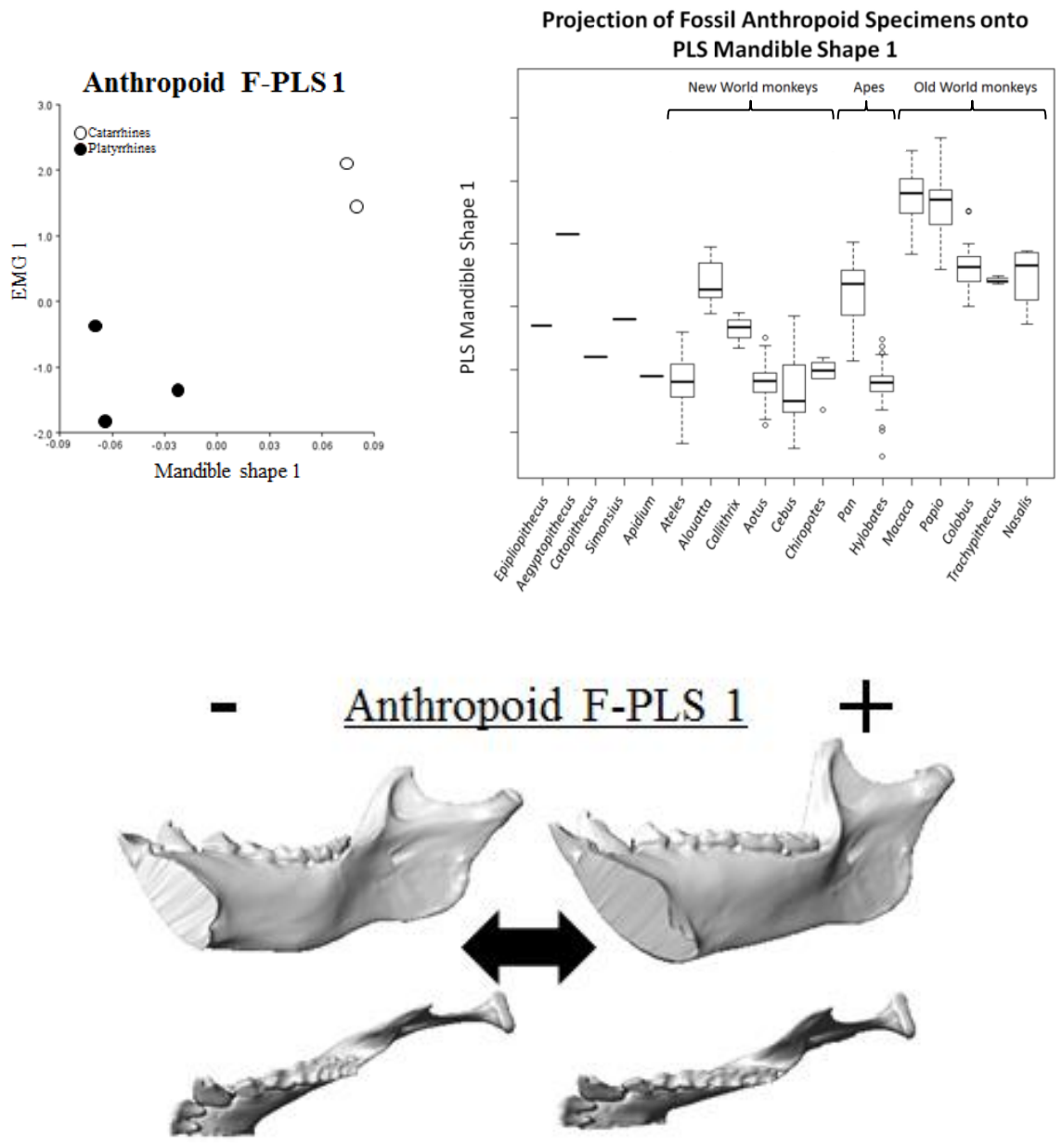


Figure 2.16: Plot of the first pair of axes of the F-PLS on the reduced landmark set including only anthropoid taxa. The boxplot shows the projection of all extant and fossil anthropoid specimens onto the first shape axis. Visualization shows mandibular shape change along the first F-PLS shape axis.

Table 2.11: Loadings for the EMG variables from an F-PLS on all anthropoid taxa with EMG data using the reduced landmark dataset. Variables with the largest loadings for each singular vector are identified with an asterisk.

<u>EMG variables</u>	<u>Data type</u>	<u>F-PLS 1</u>
Superficial masseter	W/B ratio	0.105
Deep masseter	W/B ratio	-0.066
Anterior temporalis	W/B ratio	-0.018
Posterior temporalis	W/B ratio	-0.11
WS deep masseter	Peak muscle timing	*0.648
BS superficial masseter	Peak muscle timing	*0.562
BS deep masseter	Peak muscle timing	0.066
WS anterior temporalis	Peak muscle timing	0.072
BS anterior temporalis	Peak muscle timing	*0.416
WS posterior temporalis	Peak muscle timing	-0.149
BS posterior temporalis	Peak muscle timing	0.178

Table 2.12: Statistical results from an F-PLS on anthropoid taxa with EMG data using the reduced dataset.

	<u>F-PLS 1</u>
Singular value	0.284
p-value	0.474
correlation	0.887
% covariation	81.48%

2.4 DISCUSSION

2.4.1 EMG patterns and mandibular shape

The results from the initial F-PLS analysis using the full landmark set identify new shape-function relationships and support some but not all observations from previous studies. The first pair of F-PLS axes identified a shape vector associated with the wishboning motor pattern. Delayed activity of the balancing-side deep masseter and posterior temporalis muscles are identified and correlated with a taller mandibular ramus, deeper corpus, and taller, thicker symphysis. Specifically, the labiolingually thicker mandibular symphysis and taller mandibular ramus verify previous hypotheses regarding the mandibular shapes associated with the wishboning motor pattern and loading regimes (Hylander, 1979a,b). A labiolingually thicker symphysis efficiently counters increased wishboning stress generated by the lateral pulling of the balancing-side mandible by the delayed activity of the balancing-side deep masseter, and potentially posterior temporalis muscle (Ravosa and Hogue, 2004). Ravosa et al., (2000) also postulated that a taller mandibular ramus is a key component associated with the wishboning motor pattern by affecting the orientation of the deep masseter muscles, requiring a delay in their activity in the chew cycle. Additionally, the deeper corpus and taller symphysis indicate a configuration better able to resist parasagittal bending and dorsoventral shear stress, respectively. These shape changes, in addition to increased recruitment of balancing-side adductor muscle force (through the posterior temporalis, and possibly balancing-side deep masseter), suggest that loading regimes reflecting increased recruitment of both vertical and transverse balancing-side muscle force are accounted for on the first pair of

axes. Ravosa and colleagues have previously acknowledged the importance of both dorsoventral shear and wishboning stress in the evolution of symphyseal fusion in anthropoids but only dorsoventral shear for indriids (Ravosa, 1999; Ravosa and Hogue, 2004). In contrast, the results presented here suggest that higher magnitudes of both stresses are experienced by anthropoids and indriids in comparison to other strepsirrhines with unfused symphyses.

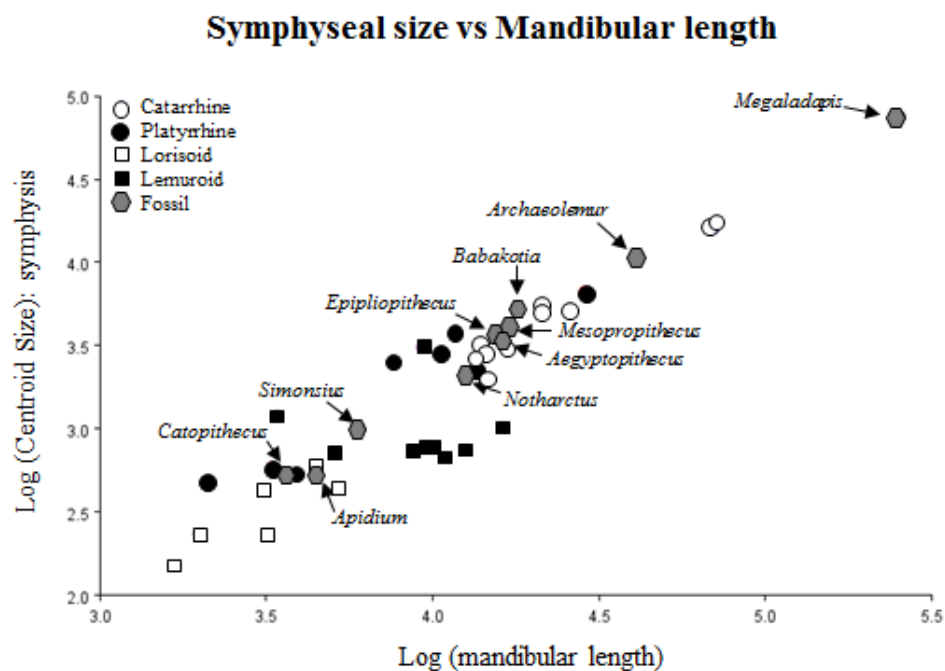


Figure 2.17: Plot of the log (centroid size) of the mandibular symphysis to log(mandibular length) including all extant species and fossil specimens.

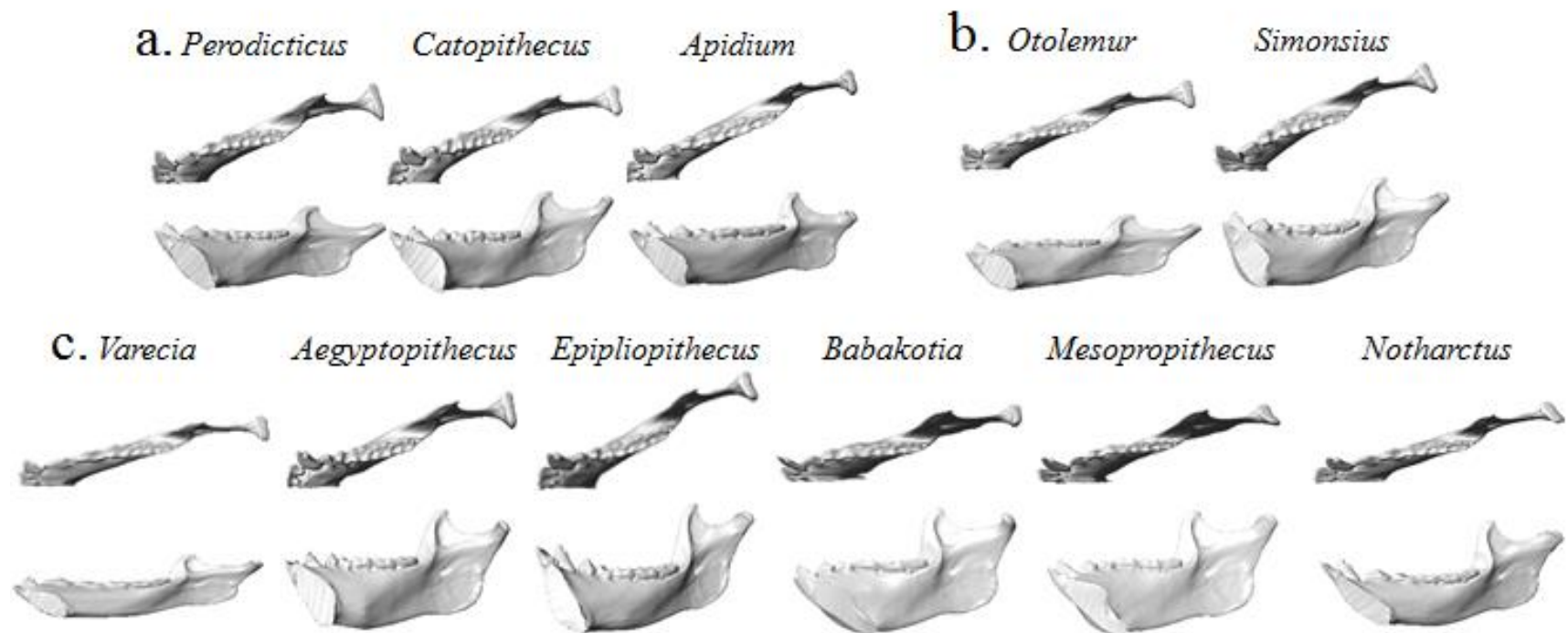


Figure 2.18: Visualization of select specimen landmark configurations that by warping a three-dimensional model of *Pan troglodytes* using a thin plate spline deformation. Each set of comparisons includes fossil specimens and the mean configuration of a strepsirrhine species with no symphyseal fusion and similar mandibular length.

It has been proposed that anthropoids exhibit increased wishboning and dorsoventral shear stress at the symphysis compared to strepsirrhines with no fusion, whereas indriids only generate greater amounts of dorsoventral shear stress (Ravosa, 1999; Ravosa and Hogue, 2004). However, the results presented here indicate that at least one indriid, *Propithecus*, exhibits masticatory patterns consistent with increased recruitment of both vertically and transversely oriented balancing-side muscle force during mastication and shape patterns consistent with resisting wishboning and dorsoventral shear stresses generated from these loading regimes (Hylander et al., 2011). This undermines the notion that fusion in anthropoids is substantively different from that found in all other primates.

Analyzing shape-function relationships in a phylogenetic context provides the opportunity to find patterns of mandibular shape and masticatory activity that are not contingent on the evolutionary history of the species studied. The first pair of axes from the P-PLS shows a separation of primates with and without symphyseal fusion (similar to the F-PLS), but *Papio* plots among unfused strepsirrhines. Even though the plot from the P-PLS generally resembles that of the F-PLS, the shape-function relationships borne out along the pairs of axes are different. The relationships between masticatory activity patterns and mandibular shape from the P-PLS are not as easily interpretable in the context of loading regimes associated with symphyseal fusion. The differences between these two analyses might suggest that aspects of mandibular shape and function related to symphyseal fusion evolved independently in indriids and early in anthropoid evolution so that these relationships are observed at higher taxonomic levels rather than along branches between subsequent nodes and tips.

Although the results from the P-PLS are difficult to interpret in relation to symphyseal fusion, they do provide an interesting insight into other aspects of masticatory shape and function. Closer inspection of the EMG variables shows that, in comparison to its nearest relative *Macaca*, *Papio* has working-side anterior and posterior temporalis muscles that reach peak activity earlier near the timing of the balancing-side superficial masseter. This additional working-side adductor activity may then account for the reduction in balancing-side superficial masseter recruitment that also loads highly on this axis. The correlated shape vector indicates a reduction in the size of the mandibular ramus which may correspond to a decreased reliance on masseter muscle force. The balancing-side deep masseter also weighs heavily on this axis. *Lemur* and *Otolemur* are known to have early peak activity of the balancing-side deep masseter compared to anthropoids and indriids, and the balancing-side deep masseter in *Papio* fires early compared to *Macaca*. Reduction in the height of the condyle above the occlusal surface of the dentition and overall ramus height (a pattern present in *Papio* in relation to *Macaca*) is correlated with early peak activity of the balancing-side deep masseter, thus providing further evidence for a link between increased condylar height, ramus height, and delayed activity of the balancing-side deep masseter muscle.

Among the anthropoids with EMG data, catarrhines and platyrrhines were found to have distinct relationships between mandibular shape and masticatory activity patterns. The working-side deep masseter muscle fires earlier in the chew cycle in catarrhines and correlates with a relatively longer mandible, less projecting gonial region, wider condyles, narrower mandibular arch, and the development of an inferior transverse torus. This relationship has multiple possible interpretations. An isolated working-side deep

masseter muscle firing early during the closing stroke would move the working-side of the jaw laterally during adduction. This could potentially cause lateral transverse bending at the symphysis due to the transverse orientation of the deep masseter muscle fibers and require additional buttressing support provided by the development of an inferior transverse torus. However, additional experimental work is needed to determine if the isolated working-side deep masseter muscle force generates significant stress at the symphysis at the beginning of the closing stroke since there does not appear to be a contralateral force on the balancing-side of the jaw. Even if the stress generated does not exceed the wishboning stress present at the end of the power stroke, additional buttressing could be necessary to prevent fatigue from repetitive loading (Hylander, 1979). Further work investigating these possible differences in underlying mechanisms for increased wishboning stress has the potential for indicating independent evolution of symphyseal fusion in catarrhines and platyrrhines; however, the current results are too preliminary to speculate. Additionally, more experimental data for larger platyrrhines and smaller catarrhines are needed to clarify whether these patterns reflect phylogeny or allometric effects of masticatory function.

Even though modern humans demonstrate shape-function patterns characteristic of primates with fused symphyses, they also exhibit relationships that are not shared with any other species. Humans manifest a mandible with a shorter ramus and corpus, shorter symphysis, and much wider mandibular arch in conjunction with reduced recruitment of the balancing-side superficial masseter which also fires earlier in the chew cycle. The independent, early firing of the balancing-side superficial masseter muscle may not require significant recruitment if it is isolated (and presumably firing concurrently with

the balancing-side medial pterygoid muscle); however, this is an assumption that requires additional investigation. Additionally, a reduction in balancing-side recruitment may simply indicate that a diminished bite force is needed to chew food. With humans doing much of their food processing externally (e.g., through cooking) (Wrangham et al., 1999; Wrangham, 2009), it is likely that less muscle force and balancing-side recruitment is needed to break down food orally for ingestion. *Homo* also has delayed firing of the working-side posterior temporalis muscle compared to other primates so that its peak activity is more in line with triplet II. Lastly, the wide mandibular arch and vertical orientation of the symphysis suggests that, unlike other anthropoids, modern humans may not generate significant wishboning stress at the symphysis. Many of the gracile features of the human mandible and dentition are presumed to reflect a reduction in the reliance of the masticatory apparatus for processing tough foods over the course of human evolution (e.g., Chamberlain and Wood, 1985; Lieberman, 2011; Wood and Collard, 1999a,b), and perhaps consequently affect the activity of the masticatory muscles. The correlation between these specific functional and morphological changes is not easily interpretable but provides a basis for future investigation into the evolution of hominin masticatory form and function.

2.4.2 Strength vs. stiffness models for symphyseal fusion

The strength and stiffness models for symphyseal fusion provide different expectations for the comparison of symphyseal shape between primates with and without fusion. The strength model predicts that symphyseal fusion evolves to resist wishboning stress (and potentially increased dorsoventral shear stress) (Ravosa and Hogue, 2004),

and thus the shape and orientation of the symphysis are not required to change to provide additional buttressing. The stiffness model interprets symphyseal fusion as a means of transferring mediolateral force across the symphysis (Lieberman and Crompton, 2000). From this perspective, additional changes to symphyseal shape and orientation are needed to resist the increased wishboning stresses generated as a result of stiffening the joint and transferring greater mediolaterally-directed forces. The results from this analysis indicate that extant primates exhibiting either complete or partial symphyseal fusion also possess symphyseal morphologies or orientations that are better suited to resist wishboning stress than their unfused counterparts. The change in shape and orientation in addition to fusion provides morphological support for the stiffness model of symphyseal fusion.

Due to the negative allometric relationship between cranial size and adductor cross-sectional area (Cachel, 1984), larger primates are expected to recruit greater balancing-side vertical adductor muscle force to maintain a similar bite force on the working-side of the jaw, resulting in greater dorsoventral shear stress at the symphysis and parasagittal bending of the corpus (Hylander, 1984). Therefore, larger primates are predicted to have a relatively larger cross-sectional area of the symphysis and deeper corpora compared to smaller primates. These shape-function relationships are expected to be observed across both anthropoid and strepsirrhine taxa since Dessem (1985) argued that unfused symphyses transfer vertically oriented muscle force across the symphysis as well as fused symphyses. Additionally, EMG studies have shown that the larger-sized *Lemur catta* recruits greater amounts of balancing-side adductor muscle force than the smaller *Otolemur crassicaudatus* (Hylander, 1977; 1979a; Vinyard et al., 2006).

These hypotheses find varying degrees of support from the results in this analysis. While an increase in overall mandibular size in anthropoids is associated with a more vertically oriented symphysis, the relative size of the symphysis does not appear to change noticeably. In unfused strepsirrhines, both the relative size of the symphysis and the corpus depth decrease as overall mandibular size increases, suggesting a reduced ability to resist larger dorsoventral shear and parasagittal bending stresses, respectively (cf., Ravosa, 1991). Further analysis and experimental data for other strepsirrhine taxa are needed to explain the incongruence of experimental and morphological evidence. Although the physiological cross-sectional area of jaw adductor muscles scales negatively with size, there does not appear to be an allometric relationship with mandibular size and ability to resist increased dorsoventral shear stress either within anthropoids or strepsirrhines (see Hylander et al., 2000; 2003). It is possible that other factors are affecting mandibular shape so that it is not solely reflecting the ability to resist the hypothesized loading regimes or that other aspects of the masticatory apparatus are scaling differently to achieve a functionally equivalent bite force for different sizes (e.g., Kay, 1975; Ravosa and Hogue, 2004).

As a curved beam structure, the mandible should experience greater wishboning stress as the curvature of the symphyseal region increases, provided the symphysis can transfer mediolaterally oriented forces across the symphysis (Hylander, 1984; 1985). Therefore, as the mandibular arch becomes relatively narrower, symphyseal region is expected to provide better buttressing against wishboning through either a thicker labiolingual dimension or an anteriorly inclined orientation (Hylander, 1984; 1985; Vinyard and Ravosa, 1998). This effect was expected to be present in only primates with

completely or partially fused symphyses, which was supported by this analysis. Any force generated in the transverse plane is expected to dissipate in the ligaments of an unfused symphysis, particularly if it does not have transversely oriented ligaments (Herring and Mucci, 1991, Lieberman and Crompton, 2000). That the predicted relationship between symphyseal curvature and symphyseal shape was found only in primates with complete or partial fusion also suggests that ossification of the joint serves, at least in part, to stiffen the symphysis for the transfer of mediolaterally directed forces.

Taken together, these results do not suggest that fusion does not also contribute to the strengthening of the symphysis to some degree, but rather highlights the requirement of stiffening the articulation between the hemimandibles for the transfer of muscle force. In this regard, mandibular symphyseal fusion, with the wishboning motor pattern, acts as an adaptation to create a transverse chewing motion rather than arising as a response to masticatory stresses generated at the symphysis.

2.4.3 Partial vs complete symphyseal fusion

The question still remains as to why some primates completely fuse their symphyses and others develop only partial fusion. If fusion functions to strengthen the symphysis against stresses at the symphysis, indriids and anthropoids appear to have found different ways to counteract similar stress patterns that may reflect possible adaptive pathways limited by phylogenetic inertia. Indriids have partially fused mandibular symphyses rather than complete fusion, which likely reflect symphyseal orientations. Since the symphysis is anteriorly inclined in strepsirrhines (Figure 1.4), thought to be a consequence of having a tooth comb, its long axis is better oriented to

resist wishboning stress. Rather than completely fusing the symphysis, indriids have instead, elongated the long axis of the symphysis compared to other strepsirrhines. In this case, partial fusion could be interpreted to best resist dorsoventral shear rather than wishboning. This is supported by previous observations that the ossified tissues at the symphysis are oriented in the dorsoventral plane (Beecher, 1977). Additionally, the anteroinferior aspect of the symphysis fuses first and the lingual aspect fuses last (Beecher, 1977), which has been used to suggest that a partially fused symphysis would not efficiently resist wishboning.

The explanation of partial fusion has been a weakness for the stiffness model for symphyseal fusion. Ravosa and Hogue (2004) argue that partial fusion is not suited to resist or transfer mediolaterally oriented muscle forces because of the labiolingual direction of fusion. However, indriids may not require complete ossification of the joint to adequately transfer mediolateral force across the symphysis. The anteriorly inclined symphyses of indriids orient the labial portion of the symphysis in a more horizontal plane. Additionally, Beecher (1977) demonstrated that, unlike strepsirrhines with no fusion, *Propithecus verreauxi* has transverse symphyseal ligaments located at the lingual aspect of the symphysis. These transverse ligaments, in addition to ossification of the labial aspect and orientation of the symphysis, may provide sufficient stiffness for the transfer of mediolateral muscle force during mastication.

2.4.4 Masticatory function and symphyseal fusion in fossil primates

All the fossil primates included in this study exhibit either partial or complete symphyseal fusion. When projected onto the F-PLS shape axis that delineates shape variations associated with EMG data, each fossil specimen plots closer to primates with

fused symphyses; however, not all are located within the range of extant primates (Figure 2.14). This is not surprising considering some of the extinct taxa may represent transitional periods in the evolution of symphyseal fusion or convergent morphologies derived from different underlying mechanisms. Therefore, direct comparisons of mandibular shape between these fossil specimens and extant primates can provide greater insight into the evolution of symphyseal fusion rather than only analyzing suites of features that are different between groups of extant primates.

Hylander et al., (2011) demonstrated that *Propithecus verreauxi* (and presumably all other indriids) have masticatory activity patterns convergent with anthropoids associated with increased transverse movement of the mandible. The results presented here support this observation by linking the wishboning motor pattern with a mandibular structure characteristic of generating and resisting significant wishboning stress. Further, this study suggests that *Babakotia*, *Mesopropithecus*, *Archaeolemur*, and *Megaladapis* exhibit similar masticatory patterns to indriids compared to other strepsirrhines. When mandibular morphology is compared between primates with complete and partial fusion, the subfossil lemurs more closely resemble indriids rather than anthropoids, except for *Archaeolemur*. Even though larger in overall size, *Babakotia* and *Mesopropithecus* resemble *Propithecus verreauxi* in symphyseal and overall mandibular shape which likely reflects similarities and masticatory function as well as a close phylogenetic relationship. Both subfossil lemur taxa have partially fused symphyses with an anteriorly inclined orientation and elongation through the long axis. *Mesopropithecus* possesses a more labially-projecting superior transverse torus than *Babakotia*. Both taxa also have taller corpora and mandibular condyles located higher above the occlusal surface of the

dentition compared to other unfused strepsirrhines. Additionally, *Mesopropithecus* and *Babakotia* are believed to have more mechanically demanding diets, similar to *Propithecus* (Godfrey et al., 1997; 2004; Muchlinski et al., 2011; Rafferty et al., 2002).

Archaeolemur and *Megaladapis* are unique in having evolved complete symphyseal fusion. In comparison to *Propithecus*, *Archaeolemur* has a symphysis that maintains a similar orientation but it not as elongated. However, the symphysis is labiolingually thicker and the corpus is buccolingually thicker in *Archaeolemur*. The more robust mandibular dimensions of *Archaeolemur* are likely an adaptation to resist different loading regimes possibly related to an omnivorous diet consisting of fruit and hard objects (Godfrey et al., 1997; 2004; 2005; Rafferty et al., 2002; Scott et al., 2009). The increased robusticity and/or fusion of the symphysis and buccolingual thickness of the corpus might reflect a greater occurrence of coronal bending in *Archaeolemur* which may be inferred from a less inverted inferior ramus compared to *Propithecus*.

Megaladapis has a unique symphyseal morphology compared to *Propithecus*, with a labial surface that appears to be concave with a projecting superior transverse torus inferiorly located on the lingual surface (to some degree resembling *Alouatta*).

Additionally, the corpus is shorter but buccolingually thicker with a mandibular condyle higher above the occlusal surface of the dentition. The morphology of *Megaladapis* reflects a decreased ability to resist vertically oriented forces but increased ability to counter mediolaterally oriented forces, possibly a consequence of allometric properties or a highly folivorous diet.

All other extinct primate specimens – *Notharctus*, *Apidium*, *Simonsius*, *Catopithecus*, *Aegyptopithecus*, and *Epipliopithecus* – more closely resemble extant

anthropoids in their mandibular morphology when compared to *Propithecus* and other subfossil lemurs. *Notharctus*, an adapoid primate from the Eocene, was previously argued to have evolved complete symphyseal fusion to resist increased dorsoventral shear stress (Ravosa, 1996). This inference was based on the assumption that the wishboning motor pattern and increased wishboning stress was characteristic of primates that have early ontogenetic fusion (i.e., crown anthropoids). *Notharctus* was predicted to have late ontogenetic fusion based on the ontogenetic timing of fusion of other adapiforms, primarily *Leptadapis magnus* and *Adapis parisiensis* (Ravosa, 1996). It has since been demonstrated that primates with partial and late ontogenetic fusion do possess the wishboning motor pattern (Hylander et al., 2011), and presumably wishboning loading regime (supported by the results in this analysis), which nullifies the previous assumptions made for *Notharctus*. Based on this analysis, *Notharctus* possesses a mandibular shape that is suited to better resist both increased dorsoventral shear and wishboning stress. Additionally, *Notharctus* has a mandibular condyle located higher above the occlusal surface of the dentition which has been associated with the wishboning motor pattern. Comparisons of diet and mandibular morphology with other adapoids and omomyoids suggests that fusion is related to allometric constraints on muscle force production and unrelated to dietary adaptations (Ravosa, 1996).

Similar arguments can be made for most of the fossil anthropoids included in this analysis. *Simonsius*, *Catopithecus*, *Aegyptopithecus*, and *Epipliopithecus* all possess symphyseal shapes that suggest they were better equipped to resist both increased dorsoventral shear and wishboning stress at the symphysis, have deeper corpora, and taller mandibular condyles. Similar to *Notharctus*, *Simonsius* was previously assumed to

have evolved complete symphyseal fusion to resist increased dorsoventral shear stress based on the ontogenetic timing of fusion (Ravosa, 1999). However, the juvenile specimen that this observation is based on is tentatively attributed to this taxon based on only the size of the specimen. The other parapithecoid in this analysis, *Apidium*, exhibits complete symphyseal fusion but possesses a pattern of mandibular morphology that is intermediate between anthropoids and strepsirrhines which has been observed in previous work (Ravosa et al., 2000).

Catopithecus provides an interesting case in that it demonstrates similar external morphology to anthropoids but only exhibits partial fusion. Previous work has characterized *Catopithecus* as evolving partial fusion primarily as an adaptation to resist increased dorsoventral shear stress, similar to other primates with partial fusion, but not resist significant wishboning stress, thought to occur only in crown anthropoids (Ravosa, 1999). This interpretation was the basis for placing *Catopithecus* as a stem anthropoid, outside of the crown anthropoid clade, and is contingent on the evolution of the wishboning motor pattern and increased wishboning stress during mastication prior to the divergence of platyrrhines and catarrhines (Ravosa, 1999). However, based on morphological comparisons of *Catopithecus*, this taxon was better equipped to resist increased dorsoventral shear and wishboning stress at the symphysis compared to similar sized, unfused strepsirrhines. Additionally the mandibular condyle is higher above the occlusal surface of the dentition, and therefore, may have had the wishboning motor pattern. Unlike indriids with partial fusion, *Catopithecus* has a more vertical symphyseal orientation that is similar to other anthropoids and has a symphyseal shape that is more comparable to *Callithrix* with a superior transverse torus that projects lingually and drops

vertically without an inferior transverse torus. The combination of anthropoid-like morphology and partial fusion makes this taxon unlike any extant primate and difficult to interpret in regard to masticatory function. If fusion occurs to primarily stiffen the symphysis to allow for efficient transfer of balancing-side muscle force, partial fusion may have been sufficient in *Catopithecus* and may represent a transitional form leading to increased reliance on recruiting transversely oriented muscle force from the balancing-side of the jaw during mastication. Additionally, *Catopithecus* is believed to have been frugivorous and likely insectivorous (Kirk and Simons, 2001; Rasmussen and Simons, 1992; Simons and Rasmussen, 1996), to which partial fusion could represent increased balancing-side muscle recruitment for a greater reliance on fruit in the diet as opposed to insects.

The fossil anthropoid specimens were also projected onto the F-PLS axis separating catarrhines and platyrrhines. Although the overall relationship tested was not found to be significant, possibly as a result of sample size, some interesting patterns emerged among individual fossil taxa. Of the fossil anthropoids included in this analysis, only *Aegyptopithecus* falls in the catarrhine range while the others plot closer to platyrrhines, including stem catarrhine *Epipliopithecus*. Although caution is needed in the interpretation of this result, the similarities between these fossil and extant platyrrhine specimens suggest that the ancestral condition for crown anthropoids may have more closely resembled the platyrrhine masticatory muscle patterns. One expectation might be that the distinctions found here are related to body size; however, *Epipliopithecus* has a slightly larger mandibular size compared to *Aegyptopithecus*, but nevertheless more closely resembles platyrrhines, suggesting body size may not be a significant factor.

2.5 CONCLUSIONS

The results from this study provide support for many previous studies differentiating between the mandibular shape of strepsirrhines and anthropoids; however, additional insights are provided for extant and extinct taxa. This work is novel for providing direct relationships between masticatory activity and mandibular shape, rather than interpreting function solely through shape, and then making inferences about fossil primates based on these relationships. Furthermore, shape-function patterns were identified that differentiate catarrhines from platyrrhines as well as modern humans from other primates that require additional investigation.

It is likely that all of the fossil primates in this study exhibited the wishboning motor pattern that evolved convergently for anthropoids and indriids. Nevertheless, *Apidium* appears to have an intermediate mandibular morphology when comparing anthropoids to strepsirrhines, which has similarly been noted for the dentition of *Apidium* (Ravosa et al., 2000). The corpus and symphyseal morphology of *Catopithecus* suggests that it was capable of resisting greater masticatory stresses than strepsirrhines with no symphyseal fusion and similar to small-bodied platyrrhines, even though it retains only a partially fused symphysis. Partial fusion in *Catopithecus*, in conjunction with a shorter and vertically-oriented symphysis, might suggest that transverse movement during mastication was less important compared to extant anthropoids and likely indicates a transitional morphology towards greater reliance on transverse mandibular movement.

Lastly, the morphological evidence presented here supports the model that symphyseal fusion in primates evolves to stiffen the symphyseal joint between the left and right hemimandibles. Additional changes to symphyseal shape occur with both

partial and complete ossification of the symphysis that would efficiently resist increased dorsoventral shear and wishboning stress. Stiffening the symphyseal region allows for greater transfer of balancing-side muscle force during mastication and increases the stress generated at the symphysis (particularly wishboning) that is not present in unfused strepsirrhines. Nevertheless, the functionality of symphyseal fusion to stiffen the mandible does not mean that ossification of the joint does not enhance the strength in any way. It is likely that fusion increases both the stiffness and strength of the symphysis, but more efficient transfer of force generates new stresses that are otherwise dissipated in the ligaments of unfused symphyses.

3 Mandibular symphyseal fusion and the wishboning motor pattern

In the previous chapter, morphometric and EMG data were analyzed conjointly to make direct links between mandibular shape and masticatory function. The timing of muscle firing patterns and recruitment of balancing-side muscle force quantified through EMG analyses are associated with different masticatory loading regimes. Particularly, the recruitment of a delayed and unopposed balancing-side deep masseter muscle is associated with mediolateral movement of the mandible that generates a wishboning loading regime at the symphysis. Additionally, dorsoventral shear of the symphysis is associated with greater recruitment of balancing-side adductor muscle force in the vertical plane. Consequently, the shape of the mandible is expected to change in predictable ways in response to the loading regimes if those regimes generate significant stress. The results from the analyses presented in Chapter 2 indicate that both anthropoids and indriids experience the motor pattern associated with the wishboning loading regime, and exhibit mandibular morphology to counter significant wishboning stress. Greater recruitment of the balancing-side posterior temporalis muscle in conjunction with changes in corpus and symphyseal morphology indicate that greater magnitudes of dorsoventral shear stress are also likely present in anthropoids and indriids relative to unfused strepsirrhines.

Whether symphyseal fusion is interpreted as a means to either strengthen or stiffen the anterior jaw impacts how the evolution of the wishboning motor pattern (WMP) and fusion are viewed together. As will be discussed in the following chapter,

proponents of the strength hypothesis have proposed that symphyseal fusion in anthropoids is a response to a newly evolved loading regime (i.e., wishboning) brought about by correlated structural changes in the skull (Ravosa et al., 2000; Ravosa and Hogue, 2004). From this perspective, symphyseal fusion is not seen as an initial adaption on its own, but as a response to stresses generated from the WMP (Ravosa et al., 2000). Conversely, based on the stiffness hypothesis, symphyseal fusion and the WMP can be viewed as co-occurring adaptations for increased mediolateral force during unilateral mastication as the stiffness provided by fusion is needed for the WMP to function (Lieberman and Crompton, 2000). Whether increased mediolateral movement and muscle force is needed as an adaption to diet or to maintain functional equivalency as a consequence of other changes in skull morphology, symphyseal fusion is a requirement for the WMP to be successful.

In both models, the wishboning motor pattern plays a significant role in generating mediolaterally oriented muscle force during mastication resulting in greater magnitudes of wishboning stress and a corresponding change in symphyseal morphology (Lieberman and Crompton, 2000; Ravosa and Hogue, 2004). Therefore, it becomes necessary to understand the underlying mechanisms driving the evolution of the WMP to assess which hypothesis has more explanatory power. An alternative to viewing the WMP as an adaptation to changing dietary mechanical properties, it is possible that changes in overall skull morphology affect the functional equivalency of the masticatory apparatus. Ravosa et al., (2000) have proposed specifically that increasing the relative size of the neurocranium results in a sequence of skull changes that ultimately leads to the WMP. In primates, larger relative brain size correlates with increased facial kyphosis

(Ross and Ravosa, 1993), which is expected to displace the dentition inferiorly and increases ramus height. As a result, the masseter muscles are oriented more vertically and mediolateral movement of the mandible is maintained through delaying peak activity of the balancing-side deep masseter muscle (Ravosa et al., 2000). This hypothesis was initially proposed based on comparisons between anthropoids and strepsirrhines, but did not take into consideration the presence of the WMP in indriids (Ravosa et al., 2000; Ross and Ravosa, 1993). In the following chapter, the relationship between skull morphology and the WMP is evaluated across anthropoids and strepsirrhines (including indriids) to determine which aspects of skull morphology are likely associated with the evolution of the WMP and whether these shape-function relationships are shared across clades which have independently evolved the WMP.

4 Morphological integration of the skull and the evolution of symphyseal fusion

4.1 INTRODUCTION

4.1.1 Mandibular symphyseal fusion in primates

Mandibular symphyseal fusion is an anatomical phenomenon that has evolved multiple times over the course of primate evolution (e.g., Fleagle, 1999; Hartwig, 2002; Martin, 1990; Scott et al., 2012b; Szalay and Delson, 1979). Among extant primates, all anthropoid species (including all catarrhines and platyrrhines) have complete fusion of the mandibular symphysis, and a small assortment of strepsirrhine species (e.g., indriids) exhibit partial fusion in adult forms. Symphyseal fusion is argued by some researchers to have evolved as a mechanism to strengthen against stresses generated at the symphysis during mastication (Ravosa and Hogue, 2004; Ravosa and Hylander 1993; 1994) while others suggest that fusion occurs to stiffen the symphysis to more efficiently transfer balancing-side muscle force during unilateral mastication (Crompton et al., 2008; Greaves, 1988; 1993; Herring et al., 2008; Lieberman and Crompton, 2000; Scapino, 1981). However, it has been shown that the shape and orientation of the mandibular symphysis also contributes to the resistance of stresses occurring at the symphysis (see Chapter 2). Therefore, both symphyseal shape and orientation need to be considered in association with the degree of fusion when trying to understand masticatory activity and mandibular loading regimes.

Previous analyses on symphyseal fusion have often focused on the differences between fused anthropoids and unfused strepsirrhines, identifying the wishboning loading

regime and motor pattern in the former but not the latter group (e.g., Hylander, 1979a, 1984; Hylander and Johnson, 1994; Hylander et al., 2000; Ravosa et al., 2000; Vinyard et al., 2006). However, more recent work has inferred the wishboning motor pattern (WMP) in *Propithecus verreauxi* as well, based on muscle activity patterns (Hylander et al., 2011). This finding, in addition to evidence based on mandibular structure (see Chapter 2), suggests the production of wishboning stress at the symphysis occurs in this and perhaps other related taxa (i.e., indriids) with partial symphyseal fusion. Previously, indriids were hypothesized to generate larger magnitudes of dorsoventral shear compared to other strepsirrhines, but not anthropoid-like wishboning, based on their partially fused symphyses and more robust symphyseal and corpus dimensions (Ravosa, 1991; Ravosa and Hogue, 2004). Nevertheless, the partial fusion and mandibular morphology of indriids also supports the hypothesis that indriids were able to resist greater wishboning loads during unilateral mastication (see Chapter 2).

With current data suggesting that both partially fused strepsirrhines and anthropoids with complete fusion generate similar motor and muscle force patterns, the variation within strepsirrhines provides an interesting opportunity to understand the relationship between jaw shape, masticatory loading regimes, and ultimately symphyseal fusion. If mandibular symphyseal fusion is associated with generating increased wishboning stress (and likely also dorsoventral shear) by recruiting greater balancing-side muscle force during mastication, strepsirrhines and anthropoids seem to be finding different combinations of symphyseal shape and orientation to resist similar symphyseal stresses. The more vertically oriented mandibular symphysis in anthropoids necessitates a labiolingual thickening of the symphysis to resist increased wishboning stress (Hylander,

1984). Conversely, the anteriorly inclined symphysis of *Propithecus* – probably oriented as a function of having a tooth comb – is already better oriented to resist wishboning stress and has instead elongated the midline through its long axis (see Chapter 2). Often, previous analyses (e.g., Ravosa, 1991; 1996) have overlooked the importance of symphyseal orientation when simply comparing labiolingual and dorsoventral dimensions with regard to resisting symphyseal stress (see Section 1.2).

The relationship between jaw fusion and dietary mechanical properties in strepsirrhines has been used as evidence for different underlying mechanisms for symphyseal fusion in anthropoids and indriids (Scott et al., 2012b). It has been hypothesized that symphyseal fusion tracks differences in dietary mechanical properties in extant strepsirrhines but not anthropoids (or even extinct strepsirrhines such as adapoids) (Ravosa, 1996; 1999; Ravosa and Hogue, 2004; Scott et al., 2012b). Strepsirrhines that eat more mechanically resistant foods such as leaves, bamboo, or seeds are characterized by partial fusion with interlocking rugosities and calcified ligaments (Beecher, 1977; Scott et al., 2012b). Those that rely on foods that are easier to process, such as ripe fruit, exudates, and insects, have smoother symphyseal plates that are not fused (Scott et al., 2012a). Increased symphyseal fusion in strepsirrhines occurs with a greater recruitment of muscle force from the balancing-side jaw adductor muscles (Ravosa, 1991; 1996; Hylander et al., 2011). Anthropoids are different in that they have no reduction in symphyseal ossification given their diverse ecological and dietary preferences (Scott et al., 2012a,b), and researchers have questioned why symphyseal fusion still occurs in primates, such as callitrichids, that have less mechanically demanding diets (Ravosa and Hogue, 2004; Scott et al., 2012b). The retention of

symphyseal fusion across anthropoids suggests that either the wishboning motor pattern and fusion retain their importance as a functional adaptation during mastication even for less mechanically demanding diets, or that it is retained through some other mechanism such as developmental canalization (Lockwood, 2007).

Currently, the best supported hypothesis links mandibular symphyseal fusion to the WMP and a reliance on transverse jaw movement and muscle force during mastication as an evolutionary package (see Ravosa and Hogue, 2004). This is the case whether symphyseal fusion functions to strengthen or stiffen the symphysis (Lieberman and Crompton, 2000; Ravosa and Hogue, 2004). The WMP creates the transversely-oriented balancing-side muscle force that is transferred across the symphysis to move the working-side mandible medially and generates wishboning stress at the symphysis. Thus rather than focusing on symphyseal fusion, it is perhaps more prudent to focus on the underlying causes and adaptive significance of the WMP.

4.1.2 The relationship between the wishboning motor pattern and loading regime

One important consideration that needs further attention is the assumed relationship between the wishboning motor pattern and the wishboning loading regime. Experimental studies using strain gauge measurements provide the best way to measure bone strain and predict stresses exhibited by the mandible, compared to inferring strain and stress through shape (Herring et al., 2008; Hylander, 1977; 1979a; 1986; Hylander and Crompton, 1986; Hylander et al., 1998). However, these particular experimental data are difficult to measure and have only been collected for a small number of primate species (Hylander, 1977; 1979a; 1984; Hylander and Crompton, 1986; Hylander and

Johnson, 1989; 1993; 1997; Hylander et al., 1992; 1998). These studies have found that primates exhibiting significant wishboning strain and stress also demonstrate a motor pattern that corresponds with delayed activity of the balancing-side deep masseter muscle. As a result, a causal relationship has been inferred for these two functional observations which has led to this specific motor pattern being designated as the wishboning motor pattern. Additional experimental work has identified the WMP in other anthropoid taxa and been used as evidence for inferring the presence of the wishboning loading regime across anthropoids. However, even though WMP has been identified in *Propithecus* (Hylander et al., 2011), little attention has been given to the presence of a wishboning loading regime in this species.

4.1.3 Evolution of the wishboning motor pattern

Hylander and colleagues have identified the WMP in at least six anthropoid species using EMG analyses (Hylander et al., 2000; 2002; 2004; Ross and Hylander, 2000; Vinyard et al., 2007; 2008) and, due to the ubiquitous nature of complete symphyseal fusion across anthropoids, the WMP is assumed to be shared among all living anthropoids (Ravosa and Hogue, 2004). As mentioned previously, the WMP has also been observed in the strepsirrhine *Propithecus verreauxi* (Hylander et al., 2011) and is thought to be common among other indriids with partially fused mandibles but has not yet been demonstrated in unfused strepsirrhines. The WMP refers to the postponed and unopposed peak activity of the balancing-side deep masseter muscle during the chewing cycle (see Ravosa and Hogue, 2004). In primates with the WMP, the working-side superficial masseter, working-side medial pterygoid, and balancing-side temporalis

muscles (Triplet II) move the working-side of the jaw medially and upward so the upper and lower dentition are in maximum occlusion (Kay and Hiiemae, 1974; Hylander, 2006). Subsequently, the balancing-side deep masseter muscle fires in relative isolation (but in conjunction with the balancing-side posterior temporalis) which is thought to cause transverse movement of the jaw at the end of the power stroke and maintain tooth contact after maximum occlusion (Hylander and Johnson, 1994). Since the balancing-side deep masseter is not counteracted by other muscles on the same side, the opposing transverse forces generated by the muscle and tooth-tooth or tooth-food contact on the working-side would create significant wishboning stress at the symphysis (Hylander and Johnson, 1994).

In contrast, the balancing-side deep masseter muscle in unfused strepsirrhines peaks earlier in the power stroke, around the same time as Triplet I, in conjunction with the balancing-side medial pterygoid muscle (Ravosa and Hogue, 2004; Ross and Iriarte-Diaz, 2014). The joint activity of these muscles contracting at the same time is thought to adduct the balancing-side of the mandible with little transverse movement and does not result in mediolaterally oriented muscle force or higher magnitudes of wishboning stress (Ravosa and Hogue, 2004). Therefore, it has been argued that the observed wishboning stress at the symphysis late in the power stroke in anthropoids and indriids derives from an unopposed, late-acting balancing-side deep masseter muscle (e.g., Hylander and Johnson, 1994).

Studies investigating differences between anthropoids and strepsirrhines have associated structural changes in skull to the evolution of the WMP, as the WMP was initially thought to be unique to anthropoids (Ravosa et al., 2000). Multiple previous

works have identified greater integration of the orbits and anterior cranial base in anthropoids compared to strepsirrhines (Dabelow, 1929; McCarthy and Lieberman, 2001; Ross and Ravosa, 1993) which results from a greater approximation of the orbits toward the midline where the orbital roof forms much of the floor anterior cranial fossa (Cartmill, 1970; 1972; Dabelow, 1929). The configuration of the orbits within anthropoids has led to a structural integration of neurocranium, face, and basicranium such that an increase in relative brain size flexes the basicranium while concurrently rotating the face downward (Ross and Henneberg, 1995; Ross and Ravosa, 1993; Spoor, 1997). This relationship is not present in strepsirrhines due to the lateral position of the orbits (Ross and Ravosa, 1993). The theoretical basis for this work was explicitly developed as the spatial-packing hypothesis by Biegert (1957; 1963) but was expanded upon and tested by other researchers (Bastir et al., 2010; DuBrul and Laskin, 1961; Enlow, 1990; Gould, 1977; Lieberman et al., 2000; 2008; McCarthy, 2001; McCarthy and Lieberman, 2001; Moss, 1958; Ross and Henneberg, 1995; Ross and Ravosa, 1993; Spoor, 1997; Strait, 1999; 2001; Vogel 1964). In his influential papers, Biegert (1957; 1963) proposed that neocortical volume and the size of the masticatory apparatus have opposite effects on flexion of the basicranium: increasing the relative size of the neurocranium increases basicranial flexion while increasing masticatory size reduces basicranial flexion. Biegert (1957; 1963) also predicted that, as a consequence of body size alone, smaller animals should have more flexed basicrania than larger animals since the masticatory apparatus scales with positive allometry and the neocortex scales with negative allometry.

Ravosa et al. (2000) evoked these ideas of skull integration to hypothesize that relative brain size, basicranial flexion, and facial kyphosis initiate a cascade of structural and functional changes that ultimately result in mandibular symphyseal fusion in anthropoids. In a separate analysis of primarily mandibular components, Ravosa et al. (2000) interpreted an increased height of the temporomandibular joint above the occlusal surface of the dentition in anthropoids as a consequence of the downward rotation of the face (e.g., Ross and Henneberg, 1995; Ross and Ravosa, 1993). A higher temporomandibular joint deepens the mandibular ramus which in turn results in more vertically oriented masseter muscles, as the masseter muscles originate on the zygomatic processes and insert onto the external ramus and gonial angle of the mandible (Figure 4.1). A vertical orientation of the masseter muscle reduces its contribution to the transverse movements of the jaw during mastication. Thus, increasing or maintaining adequate levels of transverse jaw movements during mastication delays the balancing-side deep masseter muscle activity in anthropoids compared to strepsirrhines (Ravosa et al., 2000).

Ravosa et al's., (2000) hypothesis contradicts some of Biegert's (1957; 1963) initial assertions in the spatial-packing hypothesis. Biegert (1957; 1963) does not provide specific criteria defining "increased size of the masticatory apparatus", but increasing the depth of the mandibular ramus would be one way to do this provided there is not a corresponding significant reduction in mandibular length as well. However, Ravosa et al., (2000) attribute increased ramus height ultimately to greater brain size and basicranial flexion, which is the opposite relationship proposed by Biegert's (1957; 1963) spatial-packing hypothesis. Nevertheless, Biegert (1957; 1963) highlighted the importance of

increasing the jaw joint height above the occlusal surface for masticatory adaptations, and described this configuration as the “universally specialized type” in comparison to the “generalized form.” He proposed that the “universally specialized type” can be achieved by either rotating the face upward (i.e., airorhynchy), displacing the palate and nasal chamber inferiorly from the mandibular condyle, or through palatal vaulting to inferiorly displace occlusal surface from the palate and mandibular condyle. The emphasis of Ravosa et al (2000) on facial kyphosis assumes that rotating the face downward heightens the face by displacing the occlusal surface below the jaw joint, but it is not clear whether these two morphological changes are related, and if so, do they follow the mechanisms described by Biegert (1957; 1963). The uncertainties underlying the structural relationships of these skull components highlight the necessity for further investigation into the evolution and integration of these features.

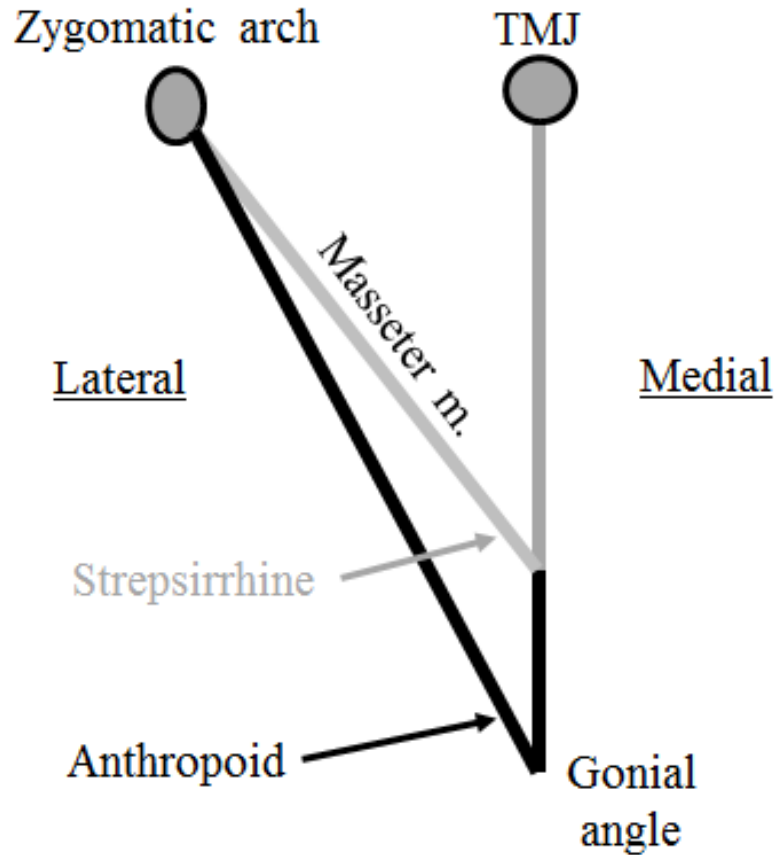


Figure 4.1: Diagram of the differences in structural configuration of the temporomandibular joint (TMJ), gonial angle, and zygomatic arches between anthropoids and strepsirrhines (modified from Ravosa et al., 2000). The line between the zygomatic arch and gonial angle represents the masseter muscle. The distance between the zygomatic arch and TMJ does not differ between anthropoids and strepsirrhines, so a deeper gonial angle in anthropoids results in a more vertical masseter muscle.

Insight from the fossil record already provides some evidence to doubt previous hypotheses regarding the underlying factors driving the evolution of the WMP and symphyseal fusion. Ravosa et al.'s (2000) model identifies increased encephalization in early anthropoid lineages as one of the instigating factors leading to symphyseal fusion. Nevertheless, fossil specimens of early stem catarrhines and platyrrhines (e.g., *Aegyptopithecus*, *Chilecebus*, and *Homunculus*) have relatively small, strepsirrhine-like

brain sizes which suggest that greater encephalization evolves later, and independently, in these primate lineages (Radinsky, 1977; Sears et al., 2008; Simons et al., 2007). The evolution of a larger relative brain size also does not evolve concurrently with mandibular symphyseal fusion as *Aegyptopithecus* has complete symphyseal fusion but retains a relatively small neurocranium. This evidence does not exclude other factors – such as facial kyphosis or facial height – from participating in the fusion of the anthropoid symphysis, but it nevertheless demonstrates a need for further investigation of craniomandibular integration and symphyseal fusion.

4.1.4 Mandibular fusion and the WMP as an Evolutionary Stable Configuration

In a discussion of the phylogenetic importance of correlated characters, Lockwood (2007) used the complex evolution of mandibular symphyseal fusion in anthropoids, as described by Ravosa and colleagues (Ravosa, 1999; Ravosa et al., 2000), to suggest these correlated characters may serve as an evolutionary stable configuration (ESC). The idea of an ESC (Schwenk, 2001; Wagner and Schwenk, 2000) was developed to describe groups of characters adapted to perform a function that are stable within taxa which possess the configuration. More specifically, an ESC is identified by three particular characteristics (Lockwood, 2007; Schwenk, 2001; Wagner and Schwenk, 2000): key components must not vary significantly in taxa with the ESC, components must vary more within taxa that do not have the ESC, and the ESC should be present in multiple environmental contexts. Lockwood (2007) described symphyseal fusion in anthropoids as an ESC by arguing that whereas fusion in strepsirrhines is a straightforward response to increased stress as a result of diet or size, in anthropoids it is

“a more complex phenomenon related to skull shape as a whole” (Lockwood, 2007: 496). However, as previously discussed, more recent recognition of the WMP in *Propithecus verreauxi* potentially challenges the notion of an ESC in anthropoids, and underscores the need for further investigation to provide a more extensive understanding of the WMP and loading regime.

Likewise, the suite of characteristics thought to contribute to an ESC related to symphyseal fusion in anthropoids has not actually been fully tested to see whether it conforms to the defined characteristics of an ESC. Ross and Ravosa (1993) demonstrated that brain size, basicranial flexion, and facial kyphosis are interrelated in anthropoids but not in unfused strepsirrhines. However, this analysis did not assess whether anthropoids display a configuration that is entirely distinct from that of strepsirrhines, or whether strepsirrhines are more variable in their overall configurations. Additionally, although Ravosa et al., (2000) did determine that the anthropoid mandibular ramus is deeper than that of strepsirrhines, they did not provide data to support the assumption that ramus height is linked to the structural relationships of the cranium as described by Ross and Ravosa (1993). Nevertheless, it is clear that symphyseal fusion and the WMP are present in multiple environmental contexts given the dietary diversity of living anthropoids, supporting the interpretation of mandibular fusion as an ESC.

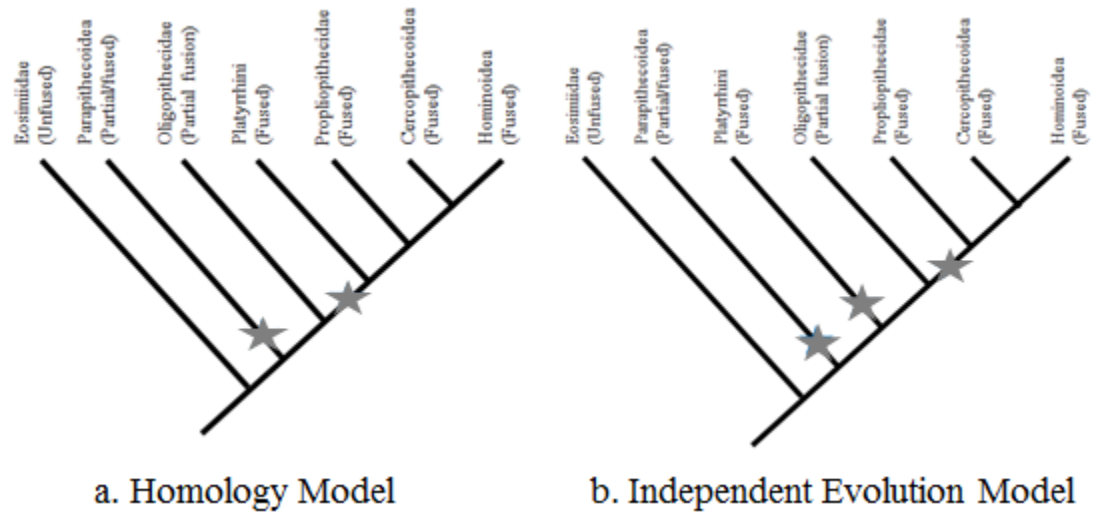


Figure 4.2: Two models for the evolution of complete symphyseal fusion (noted by gray stars) in anthropoids.

4.1.5 Evolutionary impact of mandibular symphyseal fusion

Lockwood's (2007) discussion on the phylogenetic impact and interpretation of correlated traits has a particular relevance to the evolution of mandibular symphyseal fusion in anthropoids. The hypothesized complexity of symphyseal fusion in crown anthropoids has led some researchers to argue that the integrated set of features associated with fusion likely evolved only once prior to the common ancestor of extant anthropoids rather than independently in platyrrhine and catarrhine lineages (Ravosa, 1999; Ravosa and Hogue, 2004). From this perspective, the association of multiple correlated components to create a single functional complex allows greater phylogenetic weight to be placed on this set of features as opposed to other "simple" characteristics that have been previously used to reconstruct early stem and crown anthropoid relationships (Lockwood, 2007). Phylogenetic interpretations based solely on the most parsimonious evolution of symphyseal fusion places oligopithecids (e.g., *Catopithecus*) as a stem

anthropoid the sister taxon to either crown anthropoids or the crown anthropoid-parapithecoid clade (Figure 4.2a; Ravosa, 1999). Ravosa (1999) describes early anthropoid evolution as a step-wise transition from a basal anthropoid condition with no symphyseal fusion, to a later stem anthropoid condition of generating increased dorsoventral shear stress resulting in partial fusion (exhibited by *Catopithecus*, and possibly *Arsinoea*), to the crown anthropoid condition of complete fusion to resist significant wishboning stress. Based on this model, the WMP evolved once prior to the common ancestor of all living anthropoids and is unique to crown anthropoids.

Complete symphyseal fusion evolved in multiple species from the Early Oligocene (e.g., parapithecids), but these are placed as stem anthropoids by Ravosa (1999) who suggested that complete fusion in these taxa occurs primarily from increased dorsoventral shear stress rather than exhibiting the wishboning loading regime. This inference is based on the symphyseal condition exhibited by an unassociated juvenile mandibular fragment that is consistent in size with specimens of *Simonsius* and therefore referred to that genus (Ravosa, 1999). Because this specimen is only partially fused, it suggests late ontogenetic fusion for *Simonsius*, similar to that seen in indriids. Since Ravosa and colleagues (Ravosa, 1991; 1996; 1999; Ravosa and Hogue, 2004) argue that indriids fuse the mandibular symphysis to resist dorsoventral shear stress, similar loading regimes have been inferred for parapithecids. Although the assumptions behind this interpretation are not unreasonable, they are far from definitive, leaving room for investigations into the possible loading regimes exhibited by early stem anthropoids with partial and complete mandibular fusion that are based on other sources of evidence.

Homology of the WMP complex in anthropoids has been challenged by other researchers who argued for the independent evolution of complete symphyseal fusion in catarrhine and platyrrhine lineages (Figure 4.2b) by placing greater phylogenetic value on other morphological features. Specifically, oligopithecids share similarities in postcranial morphology as well as the loss of the second premolar with other catarrhines to the exclusion of platyrrhines (Fleagle and Kay, 1987; Harrison, 1987; Seiffert et al., 2000; 2004; Seiffert and Simons, 2001; Simons and Rasmussen, 1996). This interpretation suggests that the common ancestor of platyrrhines and catarrhines exhibited an unfused symphysis or a partially fused symphysis such as that found in *Catopithecus*. From this perspective, symphyseal fusion is given little phylogenetic weight, in part due to the independent evolution of fusion in several primate lineages, and thus important for reconstructing anthropoid evolutionary relationships. However, as discussed previously, while symphyseal fusion may appear as a simple character on the surface level, its underlying mechanisms may be more complex.

4.1.6 Study goals

The purpose of this analysis is to investigate the relationship between masticatory function (particularly the WMP) and skull morphology along with the morphological integration of the skull across different taxonomic levels of primates. Specifically, the WMP has been hypothesized to result from increased relative brain size, basicranial flexion, facial kyphosis, and a deeper mandibular ramus from a higher jaw, distinguishing anthropoids from strepsirrhines (Ravosa et al., 2000). Here, this hypothesis is evaluated by directly analyzing the relationship between masticatory muscle activity and skull

shape across primates to elucidate the correlated relationship between masticatory function and skull shape. Subsequently, morphological integration of the skull is analyzed across multiple taxonomic levels to determine if the mandibular and cranial components hypothesized to produce the WMP are meaningfully integrated. Ravosa et al. (2000) evoked previous interpretations of cranial evolution (e.g., Ross and Ravosa, 1993) to explain differences in mandibular shape (particularly jaw joint and ramus height) and masticatory function between anthropoids and strepsirrhines. However, the results from Ross and Ravosa (1993) specifically address the relationship of cranial components *within* higher taxonomic levels of primates without making particular distinctions in cranial shape between anthropoids and strepsirrhines – an important assumption for Ravosa et al. (2000). Therefore, whether the mandibular variation between anthropoids and strepsirrhines identified by Ravosa et al. (2000) can be explained by the same patterns of cranial variation identified within anthropoids by Ross and Ravosa (1993) still remains untested. This study investigates patterns of covariation between the mandible and cranium at different taxonomic levels to determine if there is a potential causal link between the hypothesized cranial and mandibular shapes proposed to result in the WMP.

Table 4.1: Sample size by taxon used in this study. State of symphyseal fusion designated as complete, partial, or unfused.

	Taxon	Sample size (N)	Fusion
Cercopithecidae	<i>Macaca fascicularis</i>	25	fused
	<i>Papio anubis</i>	10	fused
	<i>Colobus guereza</i>	25	fused
	<i>Nasalis larvatus</i>	3	fused
	<i>Trachypithecus cristatus</i>	4	fused
Hominidae	<i>Pan troglodytes</i>	25	fused
	<i>Homo sapiens</i>	10	fused
Hylobatidae	<i>Hylobates lar</i>	27	fused
Atelidae	<i>Alouatta seniculus</i>	28	fused
	<i>Ateles geoffroyi</i>	25	fused
Cebidae	<i>Cebus apella</i>	25	fused
	<i>Aotus trivirgatus</i>	25	fused
	<i>Callithrix jacchus</i>	5	fused
Pitheciidae	<i>Chiropotes satanas</i>	5	fused
Lemuridae	<i>Lemur catta</i>	23	unfused
	<i>Haplemur griseus</i>	10	simple partial
	<i>Varecia variegata</i>	4	unfused
Indriidae	<i>Propithecus verreauxi</i>	23	complex partial
Galagidae	<i>Otolemur crassicaudatus</i>	10	unfused
Lorisidae	<i>Perodicticus potto</i>	4	unfused
	<i>Nycticebus coucang</i>	4	unfused
		Total: 320	

4.2 MATERIALS AND METHODS

These research questions were addressed by analyzing the skull shapes of a taxonomically diverse sample of primates that vary in the presence of the WMP and the degree of symphyseal fusion (Table 4.1). 3D models of 320 primate skulls were obtained from multiple sources. The majority of primate skulls were scanned using a Breuckmann SmartSCAN white light scanner using 90mm lenses. Additional specimens were generously made available by other researchers, from either μ CT or NextEngine 3D scans (*Callithrix jacchus*, Dr. CJ Vinyard; *Alouatta seniculus* and *Ateles geoffroyi*, Dr. Lauren Halenar). Skull shape was quantified using landmark-based morphometrics with a series of 90 landmarks and 15 semilandmark curves (Table 4.2, Figure 4.3) collected on each specimen using Stratovan Checkpoint software (Stratovan Corporation, Davis, CA). The landmarks and semilandmark curves were chosen specifically to address hypotheses related to skull structure and masticatory function. The semilandmarks curves were densely sampled initially to best approximate the morphology of each curve and then resampled to obtain a series of evenly-spaced points using RESAMPLE.exe (available at pages.nycep.org/nmg/, created by David Reddy and Johann Kimm, edited by Dr. Ryan Raaum). A more densely sampled curve provides enhanced representation of the morphology and a reduction of the error introduced when sliding semilandmarks along curve tangents. However, a densely sampled curve may include variation that is not biologically meaningful and mask the variation of interest. For this analysis, different numbers of evenly-spaced points were output for each semilandmark curve and visually inspected after superimposition to determine an appropriate density of points for each curve. For a small number of specimens, missing landmarks were estimated individually

using species-specific thin-plate spline interpolation in the Geomorph package in R (Adams and Otarola-Castillo, 2013).

A generalized Procrustes analysis was performed to superimpose each landmark configuration and remove location, orientation, scale to allow for analysis of shape variation. The application of sliding the semilandmarks along the curve is required to create a geometric homology of the semilandmarks across specimens (Bookstein et al., 1999, Gunz and Mitteroecker, 2013). There are currently two accepted methods for sliding semilandmarks along a curve or surface. One first method minimizes Procrustes distances among specimens but has been found to inappropriately slide points past each other when comparing more variable shapes, and thus works better when using specimens with similar morphology (Gunz and Mitteroecker, 2013). The other method minimizes bending energy across specimens (Bookstein 1997; Gunz et al., 2005), and although based on the non-biological properties of a thin-plate spline transformation, constrains semilandmarks from sliding past each other. Based on the sample analyzed in this study, sliding semilandmarks along tangents of the curves to minimize bending energy was the more appropriate method.

Most of the analyses presented here analyze the cranium and mandible together using a single Procrustes superimposition; however, for the certain analyses the cranium and mandible were aligned separately so shape variations specific to each component were not confounded by variation in their shared orientation. Since, both alignment procedures yielded similar results with the same interpretations, only results from the single superimposition are reported.

Table 4.2: Description of landmarks and semilandmarks used in this study

Element	Landmark number	Landmark description	Bilateral/Midline/Symmetric
<u>Mandible</u>	M1	Most medial point on the articular surface of the mandibular condyle	Bilateral
	M2	Most lateral point on the articular surface of the mandibular condyle	Bilateral
	M3	Most anterior point on the mandibular condyle at the midpoint of the mediolateral curve	Bilateral
	M4	Most posterior point on the mandibular condyle at the midpoint of the mediolateral curve	Bilateral
	M5	Coronion	Bilateral
	M6	Attachment of the anterior ascending ramus on the mandibular corpus	Bilateral
	M7	Gonion	Bilateral
	M8	Inferior border of the mandibular foramen	Bilateral
	M9	Most distal molar point projected on the alveolar margin	Bilateral
	M10	Point on the lingual alveolar margin at the midpoint of m1	Bilateral
	M11	Most inferior point on mandibular corpus under m1	Bilateral
	M12	Point on the buccal alveolar margin at the midpoint of m1	Bilateral
	M13	Premolar-molar contact projected on the buccal alveolar margin	Bilateral
	M14	Premolar-molar contact projected on the lingual alveolar margin	Bilateral
	M15	Canine-premolar contact projected on the buccal alveolar margin	Bilateral
	M16	Canine-premolar contact projected on the lingual alveolar margin	Bilateral
	M17	Most inferior point on the mental foramen	Bilateral
	M18	Most mesial point on the midline of m1	Bilateral
	M19	Contact at the apex of the central incisor	Midline
	M20	Infradentale	Midline
	M21	Gnathion	Midline
	M22	Mandibular orale	Midline
	MS1	Mandibular border curve (p=63)	Symmetric
	MS2	Coronoid process curve (p=21)	Bilateral
	MS3	Mandibular corpus outline under m1 (p=15)	Bilateral
	MS4	Mandibular symphysis outline (p=21)	Midline

Cranium

C1	Most distal molar point projected on the alveolar margin	Bilateral
C2	Premolar-molar contact projected on the lingual alveolar margin	Bilateral
C3	Premolar-molar contact projected on the buccal alveolar margin	Bilateral
C4	Canine-premolar contact projected on the lingual alveolar margin	Bilateral
C5	Canine-premolar contact projected on the buccal alveolar margin	Bilateral
C6	Most inferior point on the premaxillomaxillary suture	Bilateral
C7	Inferior margin of the largest infraorbital foramen	Bilateral
C8	Midpoint on the medial orbital margin	Bilateral
C9	Frontomalare temporale	Bilateral
C10	Midpoint on the superior orbital margin projected on the supraorbital torus.	Bilateral
C11	Malar root origin	Bilateral
C12	Jugale	Bilateral
C13	Most superior point on the zygomaxillary suture	Bilateral
C14	Most inferior point on the zygomaxillary suture	Bilateral
C15	Porion	Bilateral
C16	Anterior inflection point of the temporal line	Bilateral
C17	Superior projection of porion onto the posterior zygomatic process or temporal line	Bilateral
C18	Most inferior tip of the lateral pterygoid plate	Bilateral
C19	Anterior junction of the medial and lateral pterygoid plates	Bilateral
C20	Inferior tip of the postglenoid process	Bilateral
C21	Alveolare	Midline
C22	Most inferior point on the nasal aperture	Midline
C23	Rhinion	Midline
C24	Nasion	Midline
C25	Opisthion	Midline
C26	Basion	Midline
C27	Hormion	Midline
C28	Staphylion	Midline
C29	Incision	Midline
C30	Central incisor contact projected on the alveolar margin	Midline
CS1	Nasal aperture outline (p=21)	Symmetric
CS2	Orbit outline (p=25)	Bilateral
CS3	Temporal line curve (p=33)	Bilateral
CS4	Midsagittal cranial curve (p=52)	Midline
CS5	Foramen magnum outline (p=23)	Symmetric
CS6	Basicranium curve (p=9)	Midline
CS7	Palate curve (p=9)	Midline

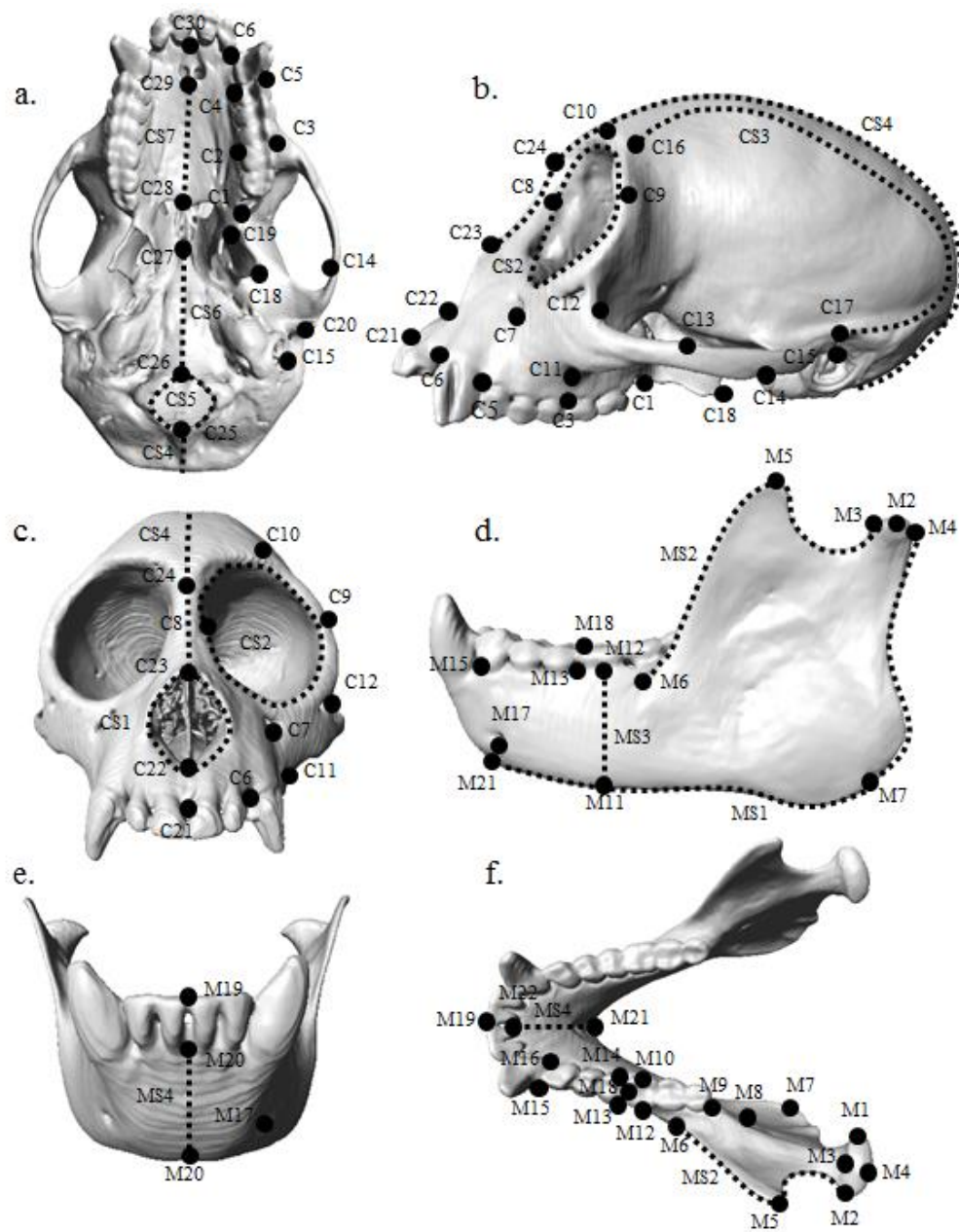


Figure 4.3: Three-dimensional landmarks and semilandmark curves used in the study.

Landmarks=black dots, semilandmarks=blue curves

The relationship between skull shape and the WMP was first investigated using a 2-block partial least squares analysis between the skull landmark configurations and data describing masticatory function. Partial least squares analysis creates pairs of (singular) axes that maximally covary with each other using a singular value decomposition of the interblock variance-covariance matrix (Rohlf and Corti, 2000) which identifies patterns of skull shape and masticatory function that have the greatest covariation. Since this analysis contains specific data on masticatory function, it will subsequently be referred to as a functional PLS (F-PLS). The functional data set consisted of electromyography measures (i.e., working-side/balancing-side ratios and timing of peak muscle activity for various masticatory muscles) that were collected from previously published studies (Hylander et al., 2000; 2002; 2004; 2005; 2011; Ross and Hylander, 2000; Vinyard et al., 2006; 2007; 2008) or generously shared through personal communication with Dr. CJ Vinyard. Working-side/balancing-side ratios are not direct measures of force generated by muscles but rather a relative assessment of the recruitment of the balancing-side muscle activity compared to the working-side muscle. Timing of peak muscle activity was calculated as the difference in milliseconds between the peak activity of the working-side superficial masseter muscle and each masticatory muscle for which published data exists. Peak times were then scaled by an estimation of the length of the power stroke, calculated as the time between peaks of the first and last muscles to fire. Scaling of peak muscle activity is necessary since larger primates have absolutely longer chewing cycles (Ross et al., 2008). The scaled peak timing of masticatory muscle activity and WS/BS ratios were standardized by the standard deviation of each variable. EMG data were only

available for nine primate species (*Homo sapiens*, *Macaca fascicularis*, *Papio anubis*, *Aotustrivirgatus*, *Callithrix jacchus*, *Cebus apella*, *Propithecus verreauxi*, *Otolemur crassicaudatus*, and *Lemur catta*) but include taxa that vary in the presence of the WMP and symphyseal fusion. Since only the mean values for the EMG data were available and the functional and shape data were not collected on the same specimens, the F-PLS was performed using the mean configurations of skull shape for each of the eight taxa. The functionally-associated shapes are visualized through thin-plate spline deformations of a specimen of *Colobus guereza* (the species nearest to the sample mean configuration) using the eigenvector of the newly constructed shape axis.

To further address the interrelationship of cranial and mandibular components, additional analyses were performed that benefitted from the inclusion of other species for which no EMG data exists. These analyses specifically test patterns of skull integration to determine if the specific components associated with the WMP are integrated as predicted. Although these analyses do not provide direct functional interpretations, they investigate the integration of cranial and mandibular components across different levels. First, skull morphology was evaluated across higher taxonomic units. Three between-group principal component analyses (BGPCA) were used to identify mean shape differences between groups with the WMP (i.e., catarrhines, platyrrhines and *Propithecus*) and strepsirrhines that do not have the WMP. BGPCA is a multivariate ordination procedure that uses group mean configurations to create new axes that summarize shape differences in low-dimensional space. The individual specimens are then projected onto the eigenvectors created by differences in group mean configurations (Boulesteix, 2005; Mitteroecker and Bookstein, 2011). Catarrhines and platyrrhines were

separated into different groups since it is uncertain whether the WMP evolved independently in each lineage or prior to the divergence of these lineages.

Morphological integration of the cranium and mandible was assessed in a phylogenetic context across all primate species in the sample using methods developed by Adams and Felice (2014). Skull shape was determined to have a phylogenetic signal (p -value < 0.0001) using the a permutation test that randomly permutes the multivariate shape data among the terminal branches of the phylogeny with a test statistic of the total amount of squared change summed overall all the branches of the tree (Klingenberg and Gidaszewski, 2010). This suggests that the shared evolutionary history needs to be considered in the analysis as it manifests as a proportional degree of phenotypic similarity across species. The non-independence of taxa was accounted for using a phylogenetic PLS (P-PLS) which performs a singular value decomposition of the interblock evolutionary covariance matrix calculated using the molecular phylogeny generated by Perelman et al., (2011) and the mean shape configurations for each species. A P-PLS was also performed using only taxa that exhibit the WMP, but the primary patterns of craniomandibular integration were similar to the results using the complete sample. Thus, only results from the analysis on the entire sample are reported. The overall covariation between the cranial and mandibular landmarks was quantified using the RV coefficient (Escourier, 1973; Klingenberg, 2009). This measure is a multivariate extension of the squared correlation coefficient between two variables (Klingenberg, 2009).

The shared within-species pattern of craniomandibular integration was subsequently analyzed across living primates that exhibit the WMP (i.e., all anthropoids

and indriids). A pooled within-species 2BPLS was performed to account for species differences and find common patterns of covariation between the cranium and mandible across taxa. Since this analysis relies on the species specific covariance pattern, those species with less than ten specimens were dropped from the analysis since they likely do not provide an adequate estimation of the covariance structure.

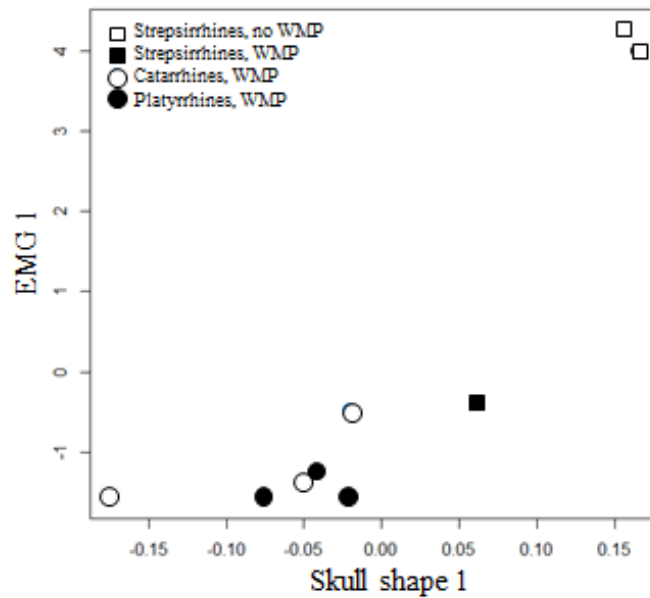
The relationships of skull components hypothesized by Ravosa et al., (2000) were more directly investigated by analyzing skull shape in relation to the angle of facial kyphosis (AFK) using multivariate regression. The AFK was measured by Ross and Ravosa (1993) as the angle between the floor of the nasal fossa and the plane of clivus ossis occipitalis at the midline. This exact angle could not be duplicated for this analysis since the majority of the 3D models used only captured the external surface morphology. Nevertheless, AFK was approximated in this study as the three-dimensional angle between the vectors of prosthion-staphylion and basion-hormion. This external measure of AFK still quantifies the orientation of the face relative to the basicranium appropriately in order to determine how the facial angle is integrated with other aspects of cranial and mandibular shape. The multivariate regression (Klingenberg, 2016; Monteiro, 1999) on AFK was performed on the aligned landmark coordinates to estimate the effects of AFK on skull shape across primates with the WMP. A phylogenetic correction was not used in this analysis since the AFK does not have a phylogenetic signal (p-value=0.491).

4.3 RESULTS

4.3.1 Analysis of the WMP and skull shape

The first pair of axes from the F-PLS investigating covariation between EMG and shape data generally distinguish primates with the WMP (anthropoids and *Propithecus*) from those without (*Lemur* and *Otolemur*) (Figure 4.4; Tables 4.3-4.4). There does not seem to be a simple linear relationship explaining the transition from an unfused to a fused symphysis, but with only a small number of species associated with EMG data, it cannot be ruled out. The relationship between EMG and shape data clearly associate *Propithecus* with the anthropoids, indicating that it shares morphological features with anthropoids related to muscle function, but as a strepsirrhine, its shape is closer to the other strepsirrhines than are the anthropoids. Also conspicuous is the position of *Homo* as the negative extreme on the shape axis. Its separation from other anthropoids may indicate a unique relationship between skull shape and masticatory function. The EMG variables that load most heavily on the first axis reflect variation in the WMP through the timing and recruitment of the balancing-side deep masseter and posterior temporalis muscles (Figure 4.4). As expected, anthropoids and *Propithecus* recruit greater balancing-side deep masseter and posterior temporalis muscle activity and delay the activity of these muscles until the end of the power stroke.

Functional PLS 1



- Functional PLS 1 +

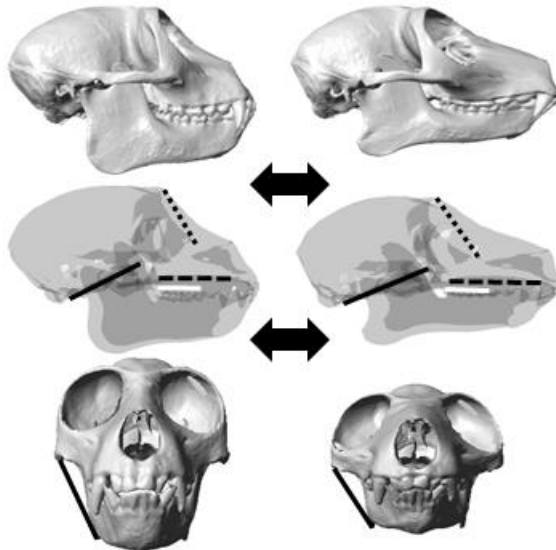


Figure 4.4: Plot of the first pair of F-PLS axes and the visualization along the shape axis. Lateral view: dotted line= orbital plane, black line= basion-hormion, dashed line= staphylion-incision, white line=m1-m3 alveolar plane. Frontal view: black line= orientation of masseter muscle from zygomatic arch to inferior ramus.

Table 4.3: Loadings for the EMG variables from an F-PLS on all taxa with EMG data. Variables with the largest loadings for each singular vector are identified with an asterisk.

<u>EMG variables</u>	<u>Data type</u>	<u>F-PLS 1</u>	<u>F-PLS 2</u>
Superficial masseter	W/B ratio	0.248	-0.109
Deep masseter	W/B ratio	0.381*	0.187
Anterior temporalis	W/B ratio	0.301	0.121
Posterior temporalis	W/B ratio	0.413*	0.263
WS deep masseter	Peak muscle timing	-0.002	-0.617*
BS superficial masseter	Peak muscle timing	0.262	-0.536*
BS deep masseter	Peak muscle timing	0.371*	0.001
WS anterior temporalis	Peak muscle timing	0.266	0.035
BS anterior temporalis	Peak muscle timing	0.203	-0.418*
WS posterior temporalis	Peak muscle timing	0.208	0.159
BS posterior temporalis	Peak muscle timing	0.413*	-0.019

Table 4.4: Statistical results from an F-PLS on all taxa with EMG data.

	<u>F-PLS 1</u>	<u>F-PLS 2</u>
Singular value	0.233	0.108
p-value	0.029	0.154
correlation	0.951	0.785
% covariation	79.40%	16.96%

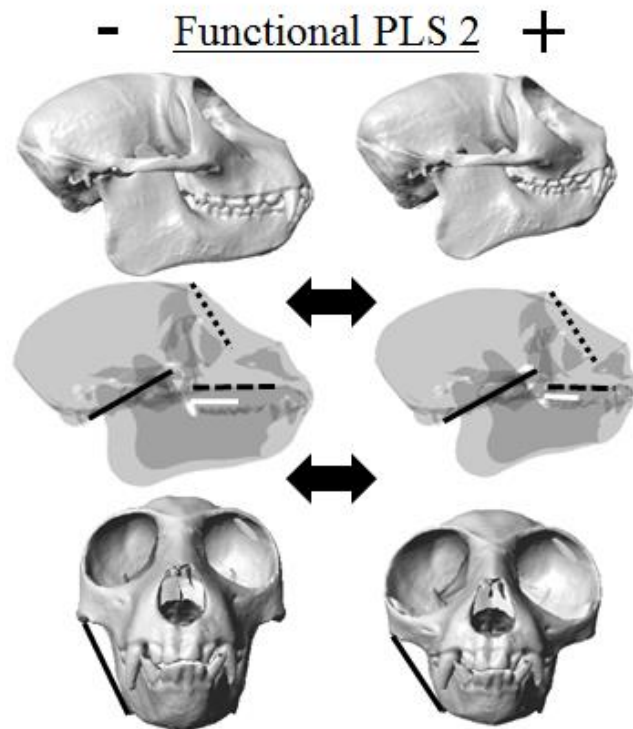
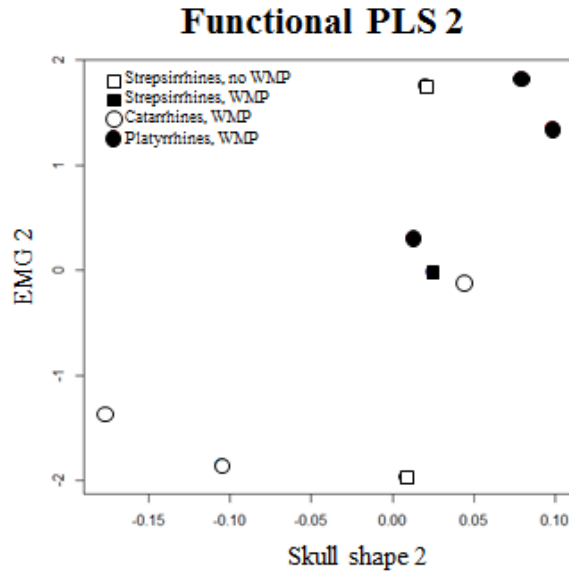


Figure 4.5: Plot of the second pair of F-PLS axes and the visualization along the shape axis. Lateral view: dotted line= orbital plane, black line= basion-hormion, dashed line= staphylion-incision, white line=m1-m3 alveolar plane. Frontal view: black line= orientation of masseter muscle from zygomatic arch to inferior ramus.

Lines are transposed on a lateral view of the skulls to demonstrate the changes in basicranial flexion, orbit and palate orientation, and postcanine tooth row position along each axis (Figure 4.4). Without the internal cranial morphology, external basicranial flexion is visualized by the angle between the basion-hormion chord and orbital plane (Strait, 2001) and facial orientation is quantified as the angle between the basion-hormion chord and midsagittal line of the palate (cf. Ross and Ravosa, 1993). The shape change along F-PLS1 provides support for many of the predictions made by Ravosa et al., (2000). The negative end of the first shape axis corresponds with a relatively larger neurocranium, more flexed basicranium, and a taller, less prognathic face with slight facial kyphosis. This configuration also has a taller mandibular ramus, due in small part to increased jaw joint height above the occlusal plane, but more definitively from expanding the inferior portion of the ramus. The small increase in jaw joint height above the occlusal surface of the dentition is a function of the palate moving inferiorly in relation to the jaw joint rather than vaulting of the palate. As a result of the orientation of the zygomatic process and inferior ramus, the masseter muscle appears to be more vertically oriented in primates with the WMP on this axis. Additional changes in skull morphology that correlate with the WMP include a taller corpus and symphysis, convergent orbits, and the medial pterygoid muscles appear to be more vertically oriented rather than in the anterior-posterior direction.

The relationship between the second pair of F-PLS axes is not statistically significant (Table 4.4). The small sample size due to the availability of EMG data reduces the statistical power for detecting significant relationships; nevertheless, the relationship is suggestive and merits interpretation. The second pair of axes primarily distinguishes

Old World monkeys from smaller-bodied New World monkeys (i.e., *Aotus* and *Callithrix*), although both *Cebus* and *Homo* plot in the middle (Figure 4.5). *Propithecus* falls near *Cebus* and *Homo* whereas *Otolemur* plots with the other platyrrhines and *Lemur* near to the catarrhines. The results from this analysis are comparable to an F-PLS including only anthropoid taxa (not reported). The negative end of the EMG axis is characterized by an earlier peak activity of the working-side deep masseter muscle at the beginning of the chew cycle along with earlier peak activities of the balancing-side superficial masseter and balancing-side anterior temporalis muscles. Peak activity of the balancing-side superficial masseter in platyrrhines occurs at approximately the same time as the working-side superficial masseter but prior to the working-side superficial masseter in catarrhines. Associated skull morphology with early peak activity of these masticatory muscles includes a less vertical symphysis with the development of an inferior transverse torus, a longer face and mandible, a less transversely-oriented masseter muscle while retaining a similar orientation of the medial pterygoid muscles, and expansion of the temporalis muscles towards the midline of the cranium (Figure 4.5).

4.3.2 Comparisons of skull shape between primates with and without the WMP

Results of a BGPCA comparing skull shapes in fused and unfused primates results in a single axis delineating the two groups. Compared to strepsirrhines without the WMP, on average catarrhines have a relatively larger neurocranium, orbits that are more convergent and frontated, and a less prognathic and taller face (Figure 4.6). The face still maintains a significant degree of subnasal prognathism with the major reduction occurring in the nasal cavity. The basicranium is greatly flexed relative to the orbital

plane in catarrhines, but the face only has a slight downward rotation. Catarrhines also have a shorter mandible with a taller ramus, corpus, and symphysis and a slightly labiolingually thicker symphysis. The corpus is not buccolingually thicker in catarrhines. The taller mandibular ramus does produce more vertically oriented masseter muscles. Increased ramus height in catarrhines is a function of both deepening the ramus inferiorly and increasing jaw joint height from the occlusal surface of the dentition through palate vaulting.

A BGPCA of platyrrhines vs. unfused strepsirrhines finds that they differ in nuanced but unique ways in comparison to the differences between catarrhines and unfused strepsirrhines. Platyrrhines do have a relatively larger neurocranium, more convergent and frontated orbits, and a shorter, taller face compared to strepsirrhines (Figure 4.7). However on average, platyrrhines do not exhibit increased facial kyphosis even with a more flexed basicranium relative to the orbital plane. Platyrrhines also have a shorter mandible with a noticeably taller mandibular ramus, achieved by expanding the gonial region, and more vertically-oriented masseter muscles. The corpus is taller but not noticeably thicker, and the symphysis is taller and more vertically-oriented. Platyrrhines do have a slightly higher jaw joint relative to the occlusal surface of the dentition due to the inferior displacement of the palate rather than vaulting of the palate.

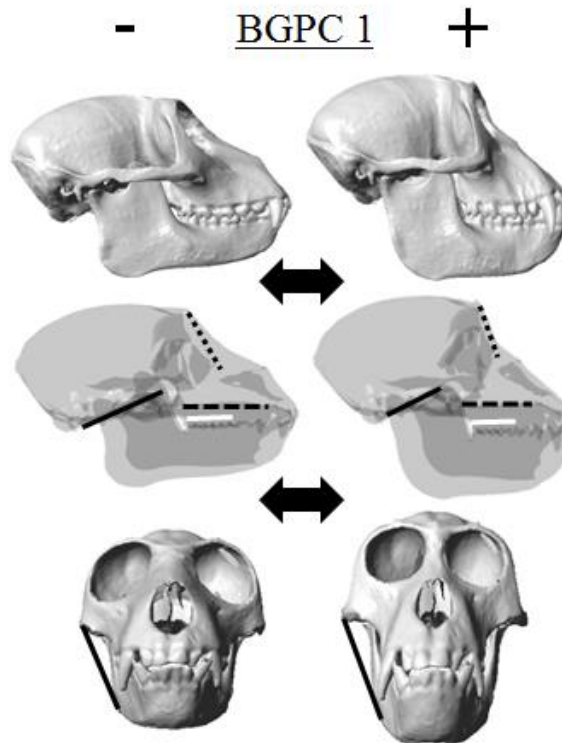
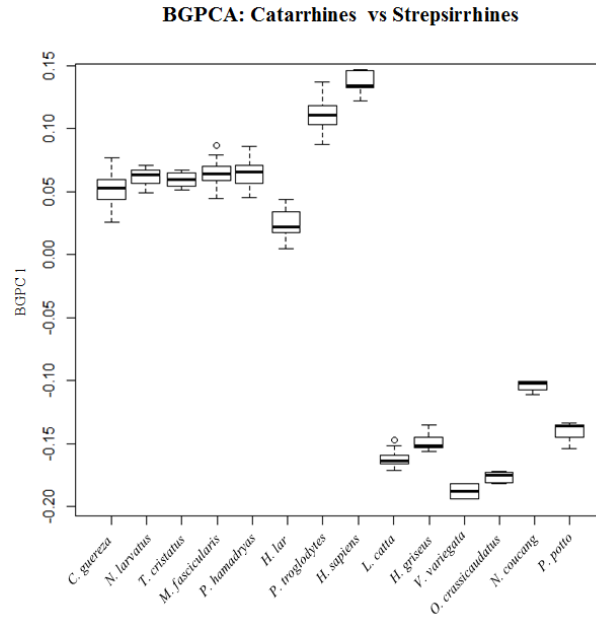


Figure 4.6: Plot of BGPCA of catarrhines and strepsirrhines without the WMP and the visualization of shape change along this axis. Lateral view: dotted line= orbital plane, black line= basion-hormion, dashed line= staphylion-incision, white line=m1-m3 alveolar plane. Frontal view: black line= orientation of masseter muscle from zygomatic arch to inferior ramus.

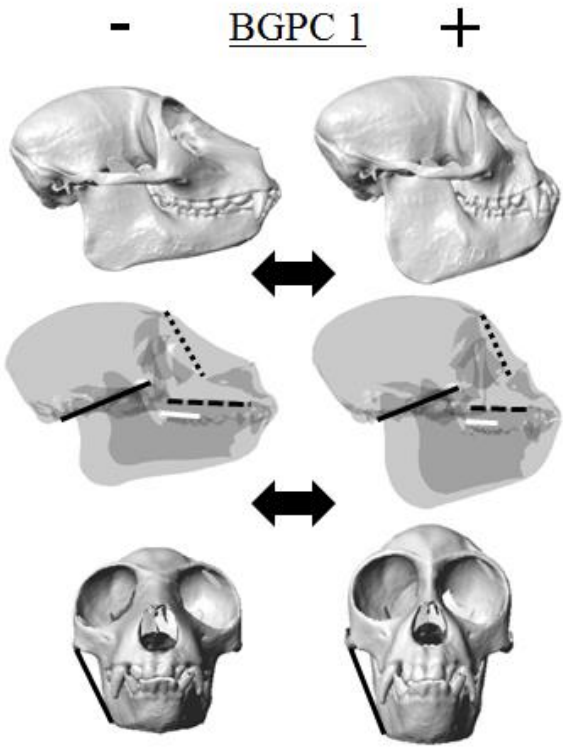
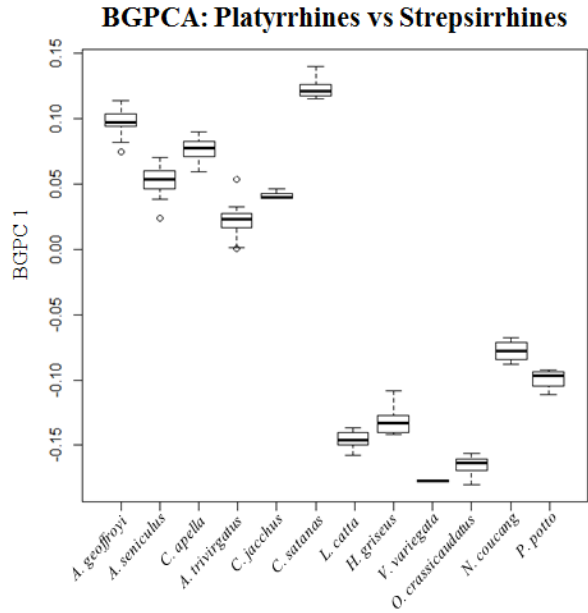


Figure 4.7: Plot of BGPCA of platyrrhines and strepsirrhines without the WMP and the visualization of shape change along this axis. Lateral view: dotted line= orbital plane, black line= basion-hormion, dashed line= staphylion-incision, white line=m1-m3 alveolar plane. Frontal view: black line= orientation of masseter muscle from zygomatic arch to inferior ramus.

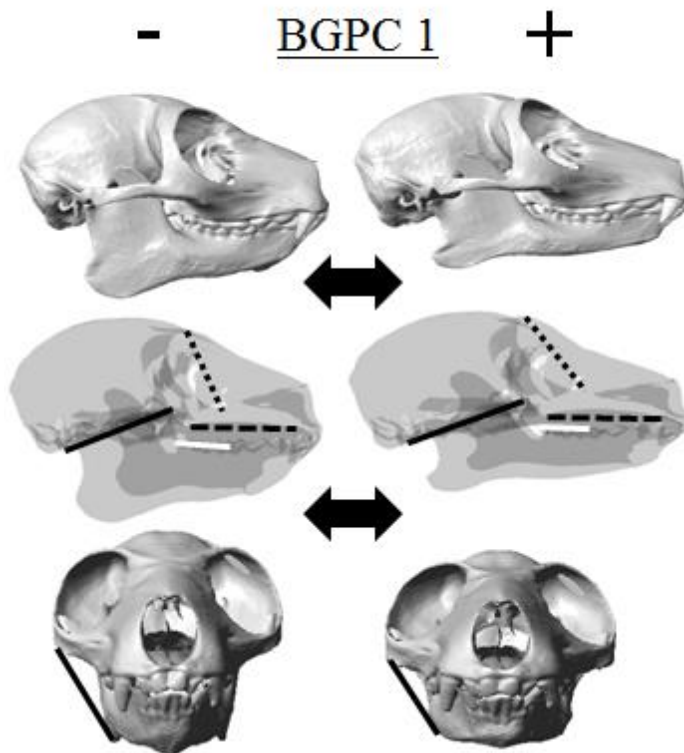
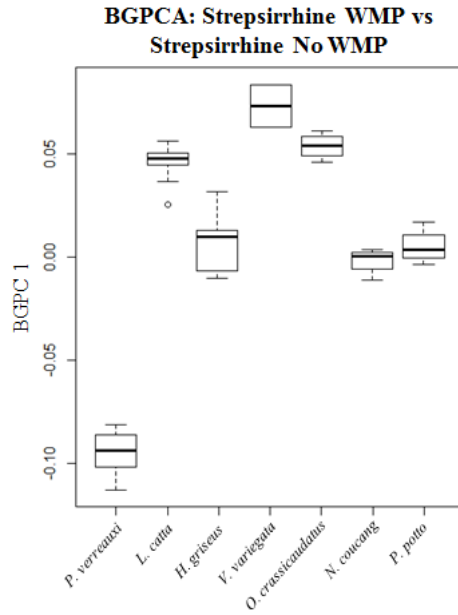


Figure 4.8: Plot of BGPCA of strepsirrhines with and without the WMP and the visualization of shape change along this axis. Lateral view: dotted line= orbital plane, black line= basion-hormion, dashed line= staphylion-incision, white line=m1-m3 alveolar plane. Frontal view: black line= orientation of masseter muscle from zygomatic arch to inferior ramus.

The BGPCA of *Propithecus* compared to unfused strepsirrhines demonstrates that the former does not have relatively larger neurocrania than other strepsirrhines, but does possess a smaller angle between the basicranium and orbital plane, likely due to greater frontation of the orbits rather than to a more flexed basicranium (Figure 4.8).

Additionally, *Propithecus* does not have a more kyphotic face even though the face is relatively shorter. The mandibular ramus is significantly taller in indriids from an expanded gonial region and, to a lesser degree, an inferior displacement of the palate. The mandibular corpus and symphysis are also both taller in indriids than other strepsirrhines.

4.3.3 Patterns of craniomandibular integration associated with the WMP

As expected, the cranium and mandible are highly integrated (RV coefficient=0.966) across primates when accounting for shared evolutionary history among taxa. The first pair of axes from the P-PLS of all primates distinguishes *Homo* (positive end) from *Alouatta*, *Pan*, and *Papio* (negative end) with other species clustered midway in-between (Figure 4.9; Table 4.5). Moving towards the positive end of each axis, relative neurocranial size increases, orbits become larger, the basicranium becomes more flexed, and the face is shorter (primarily through reduced subnasal prognathism) and rotated downward. The mandible is anteroposteriorly shorter with a more vertical and shorter symphysis, lacking the inferior projection of a transverse torus. The corpus dimensions remain constant but the corpus is everted inferiorly. A downward rotation of the face results in a reduction in jaw joint height above the occlusal surface and ramus height. The coronoid process is higher with a more pronounced mandibular notch. Overall, the ramus is smaller which is likely to reflect relatively smaller masseter muscles

that are more transversely-oriented. The inferior border of the mandible does not provide a smooth transition at the junction of the ramus and corpus but instead has a concave appearance that might be a consequence of greater facial kyphosis.

The second pair of P-PLS axes demonstrates a relatively linear relationship with *Papio* towards the negative end of the plot (Figure 4.10). Similar to the first pair of axes, increased basicranial flexion is associated with a downward rotation of the face; however, this correlates with a taller, more prognathic face, smaller and less frontated orbits and a shorter basicranium. The positioning of the orbits relative to the palate is particularly affected along this pair of axes. Relative neurocranial size does not appear to meaningfully change along this pair of axes. Increased facial kyphosis covaries with greater palatal vaulting but also with an overall shorter and smaller mandibular ramus. The symphysis is relatively shorter but labiolingually thicker. The coronoid process is taller and again there is a concave junction of the ramus and corpus associated with facial kyphosis. Even though the mandibular ramus is shorter, the orientation of the masseter muscles appears to be more vertically-oriented related to a reduction in bizygomatic breadth and laterally-projecting gonial regions.

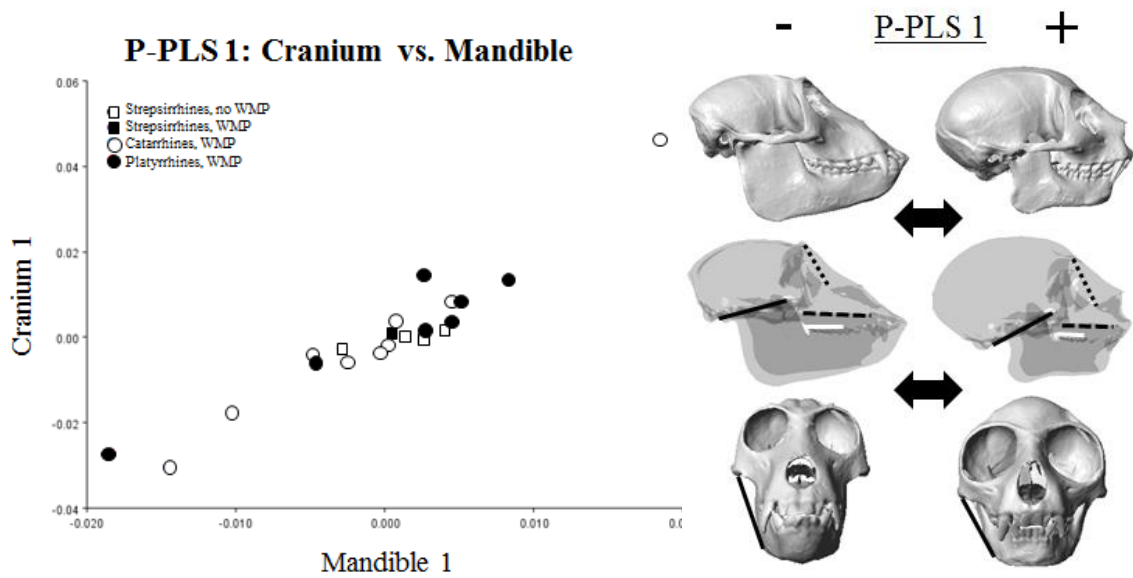


Figure 4.9: Plot of the first pair of P-PLS axes on all taxa with EMG data and the visualization along each axis. Lateral view: dotted line= orbital plane, black line= basion-hormion, dashed line= staphylion-incision, white line=m1-m3 alveolar plane. Frontal view: black line= orientation of masseter muscle from zygomatic arch to inferior ramus.

Table 4.5: Statistical results from a P-PLS on all taxa with EMG data.

	<u>P-PLS 1</u>	<u>P-PLS 2</u>	<u>P-PLS 3</u>
Singular value	0.000116	0.000047	0.000034
p-value	0.001	0.001	0.001
correlation	0.95	0.937	0.821
% covariation	42.50%	17.30%	12.40%

P-PLS 2: Cranium vs. Mandible

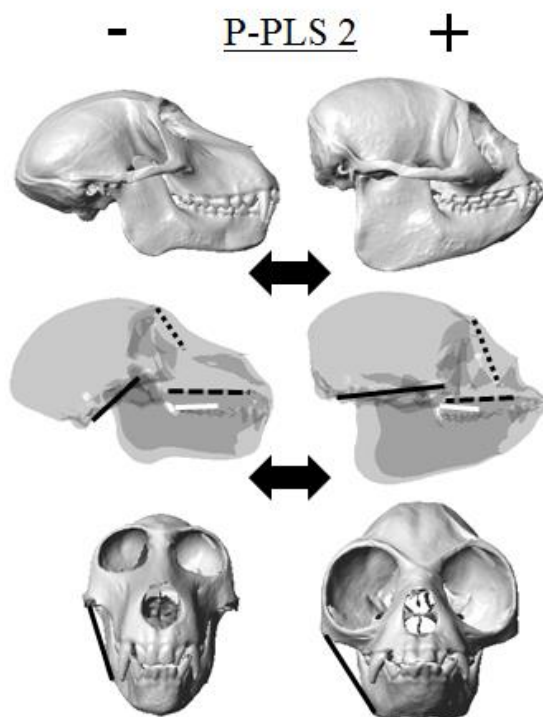
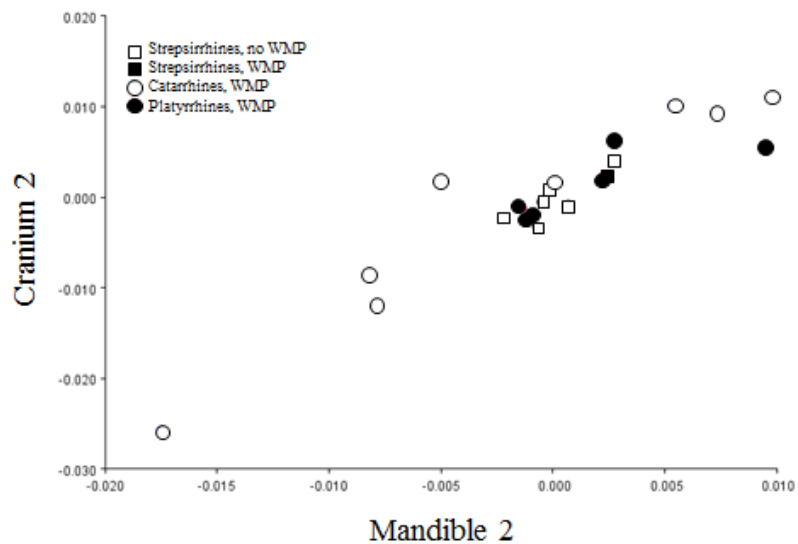


Figure 4.10: Plot of the second pair of P-PLS axes and the visualization along each axis. Lateral view: dotted line= orbital plane, black line= basion-hormion, dashed line= staphylion-incision, white line=m1-m3 alveolar plane. Frontal view: black line= orientation of masseter muscle from zygomatic arch to inferior ramus.

P-PLS 3: Cranium vs. Mandible

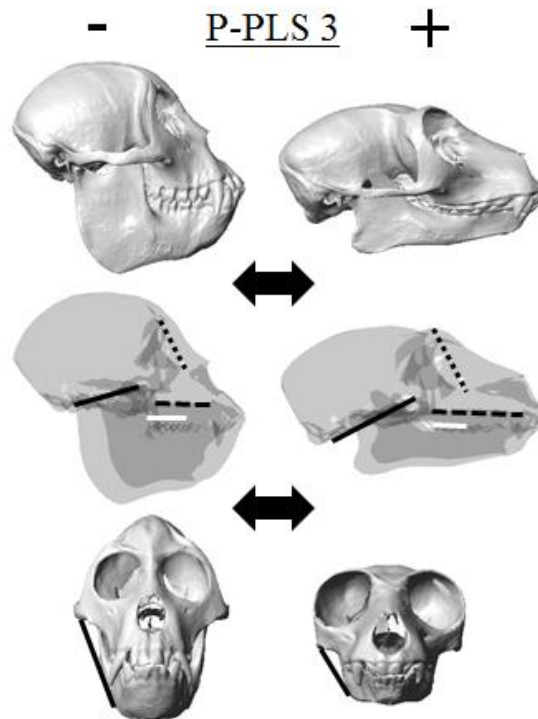
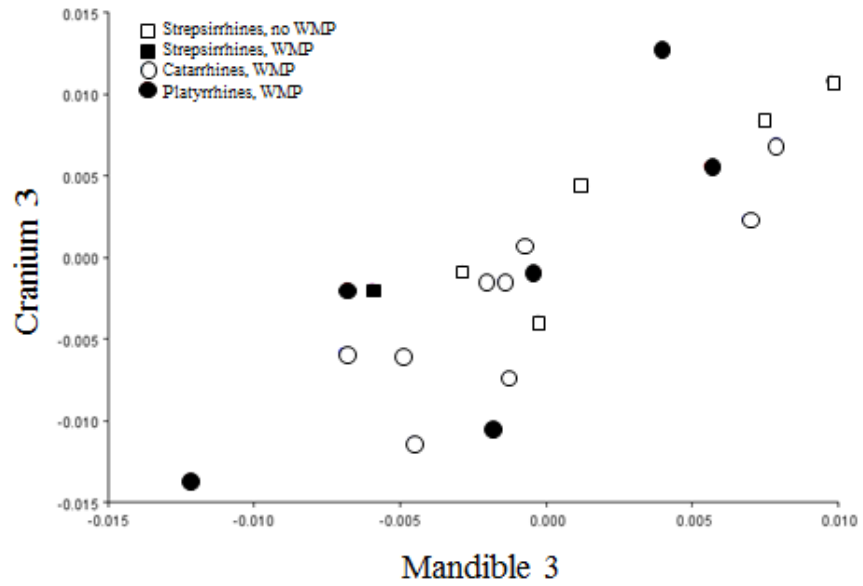


Figure 4.11: Plot of the third pair of P-PLS axes and the visualization along each axis. Lateral view: dotted line= orbital plane, black line= basion-hormion, dashed line= staphylion-incision, white line=m1-m3 alveolar plane. Frontal view: black line= orientation of masseter muscle from zygomatic arch to inferior ramus.

The third pair of significant P-PLS axes separates more gracile strepsirrhines (e.g., *Varecia*, *Lemur*, and *Otolemur*), small-bodied platyrrhines, and *Hylobates* from other primates that tend to be more robust within their respective clades (Figure 4.11). Towards the negative end of the axes, a more globular neurocranium, reduced basicranial flexion and facial kyphosis, a shorter and taller face and greater vaulting of the palate correlate with and relatively shorter but overall more robust mandible. The ramus, corpus, and symphysis are all relatively deeper with presumably larger and more vertical masseter muscles

A pooled within-species PLS analysis identified patterns of within-species covariation that are shared across the sample (Table 4.6). The first pair of axes identifies the pattern of a relatively larger neurocranium, increased basicranial flexion, a slightly taller face and a shorter ramus, corpus, and symphysis (Figure 4.12). This configuration additionally has an origin of the temporalis muscle further from the midsagittal plane and slightly more transversely oriented masseter muscles. This first pair of axes appears to be identifying shared patterns of covariation that differentiate males from females, albeit with quite a bit of overlap.

Along the second pair of axes, decreased facial kyphosis and more frontated orbits relative to the palate covary with a slightly longer mandible with a narrower arch and a less vertical symphysis with a more developed inferior transverse torus (Figure 4.13). The orientations of the masseter and temporalis muscles do not appear to be significantly affected by this pattern of covariation. A PLS analysis using separate superimpositions for the cranium and mandible yield similar results to the analysis with a simultaneous superimposition for the cranium and mandible and is not presented.

The angle between basion-hormion and the palate was calculated to determine how the angle of facial kyphosis (AFK) directly relates to changes in skull morphology using a multivariate regression. The AFK does not have a phylogenetic signal and is quite variable even within species (Figure 4.14). Primates with the WMP do not have a distinctly smaller AFK than primates without the WMP, contrary to the prediction of Ravosa et al. (2000). A multivariate regression of skull shape coordinates on AFK estimates that a reduction in the AFK covaries with a more flexed basicranium, a more prognathic face, a decrease in ramus height, a narrower mandibular arch, and a less vertical symphysis with a thicker superior transverse torus (Figure 4.15). A reduction in the height of the mandibular ramus results in more transversely-oriented masseter muscles. In the plot, one platyrrhine species, *Alouatta seniculus*, is distinct from the other primates which might indicate a unique relationship between AFK and overall skull shape (Figure 4.15). It is important to note that the multivariate regressions on AFK accounts for 14.32% of the total variation in the coordinate shape data.

Pooled PLS 1: Cranium vs Mandible coordinates

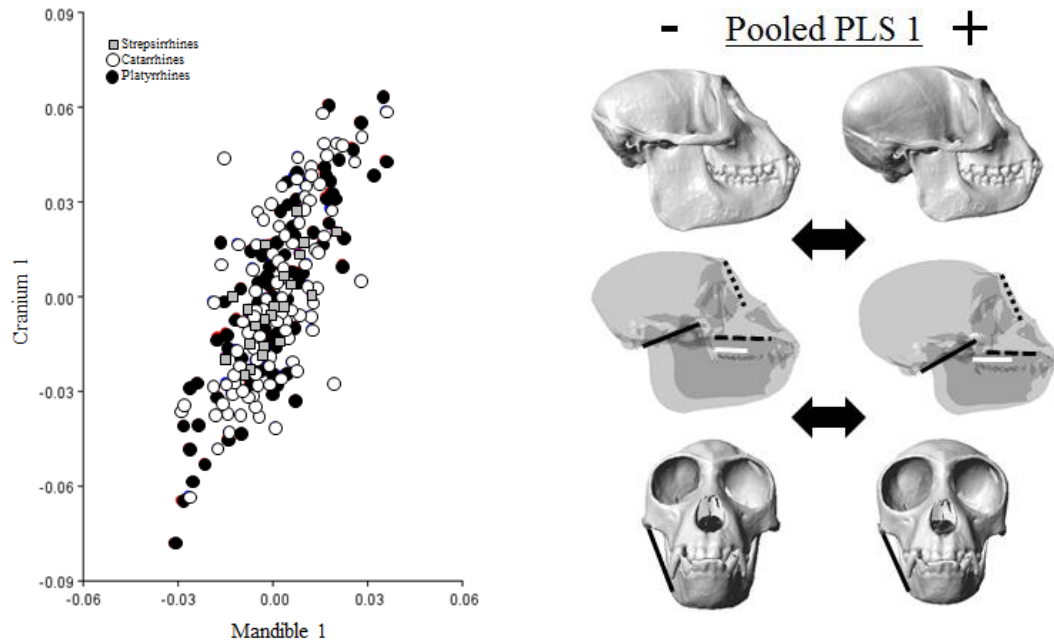
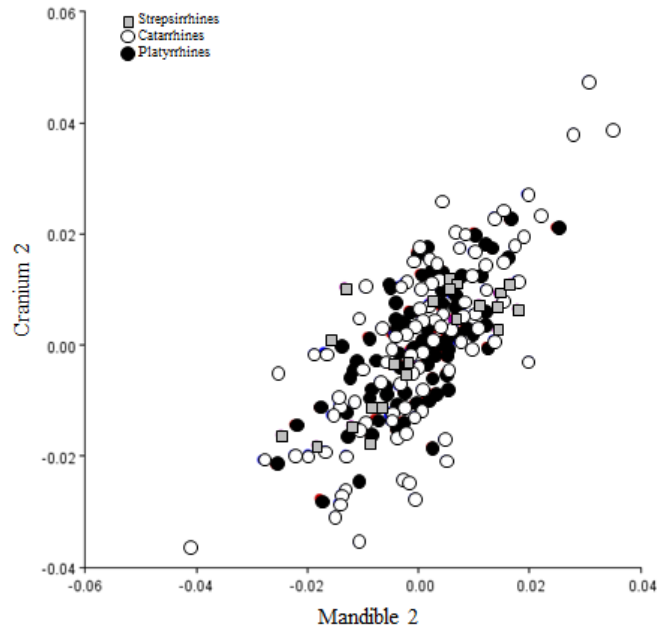


Figure 4.12: Plot of the first pair of axes from a pooled within species PLS and the visualization along each axis. Lateral view: dotted line= orbital plane, black line= basion-hormion, dashed line= staphylion-incision, white line=m1-m3 alveolar plane. Frontal view: black line= orientation of masseter muscle from zygomatic arch to inferior ramus.

Table 4.6: Statistical results from a pooled PLS on all taxa.

	<u>PLS 1</u>	<u>PLS 2</u>
Singular value	0.00028	0.0001
p-value	0.001	0.001
correlation	0.764	0.721
% covariation	75.70%	10.80%

Pooled PLS 2: Cranium vs Mandible coordinates



- Pooled PLS2 +

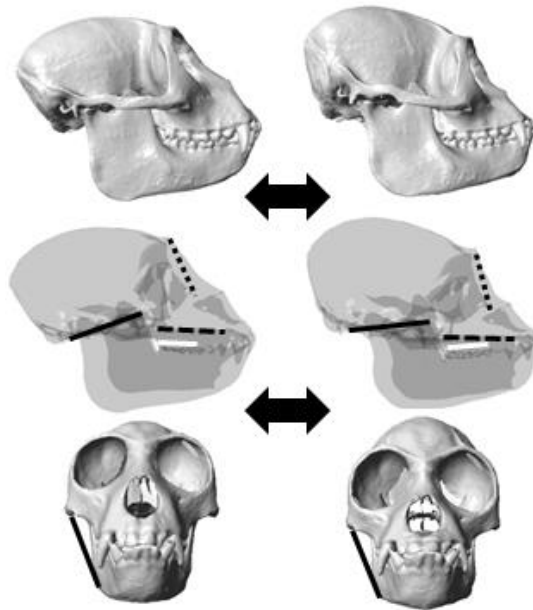


Figure 4.13: Plot of the second pair of axes from the pooled within species PLS and the visualization along each axis. Lateral view: dotted line= orbital plane, black line= basion-hormion, dashed line= staphylion-incision, white line=m1-m3 alveolar plane. Frontal view: black line= orientation of masseter muscle from zygomatic arch to inferior ramus.

4.4 DISCUSSION

4.4.1 Wishboning motor pattern and skull morphology

The purpose of this study was to investigate how specific patterns of skull shape can impact masticatory function in different groups of primates. Ravosa et al. (2000) propose that a cascade of skull features differentiating anthropoids from strepsirrhines ultimately result in the development of the WMP and symphyseal fusion in anthropoids. According to this hypothesis, anthropoids possess a jaw joint that is vertically displaced from the occlusal surface of the dentition which deepens the mandibular ramus and orients the masseter muscles vertically, necessitating a change in masticatory motor patterns to maintain transverse jaw movements during chewing (Ravosa et al., 2000). This has been linked to increases in relative brain size and shifts in the orientation of the basicranium and face (Ravosa et al., 2000; Ross and Henneberg, 1995; Ross and Ravosa, 1993). To determine if primates with the WMP exhibit these hypothesized changes in skull morphology compared to primates without the WMP, EMG data on muscle activity patterns were leveraged to extract functionally relevant shape differences rather than simply analyzing overall phenetic variation among taxa that are hypothesized to differ in masticatory function. The EMG data used in this study provide information about patterns of masticatory muscle activity that have been directly linked to changes in loading regimes occurring in the mandible associated with mandibular symphyseal fusion, particularly in anthropoids. Although the convergent evolution of the WMP in *Propithecus* has not been thoroughly addressed in previous studies, *Propithecus* was included in this analysis to provide additional insight into the underlying mechanisms associated with generating the WMP. Using EMG data to directly extract relevant

patterns of shape variation is particularly beneficial as it finds patterns of shape associated with function rather than phylogeny, which might otherwise be expected.

The results from this analysis make a primary distinction between primates with and without the WMP. Peak activity of the balancing-side posterior temporalis muscle was identified with delayed activity of the balancing-side deep masseter as part of the WMP which has been acknowledged in previous analyses (e.g., Hylander et al., 2011) but has received little attention regarding its functional significance. The balancing-side posterior temporalis muscle may assist in the transverse movement of the mandible in addition to adduction and potentially retraction of the balancing-side of the mandible. Generally the WMP covaries with a relative increase in neurocranial size, more flexed basicranium, slight facial kyphosis, a shorter and taller face with more convergent orbits, and a taller mandibular ramus. The height of the ramus increases primarily from expanding the inferior border of the ramus.

Different patterns in skull morphology are found when looking at mean differences between higher taxonomic groups that do and do not have the WMP. Compared to strepsirrhines lacking the WMP, catarrhines and platyrrhines have relatively larger neurocrania, less prognathic faces, and increased basicranial flexion relative to the orbital plane, resulting to some degree from more frontated and convergent orbits. The mandibular ramus is taller in catarrhines and platyrrhines, primarily from deepening the inferior ramus, but with some contribution from a taller jaw joint above the occlusal surface of dentition. However, this is attained in different ways in catarrhines and platyrrhines. On average, vaulting of the palate to move the dentition inferiorly is more characteristic of catarrhines, whereas platyrrhines exhibit an inferior displacement of the

palate and nasal chamber. Neither group has a significantly more kyphotic face compared to strepsirrhines. This differs from the results from the F-PLS due to the lack of taxonomic diversity for which the EMG data are available. The taxa included in the F-PLS generally have smaller angles between the palate and basicranium compared to strepsirrhines (Figure 4.14), but once other platyrrhine and catarrhine species were included, the difference in AFK appears negligible.

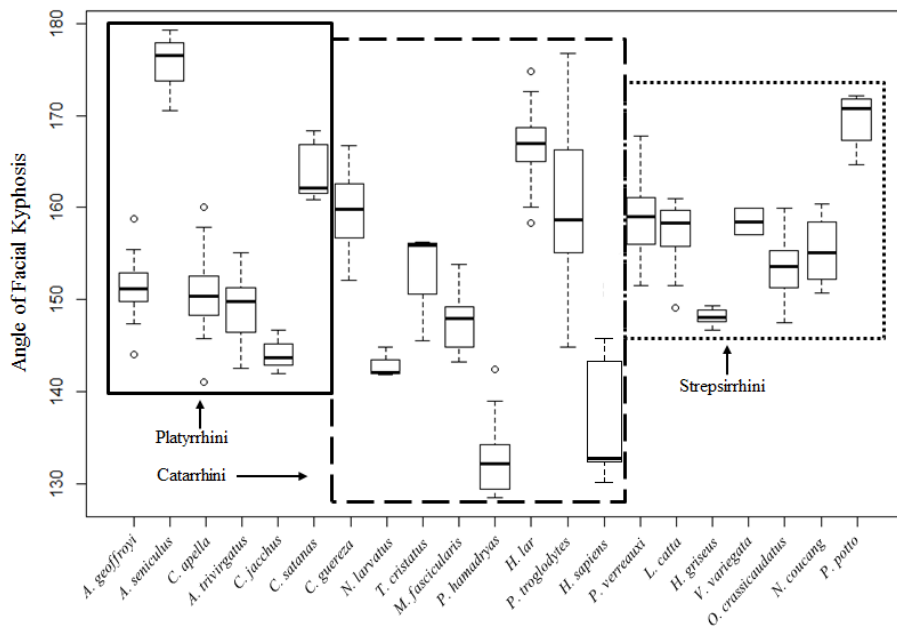


Figure 4.14: Boxplot showing the variation in the angle of facial kyphosis for each species.

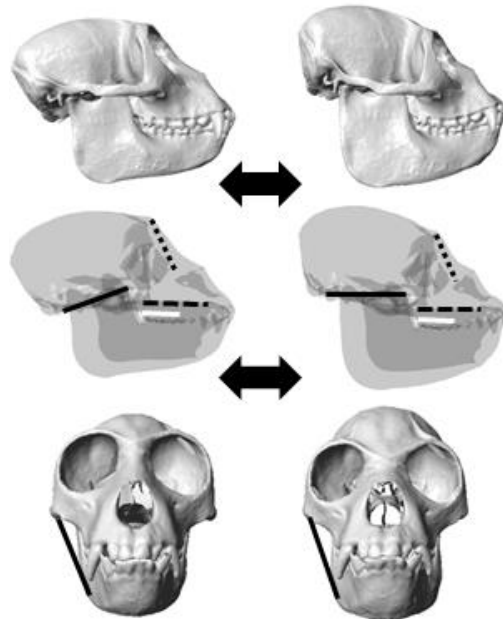
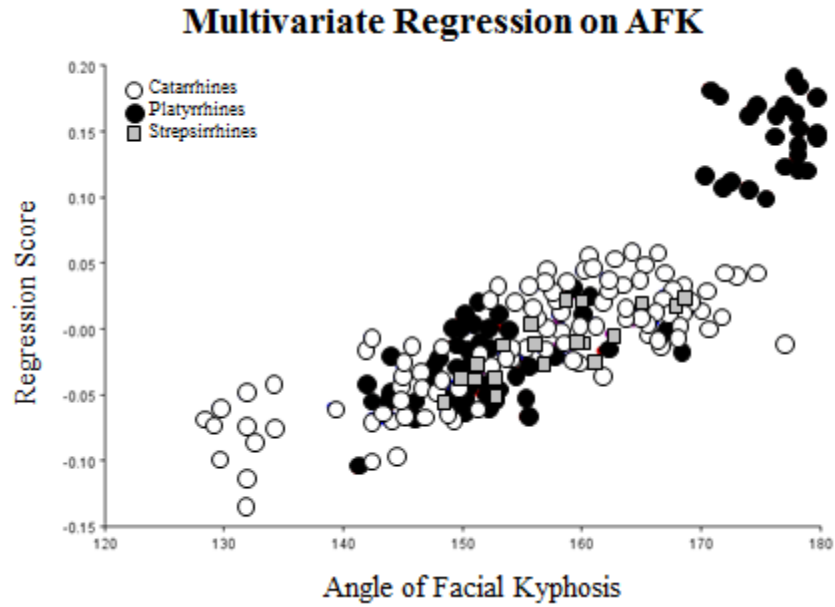


Figure 4.15: Plot the multivariate regression of skull landmark coordinates on the angle of facial kyphosis. The distinct platyrrhine group in the upper right corner is *Alouatta seniculus*. Lateral view: dotted line= orbital plane, black line= basion-hormion, dashed line= staphylion-incision, white line=m1-m3 alveolar plane. Frontal view: black line= orientation of masseter muscle from zygomatic arch to inferior ramus.

The inclusion of *Propithecus* provides a unique perspective on what drives the evolution of the WMP that is not confounded by skull characteristics that differentiate anthropoids from strepsirrhines for taxonomic rather than functional reasons. Similar to anthropoids, *Propithecus* (and likely other indriids) have more frontated orbits, increased basicranial flexion relative to the orbital plane, a less prognathic face, and no definitive change in AFK compared to other strepsirrhines lacking the WMP. The ramus is taller in *Propithecus* and, similar to platyrrhines, has a slightly taller jaw joint above the occlusal surface due to an inferior displacement of the palate. However, the main contribution to increased ramus height is below the dentition through projection of the gonial angle.

Considering all of this evidence, one must conclude that evolution of the WMP does not require the reorganizing of the skull proposed by Ravosa et al. (2000). Greater encephalization and increased facial kyphosis are not necessary for generating a taller mandibular ramus (Figures 4.8, 4.9, 4.12, and 4.15). All primates with the WMP do appear to have more frontated orbits, but it is not clear if this is directly related to ramus height. An increase in jaw joint height above the occlusal surface of dentition only partially contributes to the overall increase in ramus height between primates with and without the WMP. Additionally, jaw joint height is not related to a downward rotation of the face, as suggested by Ravosa et al. (2000), but rather through vaulting of the palate or inferior displacement of the nasal cavity and palate, two mechanisms proposed much earlier by Biegert (1957; 1963). Although the sequence of cranial changes proposed by Ravosa et al. (2000) may not be relevant to the WMP, the results from this analysis do provide support for their conclusion that a taller ramus corresponds with a more vertically-oriented masseter muscle. It has yet to be determined whether the orientation of

the deep masseter muscle has a significant impact on the transverse movements of the jaw during chewing, but the change in orientation is consistent with all primates that demonstrate the WMP. Experimental data on jaw kinematics are necessary to further address this question.

4.4.2 Morphological integration of skull components as an ESC

In addition to comparing the configuration of the skull across different groups of primates, this study investigates the morphological integration of mandibular and cranial components of the skull. Ravosa et al. (2000) refer to the conclusions drawn by other studies (Lieberman et al., 2000; Ross and Henneberg, 2005; Ross and Ravosa, 1993; Spoor, 1997) that the midline orientation of the face, basicranium, and neurocranium covary with each other to explain variations in mandibular form and masticatory function. Patterns of craniomandibular integration identified in this study do not support the hypothesis that increased encephalization, basicranial flexion, and facial kyphosis result in a higher jaw joint above the occlusal surface of the dentition and an overall increase in mandibular ramus height (Ravosa et al., 2000). Analyses of morphological integration across primate species and patterns shared within species show that increased relative neurocranial size, basicranial flexion, and facial kyphosis covary with a reduction in mandibular ramus height. However this pattern of skull integration corroborates the descriptions of skull shape patterns by Biegert (1957; 1963) with the relative size of the brain and masticatory apparatus having opposite effects on the flexion of the basicranium. These patterns are related to allometric relationships of the skull and body size as described by Biegert (1957; 1963). Smaller primates should have more flexed

basicrania due to a relatively larger neurocranium and smaller masticatory apparatus. Modern humans are unique in exhibiting the pattern of morphological integration similar to smaller primates even though it is the largest taxon included in this analysis.

From this evidence, it is unlikely that the skull morphology hypothesized to underlie the WMP constitutes an ESC, at least not in its entirety. A phenetic examination might support the anthropoid cranial reorganization proposed by Ravosa et al. (2000) hypothesis as an ESC based on general differences in skull shape between anthropoids and strepsirrhines, and on the presence of the WMP and mandibular fusion in a variety of ecological contexts across anthropoids. However upon further analysis, there is little evidence that the cranial and mandibular components evolved together as a functional unit – a requirement if they are an ESC. First, the cranial and mandibular components are not integrated in the predicted manner, both across and within primate species. This implies that greater encephalization, basicranial flexion, and facial kyphosis of the cranium did not drive the evolution of a taller mandibular ramus, the WMP, and mandibular fusion in anthropoids. The fossil record also provides some evidence for the independent evolution of these cranial and mandibular components. Multiple stem platyrrhines and catarrhines (e.g., *Aegyptopithecus*, *Chilecebus*, and *Homunculus*) have evolved complete mandibular fusion while retaining a strepsirrhine-like brain size. Second, the convergent evolution of the WMP in indriids provides insight into aspects of skull shape associated with the WMP without other confounding taxonomic differences that are not functionally relevant. Indriids (specifically *Propithecus*) do not exhibit the cranial components proposed by Ravosa et al. (2000), except for frontated orbits, when compared to other strepsirrhines but do display a taller mandibular ramus resulting in

more vertically-oriented masseter muscles. Lastly, one of the key components, facial kyphosis, does not discriminate anthropoids and strepsirrhines (Figure 4.14). Ravosa et al. (2000) suggest that a downward rotation of the face in anthropoids displaces the occlusal surface of the dentition from the jaw joint, effectively increasing mandibular ramus height. Although anthropoids do have taller mandibular rami compared to strepsirrhines, this does not appear to be directly related to facial kyphosis. Nevertheless, an ESC related to the WMP and mandibular fusion may still exist without implicating all of the proposed cranial components. A taller mandibular ramus and vertically-oriented masseter muscles are maintained in all primates exhibiting the WMP and thus may be functionally related to mandibular fusion as suggested by Ravosa et al. (2000), but ultimately determined by factors other than increased encephalization, basicranial flexion, and facial kyphosis.

4.4.3 Interpreting mandibular symphyseal fusion and the WMP

Despite extensive research on the evolution of symphyseal fusion in primates, and mammals in general, there is still no consensus on the primary function of symphyseal fusion. The arguments for fusion to provide either strength or stiffness to the symphysis lead to ultimately different interpretations regarding the underlying WMP. On one hand, the hypothesis that fusion strengthens the symphysis against greater amounts of stress ultimately characterizes fusion as a response to changes in masticatory activity patterns and loading regimes. Specifically, increased wishboning stress is caused by delayed activity of the balancing-side deep masseter muscle, which in turn results from taller ramus height and vertically-oriented deep masseter muscles. Determining the cause for

increased ramus height still remains a problem. Prior to this study greater encephalization, basicranial flexion, and facial kyphosis were thought to be the initiating factors, but the present research does not find support for this hypothesis. Interestingly, differences in the facial and palatal structure of platyrrhines and indriids versus catarrhines may provide evidence of different underlying mechanisms and independent evolution of the WMP. Nevertheless, the strength hypothesis does not interpret symphyseal fusion (at least in anthropoids) as an adaptation to changing dietary preferences but is instead ultimately a result of craniomandibular shape affecting masticatory activity patterns and loading regimes.

On the other hand, the stiffness hypothesis provides alternative interpretations for the evolution of the WMP and symphyseal fusion. Where the strength hypothesis proposes symphyseal fusion as a response to changing loading regimes, the stiffness hypothesis interprets symphyseal fusion as an adaptation to recruit and transfer mediolaterally-oriented muscle force from the balancing to working side of the mandible. A change in diet to harder or tougher foods would reasonably be expected to require recruitment of additional balancing-side muscle force. Therefore, it is possible that symphyseal fusion and delayed activity of the balancing-side deep masseter muscle evolved as an adaptive complex to transfer mediolaterally oriented muscle force across the symphysis to the working side of the jaw. The increase in ramus height that correlates with the WMP and symphyseal fusion may instead function to increase the overall size of the masseter muscles to generate greater muscle force rather than impacting the orientation and activity of the masticatory muscles. This interpretation views symphyseal fusion as an adaptation to changes in diet rather than a response to a structural

reorganization of the masticatory apparatus. However, the fossil record does not provide great support for this interpretation. Stem and early crown anthropoids do show adaptations pertaining to more frugivorous and folivorous diets (e.g., Kay et al., 1997; Kirk and Simons, 2001; Rasmussen and Simons, 1992; Simons and Rasmussen, 1996) contrary to their more insectivorous ancestors, but many extant strepsirrhines are frugivorous and retain unfused symphyses. Nevertheless, this does not necessarily prove that the evolution of the WMP and symphyseal fusion, when it occurred, would not be a beneficial adaptation to processing even marginally more mechanically demanding foods if it were to arise.

A third possibility is that the face and palatal structure initiated the WMP as described for the strength hypothesis (Ravosa and Hogue, 2004), and symphyseal fusion was needed to transfer the balancing-side muscle force to maintain the transverse movement of the mandible during the chew cycle. It is possible that unfused strepsirrhines maintain transverse movement through the working-side medial pterygoid muscle, and thus do not need to transfer mediolaterally oriented force across the symphysis. The increased height of the ramus in anthropoids and indriids could cause a more vertical orientation of the medial pterygoid muscle (similar to the masseter muscle) instigating the isolation of peak balancing-side deep masseter muscle activity at the end of the power stroke and requiring symphyseal fusion to transfer balancing-side muscle force across the symphysis. Additional experimental evidence is needed to understand the role of the medial pterygoid muscle in the chew cycle to either support or refute this hypothesis.

4.4.4 Masticatory patterns and morphology within anthropoids

Catarrhines and platyrrhines have a few distinct differences in their patterns of masticatory function. Figure 4.5 identifies patterns of masticatory function and skull shape that primarily distinguish Old World monkeys from smaller-bodied New World monkeys. The working-side deep masseter muscle fires very early and unaccompanied in the chew cycle in Old World monkeys. The working-side deep masseter muscle adducts the jaw and moves it laterally to the working-side which has the potential to create a wishboning stress at the symphysis. This peak muscle activity pattern covaries with a thicker, less vertical symphysis and the presence of an inferior transverse torus. However, these characteristics could also simply be related to other differences between platyrrhines and catarrhines. The more prognathic papionin face creates greater symphyseal curvature and thus higher wishboning stress (Vinyard and Ravosa, 1998). Increasing the anteroposterior width of the symphysis in addition to a less vertical orientation or development of an inferior transverse torus could counteract increased wishboning stress. To ascertain if the isolated activity of the working-side deep masseter muscle is a causal factor in determining symphyseal morphology, experimental evidence from strain gauge studies is needed to see if significant wishboning stress corresponds with the activity of the working-side deep masseter muscle. The force generated at the symphysis by the working-side deep masseter may be insignificant if there is not a counter force on the contralateral side of the jaw.

Conversely, the peak activity of the balancing-side superficial masseter occurs at nearly the same time as the working-side superficial masseter in small-bodied platyrrhines. A coordinated firing of the working and balancing-side superficial masseters

could twist both corpora with inferior eversion from the muscle force and superior inversion from the bite force (only on the working-side). Without counteracting forces from muscles on the ipsilateral sides (e.g., working and balancing-side medial pterygoid muscles), a twisting of the corpus would result in coronal bending at the symphysis. This hypothesis is supported by the corresponding differences in skull shape between small-bodied platyrrhines and papionins. Platyrrhines have a more transversely oriented masseter while retaining a similar orientation of the medial pterygoid muscles compared to papionins. Even if the medial pterygoids fire concurrently with the ipsilateral superficial masseters, the transverse orientation of the superficial masseters could still cause eversion of the inferior border of the corpus. Additionally, the more-vertical orientation of the symphysis and buccolingually thicker corpora in platyrrhines are better suited to resist coronal bending and torsional stress, respectively.

4.4.5 Phylogenetic context of the WMP and symphyseal fusion

The argument put forth for the evolution of mandibular fusion prior to the divergence of platyrrhines and catarrhines is based on the complexity and cascade of features associated with mandibular fusion. Proponents of this interpretation have suggested that the functional complexity of mandibular fusion in anthropoids warrants greater phylogenetic weight compared to other features (such as the loss of P2) and other instances of mandibular fusion across the primate tree (Lockwood, 2007; Ravosa, 1999). The results from this study demonstrate that the evolution of the WMP and mandibular fusion in anthropoids is not likely tied to an elaborate reconfiguration of the skull that differentiates anthropoids from strepsirrhines and may not be different from the

mechanisms exhibited by indriids. Hence the WMP and mandibular fusion should be used with caution in phylogenetic analyses as it has evolved independently in multiple lineages.

Evidence for independent evolution of the WMP in platyrrhines and catarrhines is potentially found in the manner in which members of each taxon increase the height of the mandibular ramus. Although ramus height is increased in both parvorders primarily through expanding the ramus below the dentition, the height of the mandibular condyle above the dentition also contributes to the overall ramus height, in a potentially significant way. In catarrhines, the palate is vaulted to distance the mandibular condyle from the dentition while the palate as a whole is inferiorly displaced from the condyle. Indriids share the same configuration with platyrrhines in that the inferior displacement of the palate relative to the mandibular condyle contributes a small portion to the increase in overall ramus height. Even though condylar height is only partially responsible for the increase in overall ramus height, it demonstrates separate mechanisms in platyrrhines and catarrhines for achieving an overall similar functional configuration associated with the WMP and symphyseal fusion.

A decrease in the phylogenetic importance of mandibular fusion in anthropoids (and possible evidence for independent evolution) influences the placement of fossil primates on the anthropoid evolutionary tree. In particular, *Catopithecus* and other oligopithecids have been viewed as stem anthropoids by researchers that argue for the homologous nature of mandibular fusion in anthropoids. This new insight into the evolution of the WMP and mandibular fusion in anthropoids increases the possibility that *Catopithecus* could be a basal catarrhine by reducing the phylogenetic importance of

mandibular fusion and emphasizing other features that this taxon shares with other catarrhines.

4.5 CONCLUSIONS

It is often the case with scientific research that when trying to answer one question, many more arise. The current study shows it is unlikely that the evolution of the WMP and symphyseal fusion in primates is related to greater encephalization, basicranial flexion, and facial kyphosis; however, new questions are unveiled that provide the foundation of future research. Morphological evidence supports the hypothesis that mandibular ramus height is associated with the orientation of the masseter muscles and delayed activity of the balancing-side deep masseter muscle, but underlying mechanisms driving variation in ramus height in anthropoids and strepsirrhines are still undetermined. The results presented here indicate that ramus height could partially be related to the structure of the palate and nasal cavity that are different in catarrhines and platyrrhines, potentially suggesting independent evolution. Additionally, ramus height could reflect masseter muscle size as a dietary adaptation. Fusion in strepsirrhines has historically been attributed to more mechanically demanding diets but specifically as a mechanism to resist increased dorsoventral shear stress, not as a response to the wishboning motor pattern. Studies have shown that there is a correlation between diet and symphyseal fusion in strepsirrhines, but it is unknown whether symphyseal fusion is reversible since no strepsirrhine clade has evolved symphyseal fusion and subsequently diversified into a less demanding dietary niche. In this case, fusion in strepsirrhines may also be similar to anthropoids in that once it has evolved it is not likely to reverse even with a less

mechanically demanding diet. Regardless of the ultimate factors driving increased ramus height and symphyseal fusion in different primate lineages, there is no evidence suggesting that symphyseal fusion in some clades is better for reconstructing phylogenetic relationships than in others. Symphyseal fusion should not be afforded greater weight than other characteristics in phylogenetic analyses of fossil taxa.

5 Insights into mandibular symphyseal fusion from an ontogenetic perspective

The previous few chapters have investigated the shape-function relationships of the masticatory apparatus and the impact of skull morphology on specific masticatory motor patterns. Both analyses highlighted the importance of the wishboning motor pattern and loading regime in the evolution of symphyseal morphology and fusion in all extant primates that either completely or partially fuse their symphyses. These results and interpretations challenge previous notions regarding the loading regimes associated with fusion in different primate lineages. Historically, the wishboning loading regime was explicitly tied to mandibular symphyseal fusion in crown anthropoids while partial fusion in strepsirrhines and other extinct primates was seen specifically as a response to dorsoventral shear stress (Lockwood, 2007; Ravosa, 1991; 1996; 1999; Ravosa and Hogue, 2004; Scott et al., 2012b). This interpretation was based on the ability of a partially fused symphysis to counter wishboning stress (which was addressed in Chapter 2) and the ontogenetic timing of symphyseal fusion in different primate lineages.

Extant anthropoids are the only primates known to fuse the mandible at the symphysis early on during growth and development, before or near weaning. Conversely, partial or complete fusion occurs in strepsirrhines later in ontogeny, often once dental maturity has been reached. Previous researchers have argued that this discrepancy in developmental timing of fusion reflects differences in underlying loading regimes. If adult masticatory behaviors are adopted around the time of weaning, then the presence of the wishboning motor pattern and loading regime would necessitate symphyseal fusion

around the same time (see Ravosa and Hogue, 2004). The association of dorsoventral shear with late ontogenetic fusion implies that allometric constraints of the masticatory apparatus require greater recruitment of balancing-side adductor muscle force to maintain a consistent bite force (see Ravosa and Hogue, 2004). Nevertheless, many of these assumptions had never been thoroughly tested. The aim of the following chapter is to investigate the ontogenetic trajectories of mandibular morphology in relation to expectations of different masticatory loading regimes in primates with early and late ontogenetic fusion of the mandibular symphysis. No previous studies have provided a comparative assessment of mandibular functional morphology between primates with different ontogenetic timings of symphyseal fusion and across the timing of fusion within ontogenetic series.

6 Mandibular ontogeny and the evolution of mandibular symphyseal fusion

6.1. INTRODUCTION:

Fusion of the mandibular symphysis has proven to be an enigmatic feature in the evolutionary diversification of primates. The occurrence and degree of mandibular symphyseal fusion varies across the primate and other mammalian clades and has been studied extensively over the last few decades without consensus on the underlying mechanisms driving fusion (e.g., Beecher, 1977; 1979; Crompton et al., 2008; 2010; DeGuelldre and DeVree, 1990; Greaves, 1988; 1993; Herring and Scapino, 1973; Hylander, 1979a; 1984; Hylander and Johnson, 1994; Hylander et al., 2000; Lieberman and Crompton, 2000; Ravosa, 1991; Ravosa, 1999; Ravosa et al., 2000; Scapino, 1965; 1981; Scott et al., 2012a,b; Vinyard et al., 2006; Weijs and Dantuma, 1981; Williams et al., 2008). Interspecific comparative functional and morphological studies on adult mammals have comprised the majority of attempts to understand symphyseal fusion, with few addressing fusion in an ontogenetic context (primates: Ravosa, 1996; Ravosa and Simons, 1994; Ravosa and Vinyard, 2002; Ravosa et al., 2007, rabbits: Hirschfeld et al., 1977; Weijs et al., 1989, pigs: Herring and Wineski, 1986; Herring et al., 1991; 2008; Huang et al., 1994). Nevertheless, it is known that mandibular symphyseal fusion in primates occurs postnatally, and that the ontogenetic timing of fusion varies among different primate lineages (see Ravosa and Hogue, 2004). The current study attempts to generate new hypotheses and provide insight into mandibular symphyseal fusion by

addressing the relatively unexplored relationship between mandibular symphyseal fusion and ontogeny.

6.1.1 Ontogenetic timing of symphyseal fusion

In extant anthropoids, mandibular symphyseal fusion coincides with weaning and the eruption of the first permanent molars and is characterized as early-ontogenetic fusion. This is contrasted with indriids, which display partial symphyseal fusion that occurs later in growth and development, often around the subadult or adult stage. Expectedly, the ontogenetic timing of fusion in extinct primates requires at least a partial ontogenetic series – a rarity in the fossil record. Luckily, the abundance of mandibular elements for a few extinct primate species allows estimates of ontogenetic timing of fusion for these taxa, and thereby the inference of fusion in closely related species. For example, observations of a mandibular ontogenetic series of *Archaeolemur* indicated that this genus and likely other subfossil lemurs, exhibited late-ontogenetic symphyseal fusion similar to indriids (Ravosa and Simons, 1994). Unlike indriids, however, *Archaeolemur* and some other subfossil lemurs (i.e., *Megaladapis*, *Hadropithecus*, *Archaeoindris*, and *Palaeopropithecus*) possess a fully fused or ossified mandibular symphysis. Likewise, a similar pattern of late-onset complete fusion is found in the adapoid primates *Leptadapis magnus*, *Adapis parisiensis*, and *Notharctus tenebrosus* (Ravosa, 1996). Late-ontogenetic fusion has also been proposed for the stem anthropoid, *Simonsius grangeri* (Ravosa, 1999); however, this interpretation is tenuous since it is based on a single mandibular specimen attributed to this taxon solely by size and location. Overall, current evidence

indicates that early-ontogenetic symphyseal fusion is a unique feature of the crown anthropoid clade (Ravosa, 1999).

Unfused mandibular symphyses are accompanied by a network of ligaments and fibrocartilage that hold the hemimandibles together. As discussed previously (Chapter 2), the density and orientation of ligaments varies and is likely functionally related to the transfer of muscle force or resistance of stresses generated at the symphysis. Both early- and late-ontogenetic symphyseal ossification in primates occur in the labiolingual direction (Beecher, 1977; 1979), which is perplexing given the presumed importance of wishboning stress for fusion in anthropoids (Ravosa and Hogue, 2004) and likely strepsirrhines (see Chapter 2; Hylander et al., 2011). Considering cortical bone is weaker in tension than compression and wishboning stress generates significant tension on the lingual symphysis, ossification might be expected to begin at the lingual aspect of the symphysis to fortify against wishboning stress. It is possible that the neurovascular structures housed in the lingual region of the symphysis affect the direction of fusion (Beecher, 1977; 1979; Ravosa et al., 2007), but it is also interesting to note that pigs, which experience significant lingual compression and labial tension during mastication, undergo symphyseal fusion in the opposite (i.e., lingual to labial) direction (Herring et al., 2008).

Additionally, early- and late-ontogenetic fusion have been associated with different functional underpinnings reflected in the adult masticatory loading regimes. Adult masticatory function is often inferred to be present in individuals with the eruption of the first permanent molars (Inuma et al., 1991; Smith, 1991; Vinyard and Ravosa, 1998). Early-ontogenetic fusion in crown anthropoids has been linked with the

wishboning motor pattern and loading regime, where complete symphyseal fusion provides either stiffness to transfer muscle force or strength to fortify against increased wishboning stress once adult masticatory patterns are realized. Conversely, late-ontogenetic fusion was previously argued to be functionally associated with greater recruitment of vertically-directed balancing-side adductor muscle force, either to resist increased dorsoventral shear stress or to stiffen the symphysis for transferring balancing-side muscle force to the working-side (Ravosa and Vinyard, 2002; Ravosa and Hogue, 2004). However, these interpretations likely require revisions given that EMG data suggest that sifakas have a balancing-side deep masseter recruitment pattern similar to anthropoids (Hylander et al., 2011), even though they have late-ontogenetic fusion. The combined presence of the wishboning motor pattern and morphology of the mandibular symphysis suggest that sifakas were able to resist moderate to high levels of wishboning stress (Chapter 2).

Little information exists on the ontogenetic change of jaw muscle activity in primates. Hylander et al., (1987; 1992) demonstrated that jaw muscle recruitment patterns do not change significantly between subadult and adult crab-eating macaques while other work has indicated that EMG magnitudes of the masseter becomes relatively larger compared to the temporalis during ontogeny (McNamara, 1974). Even though it is often assumed that adult masticatory function is present with the eruption of the first permanent molar, there are expectations for allometric variations in muscle force recruitment with size (Ravosa and Vinyard, 2002). Additionally, Herring et al., (2008) demonstrated variability in masticatory loading regimes with age in an ontogenetic series of pigs, supporting the notion of ontogenetic change in masticatory function.

6.1.2 Mandibular variation and function

Extensive work has focused on understanding form-function relationships of the primate mandible. Generally, these studies have analyzed interspecific variation of adult specimens either among closely related sister taxa (e.g., Daegling, 1992; Taylor and Groves, 2003; Taylor, 2005, 2006a,b; Daegling and McGraw, 2001, 2007; Terhune, 2013) or across a wider clade of primates (e.g., Bouvier, 1986a,b; Anapol and Lee, 1994; Ravosa, 1991, 1996). These analyses have tested experimentally- or theoretically-derived hypotheses that provide expectations of differences in mandibular morphology in relation to masticatory loading regimes or responses to different mechanical requirements of diet. Masticatory muscle activity and loading patterns influence the morphology of the mandible and have the potential to vary based on dietary preferences. Species with tougher diets that require greater muscle force and repetitive loading of the masticatory apparatus (e.g., folivory as opposed to frugivory) are assumed to exhibit greater masticatory loads and necessitate improved resistance to maintain similar stress and strain levels (Hylander, 1985). However, adaptations to a folivorous diet may vary among different primate clades depending on the material properties of food, masticatory behaviors, and loading patterns and regimes already in place that are in part defined by phylogenetic history (Ross et al., 2012).

Elevated levels of balancing-side jaw adductor muscle force during unilateral mastication bends the balancing-side mandibular corpus in the parasagittal plane and generates dorsoventral shear stress at the symphysis when coupled with bite point reaction forces (Hylander, 1979a,b). Experimental studies have shown that the amount of bending is directly proportional to the recruitment of balancing-side adductor muscle

force (Hylander, 1984). Resistance to parasagittal bending of the balancing-side corpus is most efficiently achieved through increasing the vertical depth of the corpus.

Additionally, dorsoventral shear stress at the symphysis is efficiently countered by increasing the cross-sectional area of cortical bone at the symphysis (Hylander, 1984).

The working-side mandibular corpus is also twisted through axial torsion about its long axis during unilateral mastication and incision (Hylander, 1979a,b, 1981). The lateral direction of the masseter muscle force resultants and medial direction of the bite force everts the inferior corpus and inverts the alveolus creating axial torsion of the corpus. This activity also generates a coronal bending of the symphysis (Hylander, 1979a,b, 1981). Even cortical bone distribution about the neutral axis to increase buccolingual thickness of the postcanine corpus most efficiently resists torsional loads while increasing the depth of the symphysis counters coronal bending (Hylander, 1979a,b, 1985). Increased muscle force or repetitive loading to process tougher foods would presumably increase the torsional loads and coronal bending at the symphysis and be reflected in the corresponding mandibular dimensions.

Experimental studies have observed wishboning stress at the symphysis (and possibly corpus) in primates that exhibit delayed activity of the balancing-side deep masseter muscle at the end of the power stroke during unilateral mastication. This muscle activity pattern and loading regime is present in anthropoids and the muscle activity pattern has been observed in indriids as well (Hylander et al., 2011). It is likely that mandibular symphyseal fusion or the presence of transversely oriented symphyseal ligaments provide the stiffness necessary for the mandible to function as a curved beam when the mandible is bent in the plane of curvature, generating wishboning stress

(Lieberman and Crompton, 2000). Without the proper symphyseal structure to transfer muscle force from balancing-side to working-side, it is feasible that the wishboning stress generated at the symphysis would diminish in the ligaments of an unfused mandibular symphysis (Herring and Mucci, 1991). Wishboning generates high tensile stress lingually and compression labially and thus increasing the labiolingual thickness or orienting the long axis of the bone more horizontally would counter increased wishboning loads (Hylander, 1985). Additionally, since the mandibular symphysis acts as a curved beam, wishboning loads increase with greater curvature of the symphysis. As symphyseal curvature tends to increase with size, larger individuals or species are expected to experience intensified wishboning stress at the symphysis (Hylander, 1985; Vinyard and Ravosa, 1998). Therefore, wishboning loads and the resulting morphological effects are expected to track size variation rather than the mechanical requirements of diet.

Other aspects of mandibular morphology are expected to vary as a result of dietary adaptations. Some researchers have argued that a shorter, deeper face with anteriorly positioned masseter muscles create a greater mechanical advantage by positioning the masticatory muscles closer to the bite point, thus improving the load-lever arm ratio and reducing the bending moments in the face (Anton, 1996; DuBrul, 1977; Hylander 1977, 1979a; Ravosa, 1990; Spencer and Demes, 1993). Additionally, bite force is inversely proportional to jaw length, so a shorter jaw increases the amount of muscle force converted into bite force (Hylander, 1979a; Spencer, 1998). Increasing the height of the temporomandibular joint above the occlusal surface is thought to more evenly distribute occlusal loads across the postcanine teeth, effectively reducing the fatigue and failure associated with repetitive loading (Herring and Herring, 1974; Ward

and Molnar, 1980). Lastly, comparative studies have shown that folivorous primates tend to have wider mandibular condyles to distribute loads across the lateral condyle during unilateral mastication (Bouvier, 1986a; Smith et al., 1983; Takahashi and Pan, 1994). This has been associated with an emphasis on postcanine food processing while anteroposterior longer condyles are associated with anterior tooth use (Smith et al., 1983; Bouvier, 1986a).

While identification of loading regimes and masticatory activity patterns in experimental studies have corresponded with expected theoretical changes in mandibular morphology, the link between diet and morphology is more tenuous. The lack of consistent relationships between diet and morphology is likely a consequence of inaccurate expectations of broad characterizations of diet and the phylogenetic history of internal and external forces associated with mastication. Dietary profiles are variable and composed of many items with different structural properties, so referring to a species as being “frugivorous” or “folivorous” may not provide enough detail of the geometric and material properties of items to generate appropriate dietary-loading regime relationships. Ultimately, dietary variation will only correspond with variation in mandibular morphology if diets differentially affect mandibular loadings regimes and stress and strain patterns in a consistent manner, which may not be expected across primate clades with different phylogenetic histories (see Ross et al., 2012).

Elongation of the jaw in many catarrhines results a larger gape which is likely to allow for the display and use of large canines for competition or defense (Hylander, 2013; Ravosa, 1996a). However, a larger gape is achieved through the elongation of masticatory muscle fibers and/or the posterior position of jaw adductor muscles that

ultimately reduce the mechanical efficiency of the masticatory apparatus (Spencer and Hogard, 2001). It is therefore expected that in a species with sexually dimorphic canines, increased gape and facial prognathism would be associated with relatively larger masticatory muscle mass to maintain functional equivalence of bite force (Hylander, 2013). Conversely, a reduction in jaw gape and more anteriorly positioned or shorter jaw muscles result in increased mechanical efficiency of the masticatory apparatus and would be expected with a reduction in canine size (Hylander, 2013). The relationship between canine size, gape, and mechanical efficiency of the masticatory apparatus provides an example of how other factors unrelated to diet can affect masticatory biomechanics.

6.1.3 Postnatal growth and development of the mandible

While interspecific analyses of adult mandibular variation have been plentiful, comparative work on the postnatal growth and development of the mandible has received less attention. Most previous ontogenetic analyses have compared scaling trajectories between closely related species using specific linear measurements associated with masticatory loading regimes and dietary adaptations in the context of heterochrony (e.g., Boughner and Dean, 2008; Cole, 1992; Daegling, 1996; Ravosa, 1992; Ravosa and Daniel, 2010; Taylor, 2002; 2003).

Regardless of the methods employed, most studies comparing ontogenetic trajectories identify prenatal or early postnatal differences in mandibular morphology between closely related species even if the overall trajectories are parallel or divergent. In *Gorilla* and *Pan*, differences in mandibular shape are present at infancy and are likely

due to prenatal developmental variation (Daegling, 1996). The two genera do not share the same slope for their ontogenetic trajectories, indicating that they have different allometric changes in mandibular shape throughout development (Daegling, 1996; Taylor, 2002). Similar conclusions have been reached for ontogenetic comparisons of *Pan paniscus* with *Pan troglodytes* (Boughner and Dean, 2008; Taylor and Groves, 2003) and *Cebus apella* with *Cebus albifrons* (Cole, 1992). These studies found that the main differences in shape between congeners are already present early in development (likely due to prenatal growth processes), although they share parallel ontogenetic trajectories during their postnatal growth (Boughner and Dean, 2008; Cole, 1992). Therefore, the shape differences between species are not simply the result extended or truncated development, but instead often result from prenatal morphological differences possibly reflecting different dietary adaptations (Cole, 1992; Taylor, 2002).

Recent ontogenetic studies by Ravosa and colleagues have sought to understand the mandibular variation across multiple strepsirrhine clades (lorises: Ravosa, 1998; 2007; galagos: Ravosa et al., 2010; indriids and lemurs: Ravosa, 1992; Ravosa and Daniels, 2010). These studies have found that much of the variation in the facial skeleton within multiple extant strepsirrhine clades is a result of extended or truncated development along similar ontogenetic trajectories (Ravosa, 1992, 1998, 2007; Ravosa and Daniel, 2010; Ravosa et al., 2010). Even though the face may be ontogenetically scaled, the mandibular dimensions exhibit divergent growth trajectories that have been interpreted as resulting from different feeding adaptations among sister taxa (Ravosa, 1992, 1998, 2007; Ravosa and Daniel, 2010; Ravosa et al., 2010).

Dental development has been identified by some authors as an important factor in mandibular morphology in hominins (Dean and Benyon, 1991), African apes (Daegling, 1996; Taylor, 2002; Taylor and Groves, 2003) and capuchins (Cole, 1992), whereas others have suggested that tooth development has little impact on mandibular morphology (Boughner and Dean, 2004, 2008). Many studies have noted the greater relative thickness of the corpus in younger individuals, and that a reduction in relative growth rates for mediolateral corpus thickness corresponds with the timing of eruption of M_1 as the influence of molar size and development on mandibular shape (Cole, 1992; Daegling, 1996; Taylor, 2002; Taylor and Groves, 2003). In contrast, Boughner and Dean (2008) argue that since the buccolingual growth of the corpus finishes after the eruption of M_1 in *Pan*, the corpus cannot contribute further space to the development of the molars. Thus, the postnatal linear ontogenetic trajectory of mandibular shape change does not coincide with the non-linear variation in tooth developmental timing (Boughner and Dean, 2008). Nevertheless, a study of the fetal development of the mandibular symphysis in humans and chimps suggests that prenatal dental development (especially of the deciduous canines) may affect the growth of the anterior corpus, with the transition of a vertical symphysis to an anteriorly inclined symphysis coinciding with the emergence of deciduous canines in chimps (Coquerelle et al., 2010). In sum, these results indicate that there is still much that is unknown about the relationship of dental development and the variation in mandibular form.

6.1.4 Study goals

The goals of this study are to quantify and compare ontogenetic patterns of shape change for primate species representing different clades, and to identify similar and disparate adaptations to masticatory loading regimes. The majority of previous studies on the growth and development of mandibular form and function have analyzed closely related species or subspecies. However, Ravosa and colleagues (Ravosa, 1992, 1998, 2007; Ravosa and Daniel, 2010; Ravosa et al., 2010) have provided some initial work on clade-wide scaling patterns of craniomandibular dimensions among strepsirrhines to interpret variations in masticatory loading regimes among species. The goal of this analysis is not only to compare ontogenetic trajectories among clades, but also to investigate potential changes in masticatory loading regimes during growth and development in association with the timing of symphyseal fusion. In this context, the ontogenetic shape changes associated with mandibular symphyseal fusion are investigated for representative species that exhibit either complete or partial symphyseal fusion. All extant primates that exhibit complete symphyseal fusion in adulthood undergo early ontogenetic fusion while partial fusion in extant primates is associated with late ontogenetic fusion. Partial and complete fusion have been hypothesized to result from different loading regimes and thus different morphologies are expected. Mandibular shapes of specimens with and without fusion in an ontogenetic series are compared to determine whether the shape changes associated with fusion reflect loading regimes within each species. To the author's knowledge, this work provides the first comparative analysis of mandibular ontogeny and the timing of symphyseal fusion between species that vary in the degree and ontogenetic timing of fusion.

6.2 MATERIALS AND METHODS

The sample in this analysis includes a mixed-sex, cross-sectional ontogenetic series of mandibles for six primate species. The species were chosen to include representatives from most of the major primate clades and include primates that demonstrate variability in mandibular symphyseal fusion: complete fusion, partial fusion, and no fusion. The ontogenetic series for each species was divided into 4 discrete age classes based on dental eruption stages: all deciduous, M₁ in occlusion, M₂ in occlusion, and M₃ in occlusion or adult (Table 6.1). When possible, each age class was represented by roughly equal numbers of males and females. Some individuals of unknown sex were included but primarily in the younger age classes. All mandibles were scanned using a Breuckmann SmartSCAN white light scanner using 90mm lenses. The individual scans for each specimen were cleaned, aligned, and merged using Geomagic Design software to create 3D models of each primate mandible.

Table 6.1: Sample size by age group for each taxon.

	Taxon	Deciduous only	M₁ in occlusion	M₂ in occlusion	M₃ in occlusion	Timing/degree of fusion
Cercopitheciidae	<i>Macaca fascicularis</i>	10	10	10	23	early/complete fusion
	<i>Colobus guereza</i>	2	3	3	25	early/complete fusion
Hominidae	<i>Pan troglodytes</i>	10	10	10	25	early/complete fusion
Cebidae	<i>Cebus apella</i>	10	10	10	25	early/complete fusion
Lemuridae	<i>Lemur catta</i>	4	3	3	23	unfused
Indriidae	<i>Propithecus verreauxi</i>	3	4	4	23	late/partial fusion
	Total:	39	40	40	144	

Table 6.2: List of mandibular landmarks and semilandmarks. Landmarks begin with “M” and semilandmarks begin with “MS”.

Landmark number	Landmark description	Bilateral/Midline/Symmetric
M1	Most medial point on the articular surface of the mandibular condyle	Bilateral
M2	Most lateral point on the articular surface of the mandibular condyle	Bilateral
M3	Most anterior point on the mandibular condyle at the midpoint of the mediolateral curve	Bilateral
M4	Most posterior point on the mandibular condyle at the midpoint of the mediolateral curve	Bilateral
M5	Coronion	Bilateral
M6	Attachment of the anterior ascending ramus on the mandibular corpus	Bilateral
M7	Gonion	Bilateral
M8	Inferior border of the mandibular foramen	Bilateral
M9	Most distal molar point projected on the alveolar margin	Bilateral
M10	Point on the lingual alveolar margin at the midpoint of m1	Bilateral
M11	Most inferior point on mandibular corpus under m1	Bilateral
M12	Point on the buccal alveolar margin at the midpoint of m1	Bilateral
M13	Premolar-molar contact projected on the buccal alveolar margin	Bilateral
M14	Premolar-molar contact projected on the lingual alveolar margin	Bilateral
M15	Canine-premolar contact projected on the buccal alveolar margin	Bilateral
M16	Canine-premolar contact projected on the lingual alveolar margin	Bilateral
M17	Most inferior point on the mental foramen	Bilateral
M18	Most mesial point on the midline of m1	Bilateral
M19	Contact at the apex of the central incisor	Midline
M20	Infradentale	Midline
M21	Gnathion	Midline
M22	Mandibular orale	Midline
MS1	Mandibular border curve (p=63)	Symmetric
MS2	Coronoid process curve (p=21)	Bilateral
MS3	Mandibular corpus outline under m1 (p=15)	Bilateral
MS4	Mandibular symphysis outline (p=21)	Midline

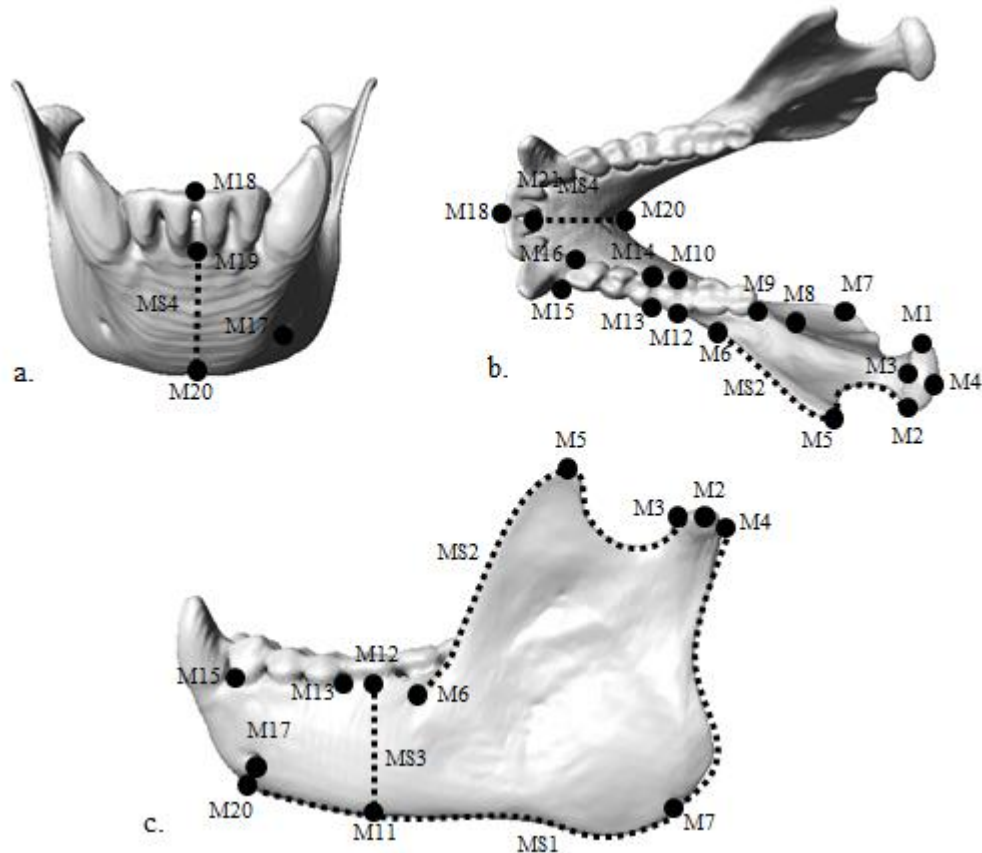


Figure 6.1: Mandibular (a-rostral, b-dorsal, c-lateral) landmarks and semilandmark curves (blue lines) used in this analysis. Both sides of the mandible were digitized, but only landmarks on the left side and midline are displayed.

A series of homologous landmarks and semilandmarks was placed on each specimen using Stratovan Checkpoint software (Stratovan Corporation, Davis, CA) (Table 6.2, Figure 6.1). Semilandmark curves were densely sampled to best approximate the actual curvature of the morphology and then resampled to obtain a series of evenly-spaced points for each curve using RESAMPLE.exe (available at pages.nycep.org/nmg/, created by David Reddy and Johann Kimm, edited by Dr. Ryan Raaum). A densely sampled curve provides greater detail of the bone's curvature and decreases the deviation of the semilandmarks off of the surface when sliding along the curve tangents.

Nevertheless, large numbers of semilandmarks capture minute details of the morphology that may not be to the research questions being asked and mask morphological patterns of interest. In this analysis, different numbers of evenly-spaced points were exported and analyzed to determine the appropriate density of semilandmarks for each curve. Missing landmarks in a few specimens were estimated within species-age categories using the thin-plate spline interpolation method in the Geomorph package in R (Adams and Otarola-Castillo, 2013).

The raw landmark configurations were superimposed to only represent shape variation among specimens using a generalized Procrustes analysis that translates each configuration to a common origin, scale configurations to a centroid size of one, and iteratively rotates the configurations to minimize the Procrustes distance between homologous landmarks (Gower, 1975; Rohlf and Slice, 1990) using the Geomorph package in R (Adams and Otarola-Castillo, 2013). During superimposition, the semilandmarks were allowed to slide along tangents to the curves under the criterion of minimizing bending energy to create geometric homology of the semilandmark curves across specimens (Bookstein, 1997; Gunz et al., 2005). Procrustes superimpositions were calculated separately for each species when analyzing each ontogenetic series but included multiple species when investigating shared patterns of shape change among age cohorts.

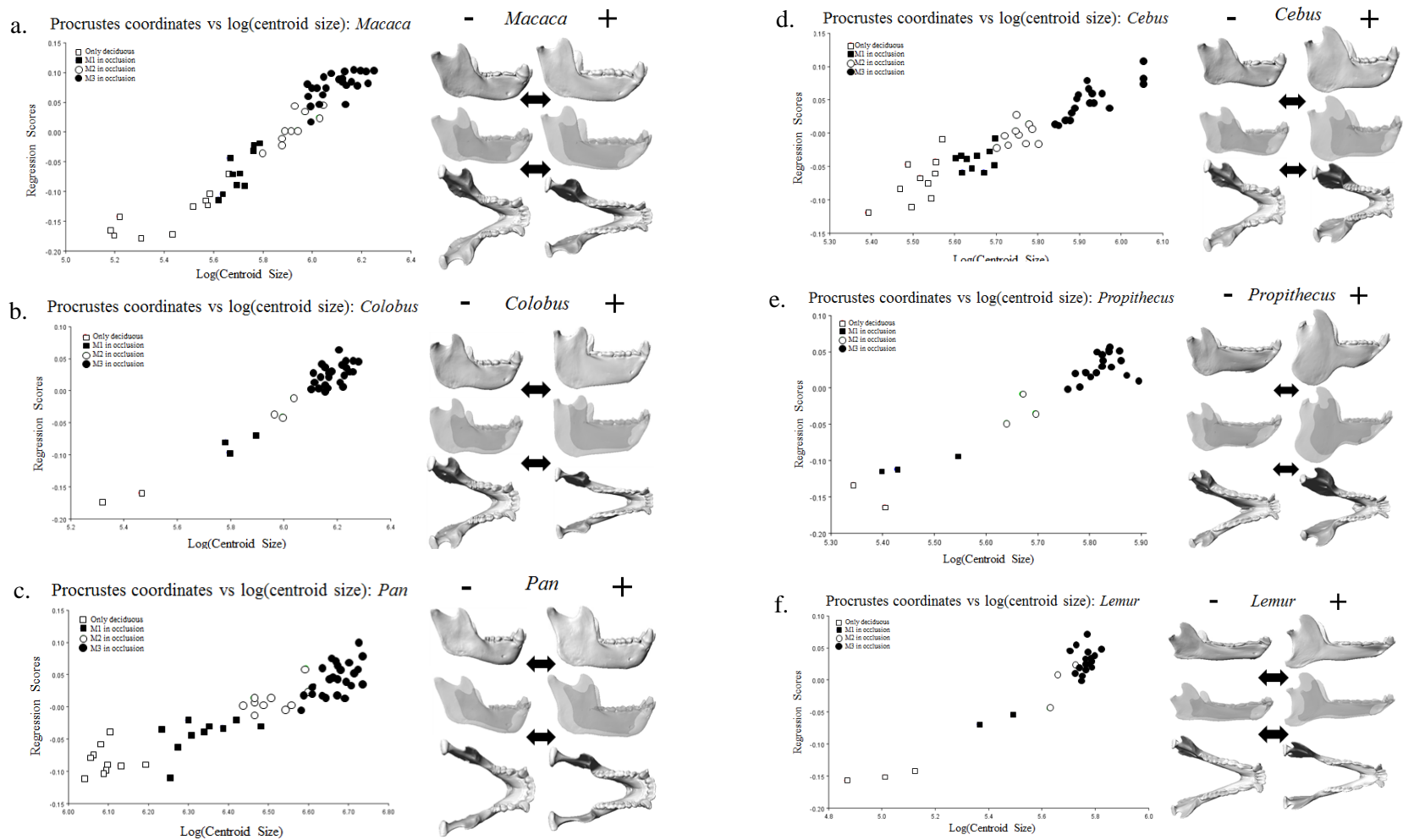


Figure 6.2: Multivariate regression of the Procrustes landmark coordinates on log centroid size for the ontogenetic series of (a) *Macaca fascicularis*, (b) *Colobus guereza*, (c) *Pan troglodytes*, (d) *Cebus apella*, (e) *Propithecus verreauxi*, and (f) *Lemur catta*. The ontogenetic allometric vector of shape change is visualized to the right of each plot from negative end (left column) to positive end (right column) of the axis.

To explore the effects of ontogenetic allometry on mandibular shape, multivariate regressions of Procrustes shape coordinates on log centroid size were computed individually for each of the six species. Multivariate regression scores were calculated and plotted against log centroid size of the mandible for each species. Multivariate regressions (Klingenberg, 2016; Monteiro, 1999) were also computed for the Procrustes shape coordinates on age class, but the resulting vectors of shape change were not interpretively different from those calculated using log centroid size for each species and therefore only the latter are reported (see Simons and Frost, 2016). Descriptions of the shape change associated with ontogenetic allometry are provided for each species and interpreted based on potential variations in loading regimes experienced during ontogeny.

Canonical variates analysis (CVA) and between-group principal component analysis (BGPCA) were used to analyze differences between age groups. Both are ordination methods that distinguish among groups by calculating eigenvectors of group mean configurations. Whereas CVA ordinated means within a space transformed to maximize group differences, and hence requires assumptions of within-group homogeneity of covariance, BGPCA is a rigid rotation of the original shape space based on differences in group mean configurations (Boulesteix, 2005; Mitteroecker and Bookstein, 2011).

Differences in age categories were first analyzed within anthropoids, *Lemur catta*, and *Propithecus verreauxi*. Anthropoids were grouped together since all experience early ontogenetic and complete fusion of the mandibular symphysis. *Lemur* retains an unfused mandibular symphysis throughout ontogeny, and *Propithecus* exhibits late ontogenetic, partial fusion. Only BGPCA was used to compare age groups within *Lemur* and

Propithecus due to small sample sizes within the various age groups. Shape changes among age groups were interpreted to highlight possible changes in loading regimes during growth and development.

Lastly, to investigate the specific shape changes associated with mandibular symphyseal fusion, between-group principal component analyses were performed separately for *Macaca fascicularis* and *Propithecus verreauxi* within the age groups associated with complete or partial fusion. This approach minimized other age-related shape variations found in the longer ontogenetic series. *Macaca* exhibits early ontogenetic fusion where the mandibular symphysis is completely ossified before the eruption of M₁. Conversely, partial symphyseal fusion generally occurs once dental adulthood is achieved in *Propithecus*. The groups that define these BGPCAs are those individuals with unfused symphyses contrasted with those that have reached the terminal state of fusion for that taxon (complete fusion in *Macaca* and partial fusion in *Propithecus*), thereby illustrating mean differences in mandibular shape associated with the development of symphyseal fusion.

6.3 RESULTS

6.3.1 Ontogenetic allometric patterns of mandibular shape in primates

In *Macaca fascicularis*, symphyseal curvature and relative mandibular length increases with size and age (Figure 6.2a). Ramus height increases with size and age through greater depth of the gonial region and increasing height of the condyle above the occlusal surface. The area of the coronoid process increases as the height of the mandibular condyle increases, so the heights of the mandibular condyle and coronoid process remain

comparable throughout ontogeny. However, the mandibular condyle becomes wider and anteroposteriorly shorter in older, larger specimens. Corpus depth increases and width decreases with size resulting in taller, thinner corpora in larger specimens. The symphyseal region becomes less vertically inclined and the inferior transverse torus becomes larger and projects further posteriorly as the mandible gets larger; however, the relative size of the superior transverse torus does not change significantly during ontogeny.

Colobus guereza demonstrates an ontogenetic allometric pattern of increase symphyseal curvature with size and age (Figure 6.2b). Larger, older individuals have a taller mandibular ramus with a deeper gonial region and taller mandibular condyle above the occlusal surface. Unlike other species in this analysis, the relative height and size of the coronoid process does not significantly change during ontogeny. Smaller specimens have a noticeably shorter condyle relative to the coronoid process. Mandibular condyles are anteroposteriorly shorter in larger specimens, but the mediolateral width does not appear to change significantly with size or age. The mandibular corpus becomes deeper and narrower as size increases while the symphysis becomes labiolingually thicker (through increased projection of both superior and inferior transverse tori) and less vertically oriented.

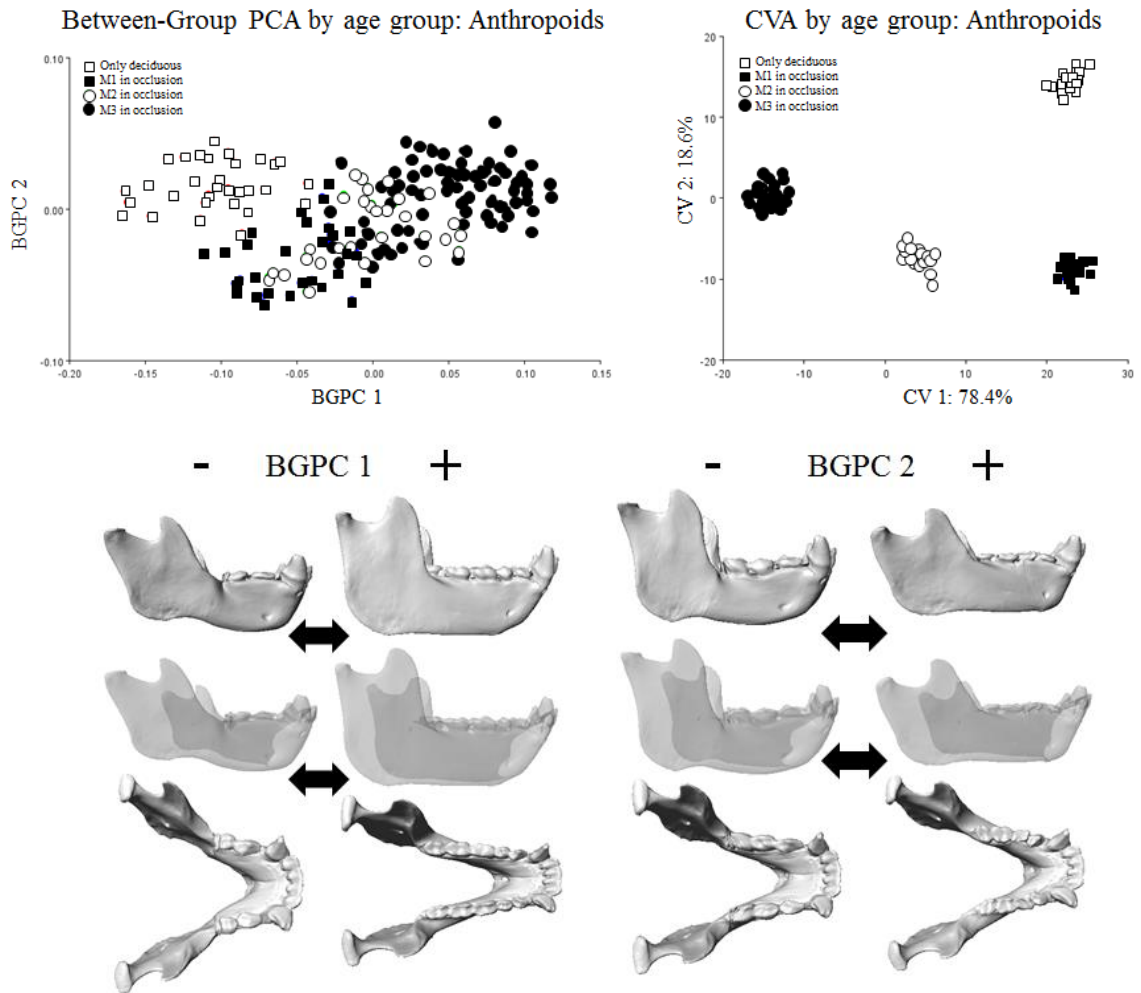


Figure 6.3: Results from a between-group PCA and canonical variates analysis of all anthropoid specimens using age group as the classifying variable. The shape vectors described by the BGPC and CV axes are similar, so only the shape vectors for the first two BGPC axes are visualized.

Between-Group PCA by age group: *Propithecus*

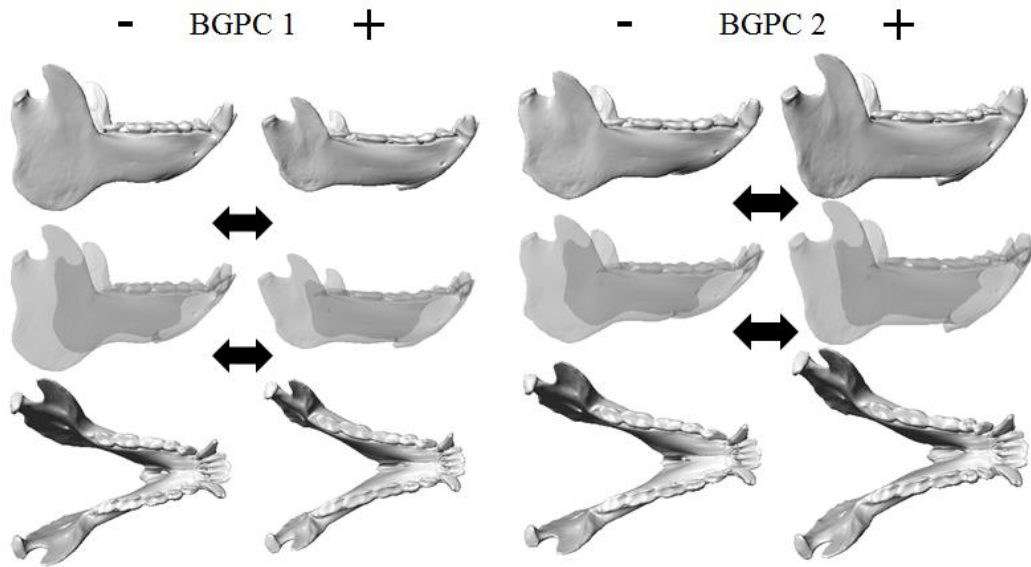
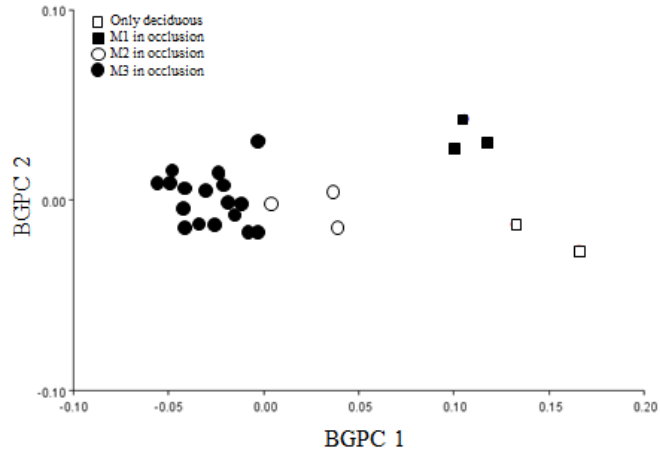


Figure 6.4: Results from a between-group PCA on the mean configurations of the different age groups of *Propithecus verreauxi*. The shape vectors for the first two BGPC axes are visualized.

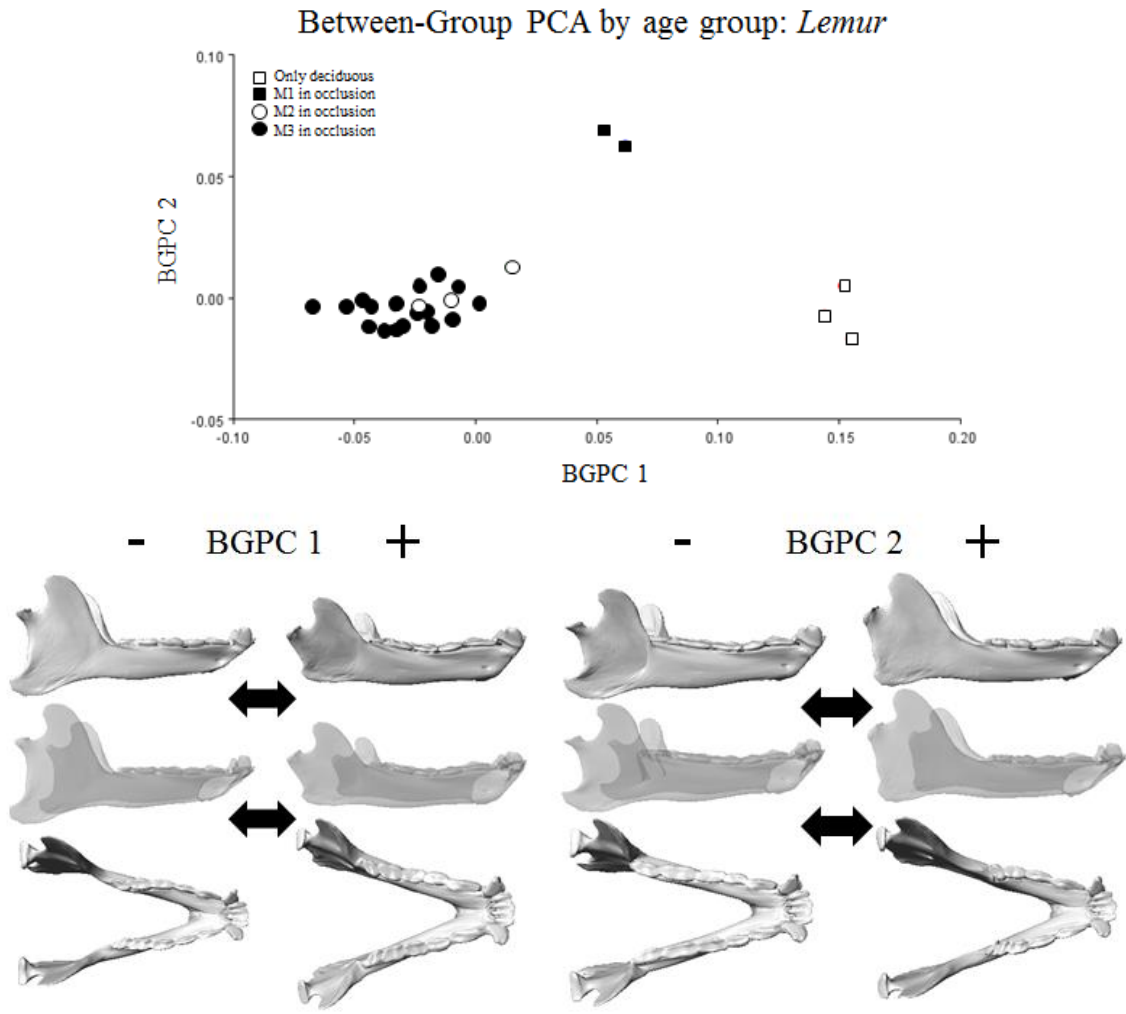


Figure 6.5: Results from a between-group PCA on the mean configurations of the different age groups of *Lemur catta*. The shape vectors for the first two BGPC axes are visualized.

Pan troglodytes shows many similarities in ontogenetic allometric patterns with *Macaca* and *Colobus* (Figure 6.2c). Larger mandibles have increased symphyseal curvature, larger surface area of the mandibular ramus, deeper gonion, and taller mandibular condyles and coronoid processes. Similar to *Macaca*, the coronoid process and mandibular condyle retain similar heights relative to each other throughout ontogeny. As mandibular size increases, the condyles become relatively wider and anteroposteriorly shorter. Additionally, the corpus becomes taller and narrower which is also demonstrated to some degree in the symphysis. Larger specimens have a labiolingually thinner symphysis with a less projecting superior transverse torus, although it is less inclined and has a more developed inferior transverse torus.

The ontogenetic trajectory of *Cebus apella* is similar to those of other anthropoids with some nuanced differences (Figure 6.2d). Symphyseal curvature does not appear to change relative to size or age when considering the curvature of the mandible from the symphysis to approximately M₁. However, the overall curvature of the mandible is more parabolic in smaller specimens and U-shaped in larger specimens, with the primary differences in shape occurring posterior to M₁. Similar to *Macaca* and *Pan*, both the coronoid process and condyle increase in height as centroid size increases; however, the coronoid process increases in size at a greater rate leading to a configuration in larger individuals where the coronoid process is significantly taller than the condyle. Smaller individuals have a coronoid process and condyle of similar height. The mandibular condyle increases in width but decreases in length as mandibular size increases. The cross-sectional area of the mandibular symphysis does not appear to change with size or

age, but larger individuals have a less vertical symphyseal orientation with a reduction in the superior transverse torus but an expansion of the inferior transverse torus.

The curvature of the mandible changes in *Propithecus verreauxi* from a more parabolic shape in smaller specimens to U-shape in larger specimens (Figure 6.2e). Thus, the curvature of the symphyseal region (from the symphysis to approximately M₁) is greater in younger specimens but the bigonial width is relatively smaller in larger specimens. During ontogeny, the gonial region deepens and the coronoid process and mandibular condyle increase in height above the occlusal surface. The coronoid process and condyle maintain similar geometric relationships relative to each other during ontogeny, as seen in *Macaca* and *Pan*. The dimensions of the mandibular condyle do not appear to change significantly during ontogeny in *Propithecus*. Unlike anthropoids, the corpus does not appear to deepen significantly during growth and development, but corpus width decreases in a manner similar to other primates. Similarly, the relative cross-sectional area of the symphysis decreases during ontogeny in *Propithecus* with a slight increase in the expansion of the inferior transverse torus and corresponding reduction in the superior transverse torus.

Lemur catta shows no change in symphyseal curvature or relative length of the mandible during ontogeny (Figure 6.2f). The inferior ramus is slightly everted with a relatively narrower bigonial width in larger specimens. During ontogeny the gonial angle is expanded and the mandibular ramus increases in height through inferior projection of gonial angle and increase in condylar height above the occlusal surface. The condyle and coronoid process both increase in height during ontogeny but maintain similar relationships as seen in *Propithecus*. The mandibular ramus becomes more vertically

oriented with an increase in centroid size. The mandibular condyle is slightly wider but anteroposteriorly shorter in older specimens. Similar to *Propithecus*, the corpus becomes relatively narrow during growth and development but does not appear to change in relative height. Similarly, relative symphyseal size decreases throughout ontogeny but the orientation is slightly less vertical with a more anterior projection of the tooth comb.

Overall *Pan*, *Macaca*, and *Colobus* exhibit greater proportional growth of the mandibular corpus relative to the ramus which also results in an overall relative increase in symphyseal size throughout ontogeny in these taxa, whereas the other taxa (*Cebus*, *Propithecus*, and *Lemur*) have greater proportional growth of the mandibular ramus and a reduction or no change in relative symphyseal size during ontogeny.

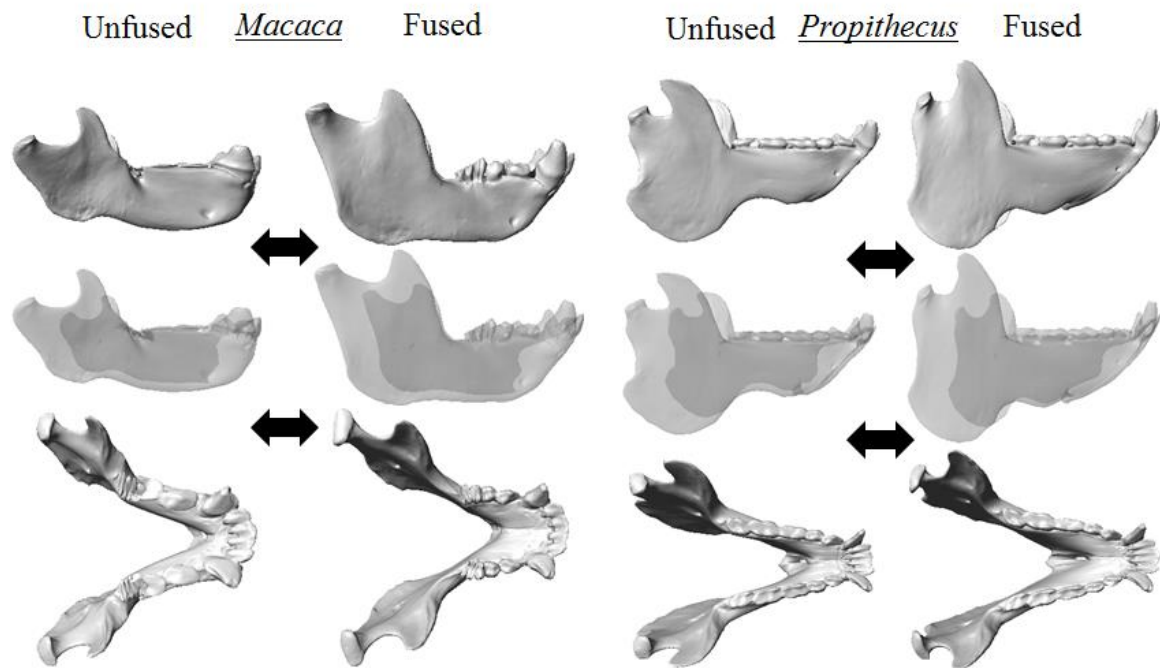


Figure 6.6: Visualization of the shape change between specimens with and without symphyseal fusion in *Macaca fascicularis* and *Propithecus verreauxi*.

6.3.2 Mandibular variation among age groups

While the CVA expectedly provides better separation among age groups than does BGPCA, both analyses yield similar shape vectors (Figure 6.3), and therefore, only the BGPCA shape visualizations are discussed. Additionally, the overlap between age groups demonstrated in the BGPCA plot provides perhaps a better representation of the continuous effects of age on morphology. Even though means were computed for discrete age groups, some individuals are inherently closer in age to the prior group while others are closer to the subsequent age group, and this is better reflected in the variance within groups of the BGPCA.

In the analysis of anthropoids, the first BGPC axes distinguish adults with fully erupted M_{3s} from those with only deciduous dentition or M_1 in occlusion (Figure 6.3). Relatively longer and narrower mandibles occur toward the end of the axis occupied by adults. This end of the axis is also characterized by mandibular condyles and coronoid processes that are higher above the occlusal surface of the dentition with a corresponding deeper gonial region. The condyles increase slightly in mediolateral width but decrease in anteroposterior length. The mandibular corpus is vertically deeper and the symphysis is less vertically oriented with a more prominent inferior transverse torus and reduced superior transverse torus. The second axis separates individuals with a fully occluded M_1 from individuals with only deciduous dentition (Figure 6.3). The other two age groups (M_2 and M_3 in occlusion) fall in between or closer to the youngest age group depending on the plot. Most of the shape patterns along this axis are similar to the first CV and BGPC axes except that the end of the axis containing juveniles with fully erupted M_{1s} demonstrate both larger superior and inferior transverse tori in addition to a taller ramus

and higher mandibular condyles and coronoid processes above the occlusal surface of dentition.

The BGPCAs on the age groups of *Propithecus verreauxi* and *Lemur catta* yield similar plots to the analyses of anthropoids by separating specimens with only deciduous dentition and adults with fully erupted M₃s on the first axis and those with M₁ in occlusion from the other groups on the second axis. Along the first BGPC axis using the *Propithecus* ontogenetic series (Figure 6.4), adults with fully erupted M₃s plot at the end characterized by relatively shorter mandibles with taller condyles and coronoid processes along with a larger, deeper gonial region. Moving from negative to positive along this axis, the mandibular arch becomes narrower anteriorly and wider posteriorly describing a more V-shaped mandible in specimens with only deciduous dentition and a U-shaped mandible in adult specimens. The mandibular condyles increase in mediolateral width moving toward the end of the axis occupied by adult specimens. Along the second BGPC axis, individuals with M₁ in occlusion occupy the end of the axis that represents a higher coronoid process and larger inferior transverse torus in comparison to specimens with only deciduous dentition.

The first axis of the BGPCA on the ontogenetic series of *Lemur* resembles that of both anthropoids and *Propithecus* in that the end of the axis occupied by adults with M₃ in occlusion is characterized by a taller mandibular ramus and higher condyles and coronoid processes above the occlusal surface of dentition (Figure 6.5). However, an increase in the dimensions of the ramus does not coincide with a deeper mandibular corpus or more robust symphysis. Conversely, the mandibular symphysis becomes less vertically oriented but relatively smaller. The M₁ age group is separated from the other

age groups along the second axis by plotting at the end of the axis associated with a posteriorly expanded coronoid process, anteroposteriorly longer mandibular condyles, less posteriorly projecting gonial region, and a taller but narrower symphysis.

6.3.3 *Intraspecific mandibular shape and symphyseal fusion*

A BGPCA was run on specimens of *Macaca fascicularis* that have only erupted deciduous dentition in order to determine the mandibular variation occurring during the process of mandibular symphyseal fusion (Figure 6.6). Within this dental age group, symphyseal fusion occurs with an overall larger mandibular ramus by increasing the height of the mandibular condyle and coronoid process and deepening the gonial region. The mandibular symphysis is less vertically oriented but has more projecting superior and inferior transverse tori and no change in the relative height of the corpus. Additionally, the relative length and curvature of the mandibular symphysis does not appear to differ between fused and unfused *Macaca* specimens with only erupted deciduous dentition.

The pattern of variation displayed in the late fusing *Propithecus verreauxi* resembles many of the shape changes associated with complete fusion in *Macaca fascicularis* (Figure 6.6) Among dental adult specimens of *Propithecus*, those with partial symphyseal fusion on average have taller mandibular condyles and coronoid processes above the occlusal surface of the dentition in addition to deeper gonial regions. Additionally, the mandibular symphysis is slightly less vertical with a more projecting inferior transverse torus. However, unlike *Macaca*, *Propithecus* specimens with partial fusion also have deeper corpora relative to their unfused counterparts.

6.4 DISCUSSION

6.4.1 Comparison of ontogenetic allometric patterns of mandibular shape and function among primate species

Some patterns in the growth and development of the mandible are conserved among primates. Anthropoids and strepsirrhines alike increase the relative size of the mandibular ramus in older specimens. The mandibular ramus broadens, the gonial region deepens, and both the coronoid process and mandibular condyle increase in height above the occlusal surface of dentition. The increase in area of the coronoid process and mandibular ramus suggest an increase in relative size of the masticatory muscles since they are the attachment sites for the temporalis and masseter muscles, respectively. Masticatory muscle size has been used as a reflection for the ability to generate muscle force and subsequently bite force (Anton, 1996; Hylander, 1979a,b; Ravosa, 1990; Taylor, 2002). Masseter muscle size has been shown to increase with positive allometry in ontogenetic series of *Gorilla* and *Cebus* suggesting that older, larger specimens are able to generate greater muscle and bite force (Cole, 1992; Taylor, 2002). The results in this analysis not only corroborate these previous studies and demonstrate similar patterns in two strepsirrhine taxa, but additionally find that greater bite force likely occurs in larger, older individuals specifically through a relatively larger temporalis muscle in addition to the masseter muscle.

Previous work has suggested that the shape of the mandibular condyles reflects the primary locations along the dental arcade used for processing food (Bouvier, 1986a,b; Smith et al., 1983; Takahashi and Pan, 1994). Mediolaterally wider condyles are associated with repetitive loading along the postcanine dentition while anteroposteriorly

longer condyles are thought to reflect greater usage of the anterior dentition. Each of the primates in this analysis demonstrates a shift in condylar shape toward mediolaterally wider but anteroposteriorly shorter mandibular condyles with increased age or size. This is not to suggest that individuals transition from loading the anterior dentition to postcanine dentition as they age, but perhaps that the muscle or bite force generated at the postcanine dentition during mastication increases with age. This would support the interpretations of masticatory muscle size based on the relative sizes of the attachment sites. Unfortunately, ontogenetic series of tree-gouging primates such as marmoset or tamarins which exhibit significant loading of the anterior dentition were not sampled for this study. Future ontogenetic investigations into the mandibular growth and development of primate species that preferentially load different aspects of the mandible would be very insightful.

The morphology of the mandibular symphysis and corpus are expected to reflect masticatory loading regimes and the stresses generated in the mandible from muscle and bite force (Hylander, 1985). The anthropoids in this study all develop a more prominent inferior transverse torus during ontogeny but either experience no change or a reduction in the relative size of the superior transverse torus. Additionally, the orientation of the long axis of the symphysis becomes anteriorly inclined with age in anthropoids, although *Cebus* experiences a less drastic shift in the orientation of the symphysis during growth and development. The development of the inferior transverse torus and orientation of the symphysis suggests that older individuals are better equipped to resist increased wishboning stress than younger individuals of the same species. With the increase in size of the masseter muscles, it is likely that greater wishboning stress is generated from an

increase in balancing-side deep masseter muscle force during unilateral mastication. Additionally, the wishboning loading regime is also expected to increase with age as a reflection of the geometric properties of the mandible. Older, larger specimens have longer mandibles with greater symphyseal curvature that generate greater wishboning stress (Hylander, 1985; Vinyard and Ravosa, 1998). The change in orientation of the symphysis appears to transfer the primary effect of resisting symphyseal wishboning stress from the superior transverse torus to the inferior transverse torus. A reduction in the vertical orientation of the symphysis is associated with development of the inferior transverse torus and often a decrease in size of the superior transverse torus. With a less vertical orientation, an increase in symphyseal thickness through the superior transverse torus is not directly oriented in the labiolingual plane that would most efficiently resist wishboning stress. Thus, the projection of the inferior transverse torus in conjunction with the orientation of the long axis of the symphysis likely provides a better approximation of the ability to resist wishboning stress. Consequently, many previous studies have utilized the labiolingual thickness of the symphysis (at the superior transverse torus) as a proxy for the ability to resist wishboning stress by measuring the greatest thickness of the symphysis perpendicular to the long axis of the symphysis (e.g., Hylander, 1985; Ravosa, 1991; Ravosa and Daniel, 2010; Vinyard and Ravosa, 1998). However, this approach does not account for symphyseal orientation or the inferior transverse torus as a factor in resisting wishboning stress.

In comparison, *Propithecus* exhibits some changes in symphyseal shape and orientation that are similar to changes found in anthropoids, particularly the reduction of the superior transverse torus while the inferior transverse torus becomes more prominent

with age. However, symphyseal curvature does not appear to increase with age as it does in anthropoids suggesting that changes in the geometric properties of the mandible may not result in increased wishboning stress with age. It may also be the case that the lack of symphyseal fusion throughout most of growth and development does not permit an efficient transfer of transversely oriented balancing-side muscle force across the symphysis (Lieberman and Crompton, 2000), limiting the amount of wishboning stress generated during chewing. In contrast to anthropoids, the symphysis of *Lemur* becomes more elliptical in shape but reduced in relative size with age. Older *Lemur* individuals would therefore be less able to resist increased levels of wishboning stress than younger individuals. This is not surprising considering experimental studies and interspecific comparisons of mandibular shape suggest that the wishboning loading regime and transverse movement of the mandible is not of great importance in *Lemur* and other strepsirrhines lacking fusion.

In anthropoids, the depth of the corpus increases with age suggesting the corpus in older individuals is structured to resist greater amounts of parasagittal bending and/or larger working-side bite and muscle forces resulting in greater shear behind the bite point than in younger individuals. Hylander (1985) has suggested that direct shear behind the bite point on the working-side of the jaw might have the greatest impact on corpus morphology. Increased balancing-side parasagittal bending from greater recruitment of vertically oriented balancing-side muscle force is also expected to correspond with increased cross-sectional area of the symphysis to resist dorsoventral shear stress. A larger symphyseal cross-section is only demonstrated in *Macaca* and *Colobus* indicating possible increased recruitment of vertically oriented balancing-side adductor muscle

force with age. Although symphyseal orientation and shape in *Pan* and *Cebus* change during ontogeny, the overall cross-sectional surface area of the symphysis does not appear to change significantly during growth and development. Therefore, it is possible that the increase in corpus height in *Pan* and *Cebus* may simply reflect resistance to greater muscle force generated on the working-side corpus rather than increased recruitment of balancing-side vertical muscle force with age (which is hypothesized for *Macaca* and *Colobus*). These differences in ontogenetic patterns of corpus shape provide testable hypotheses for ontogenetic differences in masticatory loading regimes within anthropoids, but ontogenetic experimental studies are necessary to confirm these hypotheses. Nevertheless, the results of this analysis support previous interpretations that the diminishing buccolingual thickness of the corpus with age likely reflects the size of the postcanine dentition (Cole, 1992; Daegling, 1996; Taylor, 2002) and obscures the relationship between corpus width and mandibular loading regimes.

Interestingly, the relative symphyseal cross-sectional area and corpus height do not appear to change significantly with age or size in the *Propithecus* and *Lemur*. This would suggest that neither *Propithecus* nor *Lemur* are structured to resist greater parasagittal bending of the corpus and dorsoventral shear of the symphysis from greater recruitment of balancing-side vertical adductor muscle force, not unlike *Pan* and *Cebus*. However, the static configuration of corpus height also suggests that there was no significant increase in direct shear of the working-side corpus from larger working-side muscle and bite forces.

6.4.2 Mandibular shape variation associated with early and late ontogenetic fusion

Weaning in primates occurs with the eruption of the first permanent molars and has been thought to coincide with the adoption of adult masticatory patterns and loading regimes (Iinuma et al., 1991; Smith, 1991; Vinyard and Ravosa, 1998). The early timing of symphyseal fusion in anthropoids has been inferred to result from adopting an adult masticatory loading regime that relies on the late activity of the balancing-side deep masseter muscle to generate mediolateral movement of the jaw at the end of the power stroke (Ravosa and Hogue, 2004). Therefore, symphyseal fusion is necessary prior to weaning to either resist the wishboning stress generated at the symphysis or transfer transversely oriented muscle force across the symphysis. When comparing mandibular shape between anthropoid specimens before weaning (only deciduous dentition) and after weaning (M_1 in occlusion), the resulting shape differences provide support for the assumption of adopting adult-like masticatory function associated with generating wishboning stress. Individuals with M_1 in occlusion have a taller mandibular ramus with higher condyles above the occlusal surface of the dentition which has previously been associated with delayed activity of the balancing-side deep masseter muscle and increased wishboning stress. The mandibular symphysis is larger in cross-sectional area with better developed superior and inferior transverse tori. This is opposed to the overall pattern of symphyseal shape associated with growth and development within anthropoid species that demonstrates a reduction in the superior transverse torus with an increase in age. These changes in symphyseal morphology produce a symphysis that is better equipped to resist increased dorsoventral shear and wishboning stress. Similar results are found when making comparisons between fused and unfused macaques with only

deciduous dentition except that the mandibular symphysis is also more horizontally inclined and therefore better equipped to resist wishboning stress in specimens with symphyseal fusion.

With the assumption that weaning benchmarks the acquisition of adult masticatory patterns (Iinuma et al., 1991; Smith, 1991; Vinyard and Ravosa, 1998), late symphyseal fusion in indriids has previously been attributed to resisting increased dorsoventral shear stress generated through greater recruitment of balancing-side adductor muscle force later in development. Delayed activity of the balancing-side deep masseter muscle associated with transverse movement of the jaw during mastication and wishboning stress has been identified in adult indriids (Hylander et al., 2011). Therefore, the expectation of adopting adult masticatory function post-weaning and the late development of symphyseal fusion in indriids suggest initially that fusion does not occur as a result of mediolateral jaw movements or increased wishboning stress, but instead from greater dorsoventral shear by recruiting vertically oriented balancing-side muscle force. However, this study demonstrates through ontogenetic shape changes that partial symphyseal fusion in *Propithecus verreauxi* coincides with the production of increased wishboning stress and transverse jaw movements during mastication. *Propithecus* specimens with M₁ in occlusion differ from specimens with only deciduous dentition by primarily having an overall more robust symphysis, deeper corpora, and larger coronoid processes. An overall greater cross-section of the symphysis provides better resistance for increased dorsoventral shear stress which possibly coincides with greater balancing-side adductor muscle force from a larger temporalis muscle (inferred by larger coronoid processes). The lack of any change in ramus or condylar height and no change in

orientation of the symphysis indicates that *Propithecus* does not exhibit improved resistance to wishboning stress or mandibular shapes associated with the wishboning loading regime. Conversely, comparisons between dental adults with and without partial symphyseal fusion identify patterns of mandibular shape variation generally associated with the wishboning loading regime. *Propithecus* adults with partial fusion display a taller mandibular ramus and condyles higher above the occlusal surface of the dentition. Additionally, the symphysis has a long axis that is more horizontally oriented orientation and elongated which would specifically provide better resistance to increased wishboning stress. This morphological evidence provides tentative support for the relationship between late ontogenetic symphyseal fusion in indriids and the wishboning loading regime, contrasting previous inferences that highlight dorsoventral shear stress as the primary factor in indriids fusion (c.f. Ravosa, 1991; 1999; Ravosa and Hogue, 2004). Additionally, these results also provide support for the hypothesis that delayed activity of the balancing-side deep masseter muscle is delayed as a result of a taller mandibular ramus and vertically oriented masseter or medial pterygoid muscles (Ravosa et al., 2000). Ramus height increases with age and size in *Propithecus* and may reach a point where the masseter and/or medial pterygoid are not able to provide adequate transverse mandibular movements, requiring a shift to the WMP. If true, this muscle orientation threshold would be crossed late in ontogeny and coincide with stiffening of the mandibular symphysis through partial fusion and changes in symphyseal shape that resist higher magnitudes of wishboning stress. This analysis introduces new testable hypotheses for the development of the wishboning motor pattern later in ontogeny in indriids rather than assuming the adoption of adult masticatory function soon after weaning.

6.4.3 An ontogenetic perspective on the strength and stiffness hypotheses for symphyseal fusion

Debate remains as to whether symphyseal fusion functions primarily to strengthen the mandibular symphysis to resist increased stress generated during mastication or to stiffen the symphysis to allow for the efficient transfer of balancing-side muscle force across the symphysis to the working-side of the jaw. The difficulty is in separating whether symphyseal fusion is necessary to transfer mediolaterally oriented muscle force and generate transverse mandibular movements or whether an unfused symphysis is adequate to transfer mediolateral muscle force and fusion is a consequence providing resistance to the wishboning stress resulting from those masticatory forces. In either case, symphyseal fusion is expected to occur with the ontogenetic development and evolution of the wishboning motor pattern and loading regime. However, the hypothesis for symphyseal fusion to create a stiff articulation of the hemimandibles to transfer balancing-side muscle force also predicts that symphyseal shape and orientation should reflect resistance to increased wishboning stress at the symphysis as a result of the transfer of force. Conversely, if symphyseal fusion is occurring to strengthen the symphysis against increased wishboning stress, no additional changes in symphyseal shape or orientation are necessarily expected. In anthropoids and strepsirrhines, intraspecific comparisons of mandibular shape between specimens with and without fusion in an ontogenetic context find that timing of fusion during ontogeny corresponds with changes in symphyseal orientation and shape that are best interpreted as providing resistance to increased wishboning stress. These results indicate that either symphyseal fusion

primarily functions to stiffen the mandibular symphysis or that fusion alone does not adequately strengthen the symphysis to resist wishboning stress, and additional structural changes are required.

While morphological evidence appears to support the stiffness model for symphyseal fusion (see Chapter 2), future experimental EMG studies on an ontogenetic series of *Propithecus verreauxi* could provide the adequate proof needed to settle the strength versus stiffness debate, or elaborate that both may play a part in causing fusion. The morphological evidence in this analysis (based as well on previous interspecific work associating particular mandibular morphologies with the wishboning motor pattern and loading regime; Chapter 2) suggests that the wishboning loading regime does not develop until later in ontogeny in *Propithecus*, in conjunction with partial symphyseal fusion. If this hypothesis were supported by experimental studies, at least partial symphyseal fusion would appear to be necessary to stiffen the symphysis to transfer balancing-side muscle force across the symphysis. However, if the wishboning motor pattern and loading regime are demonstrated in juveniles immediately after weaning, the lack of symphyseal fusion in these specimens would suggest that the ligamentous articulations in an unfused mandibular symphysis are adequate to transfer mediolaterally oriented muscle force across the symphysis. As such, symphyseal fusion would likely occur later in ontogeny to resist increased recruitment of balancing-side muscle force (likely dorsoventral shear stress) at the symphysis. These circumstances would additionally require a reexamination of the mandibular shape changes associated with the wishboning loading regime, as many of the diagnosed patterns of mandibular shape are not present in the indriid mandible post-weaning, as previously discussed.

6.5 CONCLUSIONS

Ontogenetic patterns of mandibular shape change can be used to generate hypotheses as to how masticatory loading regimes, stress, and strain patterns change during growth and development. Comparisons across primate clades find that some mandibular ontogenetic allometric patterns are conserved in primates. Areas for the attachments of the temporalis and masseter muscles increase in relative size with age suggesting an ability to generate greater muscle and perhaps bite force with in older individuals. This is also supported by the increase in corpus height demonstrated in each anthropoid ontogenetic series indicating an increased ability to resist parasagittal bending from greater muscle and bite forces during unilateral mastication. However, relative corpus height does not appear to change in the strepsirrhine ontogenetic series. This might indicate that masticatory muscle size increases only to maintain functional equivalency rather than increasing the amount of stress or strain experienced by the corpus. Interestingly, primates with complete or partial symphyseal fusion demonstrate a greater ability to resist increased wishboning stress with age through the development of an inferior transverse torus and anterior inclination of the symphysis and a presumed decreased reliance on the superior transverse torus for resisting wishboning stress.

Previous studies have linked wishboning stress to early-ontogenetic, complete fusion in anthropoids and dorsoventral shear stress to late-ontogenetic, partial fusion in indriids. Observations of mandibular shape variation associated with the ontogenetic occurrence of symphyseal fusion in anthropoids supports the hypothesis that fusion is a function of the wishboning loading regime. Remarkably, the mandibular shape patterns associated with the early-occurrence of fusion in anthropoids are similar to those

observed during the transition to a partially fused symphysis in indriids, late in ontogeny. If mandibular shape provides a reliable predictor of masticatory loading regimes (wishboning in particular), then fusion in anthropoids and indriids likely occur from the adoption of similar loading regimes and may signify significant changes in masticatory activity later in growth and development for indriids.

7 Summary

Previous discussions of mandibular symphyseal fusion in primates have created a narrative that supports an ancestral crown anthropoid morphotype with a completely fused symphysis and distinct underlying factors associated with fusion in anthropoids compared to strepsirrhines. This interpretation has support in the observations that anthropoids differ from strepsirrhines in both the ontogenetic timing and degree of symphyseal fusion. Comparative morphological studies between anthropoids and those strepsirrhines without symphyseal fusion have led researchers to hypothesize that an increase in brain size and other correlated changes in skull morphology led to the development of the wishboning motor pattern, ultimately requiring complete symphyseal fusion in anthropoids to withstand these new masticatory forces and stresses. Conversely, partial fusion in strepsirrhines has been attributed strictly to resisting increased masticatory forces and stresses generated from eating more mechanically demanding diets. Ultimately, this explanation has led to the use of mandibular symphyseal fusion in the reconstruction of early anthropoid evolutionary relationships to the extent of excluding oligopithecids from the crown anthropoid clade.

However, some evidence has cast doubt in these interpretations. First, fossil evidence indicates that stem catarrhines and platyrrhines with fused symphyses retained relative brain sizes, similar to strepsirrhines rather than extant anthropoids (Radinsky, 1977; Simons et al., 2007; Sears et al., 2008), suggesting that increases in brain size were not a driving factor in the evolution of symphyseal fusion in anthropoids. Second, Hylander et al., (2011) observed that *Propithecus verreauxi* shares the wishboning motor

pattern with anthropoids, previously thought to be unique to the anthropoid clade. Lastly, other researchers have provided evidence supporting the alternative, yet not entirely distinct, hypothesis that mandibular symphyseal fusion functions to stiffen the symphysis to transfer balancing-side muscle force rather than strengthening it against masticatory stresses (Lieberman and Crompton, 2000). These doubts bring skepticism to the current narrative and prompted the present studies analyzing previously held notions regarding symphyseal fusion.

An interspecific examination of mandibular morphology in relation to biomechanical variables associated with different masticatory loading regimes identifies shape-function relationships associated with wishboning in anthropoids but also in indriids with partial fusion. Evaluating fossil anthropoids in the context of these shape-function relationships (and in general comparison to strepsirrhines without fusion) indicated that these taxa were capable of resisting greater amount of dorsoventral shear and wishboning stress and possess mandibular shapes accompanying the wishboning loading regime. One of these fossil anthropoids is *Catopithecus browni*, an oligopithecoid previously assigned as a stem anthropoid based on the assumption that it lacked the wishboning loading regime and whose phylogenetic placement has been greatly debated among researchers. The symphyseal morphology suggests *Catopithecus* was able to resist higher magnitudes of wishboning and dorsoventral shear stress compared to similar sized strepsirrhines, although the retention of only a partially fused symphysis remains enigmatic.

The hypothesis that brain size is related to changes in the masticatory apparatus that could ultimately result in mandibular symphyseal fusion had never been previously

tested until this study. While extant anthropoids generally differ from strepsirrhines in relative brain size and other skull features, analyses investigating the integration of these components with the morphology of the masticatory apparatus show that they are not integrated with a configuration associated with the wishboning loading regime. Rather, integrated patterns within the masticatory apparatus hint at the idea that catarrhines and platyrrhines may have evolved the wishboning loading regime, and therefore symphyseal fusion, independently.

The evaluation of mandibular symphyseal fusion from an ontogenetic perspective indicates that the ability to resist wishboning stress in primates with complete or partial fusion increases with age through an anterior inclination of the symphysis and development of an inferior transverse torus. Additionally, even though anthropoids and strepsirrhines have different ontogenetic timing of fusion, analyses of mandibular shape changes occurring at the specific timing of fusion in each indicates that the fusion is likely accompanied by the wishboning motor pattern and loading regime in both cases.

Overall, the results from these analyses tentatively support the hypothesis that fusion functions to stiffen the symphysis to allow for the transfer of force across the symphysis. This does not preclude the idea that ossifying the halves of the symphysis would strengthen the joint as well, but the additional changes in shape and orientation accompanying fusion suggest that these other methods may be better suited to countering increased wishboning stress. Nevertheless, as discussed in the previous chapter, determining the ontogenetic onset of the wishboning motor pattern in *Propithecus verreauxi* through experimental EMG studies might provide enough evidence to

determine which model is most appropriate for the function of mandibular symphyseal fusion.

8 References

- Adams, D. C., & Felice, R. N. (2014). Assessing trait covariation and morphological integration on phylogenies using evolutionary covariance matrices. *Plos One*, 1-8.
- Adams, D. C., & Otarola-Castillo, E. (2013). Geomorph: an R package for the collection and analysis of geometric morphometric shape data. *Methods in Ecology and Evolution*, 4, 393-399.
- Anapol, F., & Lee, S. (1994). Morphological adaptations to diet in platyrrhine primates. *American Journal of Physical Anthropology*, 239-261.
- Anton, S. C. (1996). Cranial adaptation to a high attrition diet in Japanese macaques. *International Journal of Primatology*, 401-427.
- Bastir, M., Rosas, A., Stringer, C., Cuetara, J. M., Kruszynski, R., Weber, G. W., et al. (2010). Effects of brain and facial size on basicranial form in human and primate evolution. *Journal of Human Evolution*, 58, 424-431.
- Beard, C. K., Qi, T., Dawson, M. R., Wang, B., & Li, C. (1994). A diverse new primate fauna from middle Eocene fissure-fillings in southeastern China. *Nature*, 604-609.
- Beard, K. C., Tong, Y., Dawson, M., Wang, J., & Huang, X. (1996). Earliest complete dentition of an anthropoid primate from the late middle Eocene of Shanxi Province, China. *Science*, 272, 82-85.
- Beecher, R. (1977). Function and fusion at the mandibular symphysis. *American Journal of Physical Anthropology*, 47, 325-336.
- Beecher, R. (1979). Functional significance of the mandibular symphysis. *Journal of Morphology*, 47, 117-130.
- Biegert, J. (1957). Der Formandel des Primateschindels und seine Beziehungen zur ontogenetischen Entwicklung und den phylogenetischen Spezialisierungen der Kopforgane. *Morph Jahrb*, 77-199.
- Biegert, J. (1963). The evaluation of characteristics of the skull, hands and feet for primate taxonomy. In S. L. Washburn, *Classification and Human Evolution* (pp. 116-145). Chicago: Aldine Publishing Co.
- Bookstein, F. L. (1991). *Morphometric tools for landmark data: Geometry and Biology*. New York: Cambridge University Press.

- Bookstein, F. L. (1997). Landmark methods for forms without landmarks: morphometrics of group differences in outline shape. *Medical Image Analysis*, 225-243.
- Bookstein, F. L. (2015). The relation between geometric morphometrics and functional morphology, as explored by Procrustes interpretation of individual shape measures pertinent to function. *The Anatomical Record*, 314-327.
- Boughner, J. C., & Dean, C. M. (2004). Does space in the jaw influence the timing of molar crown initiation? A model using baboons (*Papio anubis*) and great apes (*Pan troglodytes*, *Pan paniscus*). *Journal of Human Evolution*, 255-277.
- Boughner, J. C., & Dean, C. M. (2008). Mandibular shape, ontogeny, and dental development in bonobos (*Pan paniscus*) and chimpanzees (*Pan troglodytes*). *Evolutionary Biology*, 296-308.
- Boulesteix, A. L. (2005). A note on between-group PCA. *International Journal of Pure and Applied Mathematics*, 19, 359-366.
- Bouvier, M. (1986a). A biomechanical analysis of mandibular scaling in Old World monkeys. *American Journal of Physical Anthropology*, 69, 473-482.
- Bouvier, M. (1986b). Biomechanical scaling of mandibular dimensions in New World monkeys. *International Journal of Primatology*, 7(6), 551-567.
- Cachel, S. (1984). Growth and allometry in primate masticatory muscles. *Archives of Oral Biology*, 29(4), 287-293.
- Cartmill, M. (1970). *The orbits of arboreal mammals*. Ph.D. Dissertation: University of Chicago.
- Cartmill, M. (1972). Arboreal adaptations and the origin of the order Primates. In R. Tuttle, *The functional and evolutionary biology of primates* (pp. 97-122). New York: Aldine de Gruyter.
- Cole, T. M. (1993). Postnatal heterochrony of the masticatory apparatus in *Cebus apella* and *Cebus albifrons*. *Journal of Human Evolution*, 253-282.
- Coquerelle, M., Bookstein, F. L., Braga, J., Halazonetis, D. J., & Weber, G. W. (2010). Fetal and infant growth patterns of the mandibular symphysis in modern and human chimpanzees. *Journal of Anatomy*, 507-520.
- Crompton, A. W., Lieberman, D. E., Owerkowicz, T., Baudinette, R. V., & Skinner, J. (2008). Motor control of masticatory movements in the southern hairy-nosed

- wombat. In C. J. Vinyard, M. J. Ravosa, & C. E. Wall, *Primate Craniofacial Function and Biology* (pp. 84-111). New York: Springer.
- Crompton, A. W., Owerkowicz, T., & Skinner, J. (2010). Masticatory motor pattern in the Koala (*Phascolarctos cinereus*): a comparison of jaw movements in marsupial and placental herbivores. *Journal of Experimental Zoology A: Ecology Genetics and Physiology*, 564-578.
- Currey, J. D. (1984). *The mechanical adaptations of bones*. Princeton: Princeton University Press.
- Dabelow, A. (1929). Über korrelationen in der phylogenetischen Entwicklung der Schadelform. *Morph Jahrb*, 1-49.
- Daegling, D. J. (1992). Mandibular morphology and diet in the genus *Cebus*. *International Journal of Primatology*, 545-570.
- Daegling, D. J. (1996). Growth in the mandibles of African apes. *Journal of Human Evolution*, 315-341.
- Daegling, D. J. (2001). Biomechanical scaling of the hominoid mandibular symphysis. *Journal of Morphology*, 12-23.
- Daegling, D. J., & Grine, F. E. (1991). Compact bone distribution and biomechanics of early hominid mandibles. *American Journal of Physical Anthropology*, 321-339.
- Daegling, D., & McGraw, S. (2001). Feeding, diet, and jaw form in western African *Colobus* and *Procolobus*. *International Journal of Primatology*, 22(6), 1033-1055.
- Daegling, D., & McGraw, S. (2007). Functional morphology of the mangabey mandibular corpus: Relationship to dental specializations and feeding behavior. *American Journal of Physical Anthropology*, 134, 50-62.
- Dean, M. C., & Beynon, A. D. (1991). Tooth crown heights, tooth wear, sexual dimorphism and jaw growth in hominoids. *Zeitschrift für Morphologie und Anthropologie*, 425-440.
- DeGueudre, G., & DeVree, F. (1990). Biomechanics of the masticatory apparatus of *Pteropus giganteus* (Megachiroptera). *Journal of Zoology*, 311-332.
- Dessem, D. (1985). The transmission of muscle force across the unfused symphysis in mammalian carnivores. *Fortschritte Der Zoologie*, 289-291.
- Dryden, I. L., & Mardia, K. V. (1992). Size and shape analysis of landmark data. *Biometrika*, 57-68.

- DuBrul, E. L. (1977). Early hominid feeding mechanisms. *American Journal of Physical Anthropology*, 305-320.
- DuBrul, E. L. (1977). Early hominid feeding mechanisms. *American Journal of Physical Anthropology*, 305-320.
- DuBrul, E. L., & Laskin, D. M. (1961). Preadaptive potentialities of the mammalian skull: an experiment in growth and form. *American Journal of Anatomy*, 117-132.
- DuBrul, E. L., & Sicher, H. (1954). *The Adaptive Chin*. Springfield, Il: Charles C. Thomas.
- Enlow, D. H. (1990). *Facial Growth*. Philadelphia: Saunders.
- Escoufier, Y. (1973). Le traitement des variables vectorielles. *Biometrics*, 751-760.
- Fleagle, J. G. (1999). *Primate Adaptation and Evolution*. New York: Academic Press.
- Fleagle, J. G., & Kay, R. F. (1987). The phyletic position of the Parapithecidae. *Journal of Human Evolution*, 16, 483-532.
- Gebo, D. (2002). *Adapiforms: Phylogeny and adaptation*. Cambridge University Press.
- Giebel, C. G. (1874-1883). In *Bronn's Klassen und Ordnungen des Thierreiches: Säugethiere, Bd. 6: Abt. 5, Buch 1*, (pp. 81-90). Leipzig: C. F. Winter'sche Verlaghandlung.
- Godfrey, L. R., Jungers, W. L., Reed, K. E., Simons, E. L., & Chatrath, P. S. (1997). Subfossil lemurs: inferences about past and present primate communities. In S. M. Goodman, & B. Patterson, *Natural Change and Human Impact in Madagascar* (pp. 218-256). Washington: Smithsonian Institution Press.
- Godfrey, L. R., Samonds, K. E., Jungers, W. L., Sutherland, M. R., & Irwin, M. T. (2004). Ontogenetic correlates of diet in Malagasy lemurs. *American Journal of Physical Anthropology*, 250-276.
- Godfrey, L. R., Semperebon, G. M., Schwartz, G. T., Burney, D. A., Jungers, W. L., Flanagan, E. K., et al. (2005). New insights into old lemurs: The trophic adaptations of the Archaeolemuridae. *International Journal of Primatology*, 825-854.
- Goodall, C. R. (1991). Procrustes methods in the statistical analysis of shape. *Journal of the Royal Statistical Society, Series B*, 285-339.
- Gould, S. J. (1977). *Ontogeny and Phylogeny*. Cambridge, Ma: Harvard University Press.

- Gower, J. C. (1975). Generalized Procrustes Analysis. *Psychometrika*, 40(1), 33-51.
- Greaves, W. S. (1988). A functional consequence of an ossified mandibular symphysis. *American Journal of Physical Anthropology*, 53-56.
- Greaves, W. S. (1993). Reply to Drs. Ravosa and Hylander. *American Journal of Physical Anthropology*, 513-514.
- Gunz, P., & Mitteroecker, P. (2013). Semilandmarks: A method for quantifying curves and surfaces. *Hystrix, the Italian Journal of Mammalogy*, 1-7.
- Gunz, P., Mitteroecker, P., & Bookstein, F. L. (2005). Semilandmarks in three dimensions. In D. E. Slice, *Modern Morphometrics in Physical Anthropology* (pp. 73-98). New York: Plenum Publishers.
- Hannam, A. G., Inkster, W. C., & Scott, J. D. (1975). Peak electromyographic activity and jaw closing force in man. *Journal of Dental Research*, 694.
- Happel, R. (1988). Seed-eating by West African cercopithecines, with reference to the evolution of bilophodont molars. *American Journal of Physical Anthropology*, 303-327.
- Harrison, T. (1987). The phylogenetic relationships of the early catarrhine primates: A review of the current evidence. *Journal of Human Evolution*, 16, 41-80.
- Hartwig, W. C. (2002). *The Primate Fossil Record*. Cambridge: Cambridge University Press.
- Herring, S. W., & Herring, S. E. (1974). The superficial masseter and gape in mammals. *The American Naturalist*, 561-576.
- Herring, S. W. (1985). The ontogeny of mammalian mastication. *American Zoologist*, 25, 339-349.
- Herring, S. W., & Mucci, R. J. (1991). In vivo strain in cranial sutures: the zygomatic arch. *Journal of Morphology*, 225-239.
- Herring, S. W., & Scapino, R. P. (1973). Physiology of feeding in miniature pigs. *Journal of Morphology*, 427-460.
- Herring, S. W., & Wineski, L. E. (1986). Development of the masseter muscle and oral behavior in the pig. *Journal of Experimental Zoology*, 191-207.
- Herring, S. W., Anapol, F. C., & Wineski, L. E. (1991). Motor-unit territories in the masseter muscle of infant pigs. *Archives of Oral Biology*, 867-873.

- Herring, S. W., Rafferty, K. L., Liu, Z. J., & Sun, Z. (2008). A nonprimate model for the fused symphysis: In vivo studies in the pig. In C. J. Vinyard, M. J. Ravosa, & C. Wall, *Primate Craniofacial Function and Biology* (pp. 19-38). Springer.
- Hiiemae, K. M., & Kay, R. F. (1973). Evolutionary trends in the dynamics of primate mastication. *Symposium of the Fourth International Congress of Primatology*, 28-64.
- Hiiemae, K., & Kay, R. F. (1972). Trends in the evolution of primate mastication. *Nature*, 486-487.
- Hirschfeld, Z., Michaeli, Y., & Weinreb, M. M. (1977). Symphysis menti of the rabbit: Anatomy, histology, and postnatal development. *Journal of Dental Research*, 850-857.
- Huang, X., Zhang, G., & Herring, S. W. (1994). Age changes in mastication in the pig. *Comparative Biochemistry and Physiology*, 647-654.
- Huttenberger, S. M., & Mitteroecker, P. (2011). Invariance and meaningfulness in phenotype spaces. *Evolutionary Biology*, 335-351.
- Hylander, W. (1979a). Mandibular function in *Galago crassicaudatus* and *Macaca fascicularis*: An in vivo approach to stress analysis of the mandible. *Journal of Morphology*, 159(2), 253-296.
- Hylander, W. (1979b). The functional significance of the primate mandibular form. *Journal of Morphology*, 160, 223-240.
- Hylander, W. (1984). Stress and strain in the mandibular symphysis of primates: A test of competing hypotheses. *American Journal of Physical Anthropology*, 64, 1-46.
- Hylander, W. L. (1975). Incisor size and diet in anthropoids with special reference to Cercopithecidae. *Science*, 1095-1098.
- Hylander, W. L. (1977). In vivo bone strain in the mandible of *Galago crassicaudatus*. *American Journal of Physical Anthropology*, 309-326.
- Hylander, W. L. (1981). Patterns of stress and strain in the macaque mandible. In C. S. Carlson, *Craniofacial biology. Monograph #10, Craniofacial Growth Series* (pp. 1-37). Ann Arbor: University of Michigan.
- Hylander, W. L. (1985). Mandibular function and biomechanical stress and scaling. *American Zoologist*, 25, 315-330.

- Hylander, W. L. (1986). In-vivo bone strain as an indicator of masticatory bite force in *Macaca fascicularis*. *Archives in Oral Biology*, 149-157.
- Hylander, W. L. (1988). Implications of in vivo experiments for interpreting the functional significance of "robust" australopithecine jaws. In F. E. Grine, *Evolutionary history of the "robust" australopithecines* (pp. 55-83). New York: Aldine.
- Hylander, W. L. (2006). Functional Anatomy and Biomechanics of the Masticatory Apparatus. In D. M. Laskin, C. Greene, & W. L. Hylander, *Temporomandibular Disorders: An Evidence Based Approach to Diagnosis and Treatment* (pp. 3-34). Quintessence Publishing Co.
- Hylander, W. L. (2013). Functional links between canine height and jaw gape in catarrhines with special reference to early hominins. *American Journal of Physical Anthropology*, 247-259.
- Hylander, W. L., & Crompton, A. W. (1986). Jaw movements and patterns of mandibular bone strain during mastication in the monkey *Macaca fascicularis*. *Archives of Oral Biology*, 841-848.
- Hylander, W. L., & Johnson, K. R. (1985). Temporalis and masseter muscle function during incision in macaques and humans. *International Journal of Primatology*, 289-322.
- Hylander, W. L., & Johnson, K. R. (1989). The relationship between masseter force and masseter electromyogram during mastication in the monkey *Macaca fascicularis*. *Archives of Oral Biology*, 713-722.
- Hylander, W. L., & Johnson, K. R. (1993). Modelling relative masseter force from surface electromyograms during mastication in non-human primates. *Archives of Oral Biology*, 233-240.
- Hylander, W. L., & Johnson, K. R. (1994). Jaw muscle function and wishboning of the mandible during mastication in macaques and baboons. *American Journal of Physical Anthropology*, 523-547.
- Hylander, W. L., & Johnson, K. R. (1997). In vivo bone strain patterns in the zygomatic arch of macaques and the significance of these patterns for functional interpretations of craniofacial form. *American Journal of Physical Anthropology*, 203-232.

- Hylander, W. L., Johnson, K. R., & Crompton, A. W. (1992). Muscle force recruitment and biomechanical modeling: An analysis of masseter muscle function during mastication in *Macaca fascicularis*. *American Journal of Physical Anthropology*, 88, 365-387.
- Hylander, W. L., Vinyard, C. J., Ravosa, M. J., Ross, C. F., Wall, C. E., & Johnson, K. R. (2004). Jaw adductor force and symphyseal fusion. In F. Anapol, R. Z. German, & N. G. Jablonski, *Shaping Primate Evolution: Form, Function, and Behavior* (pp. 229-257). Cambridge University Press.
- Hylander, W. L., Vinyard, C. J., Wall, C. E., Williams, S. H., & Johnson, K. R. (2011). Functional and evolutionary significance of the recruitment and firing patterns of the jaw adductors during chewing in Verreax's sifaka (*Propithecus verreauxi*). *American Journal of Physical Anthropology*, 146, 531-547.
- Hylander, W., Johnson, K., & Crompton, A. (1987). Loading patterns and jaw movements during mastication in *Macaca fascicularis*: A bone-strain, electromyographic, and cineradiographic analysis. *American Journal of Physical Anthropology*, 72, 287-314.
- Hylander, W., Ravosa, M., Ross, C., & Johnson, K. (1998). Mandibular corpus strain in primates: Further evidence for a functional link between symphyseal fusion and jaw-adductor muscle force. *American Journal of Physical Anthropology*, 107, 257-271.
- Hylander, W., Ravosa, M., Ross, C., Wall, C., & Johnson, K. (2000). Symphyseal fusion and jaw-adductor muscle force: An EMG study. *American Journal of Physical Anthropology*, 112, 469-492.
- Hylander, W., Wall, C., Vinyard, C., Ross, C., Ravosa, M., Williams, S., et al. (2005). Temporalis function in anthropoids and strepsirrhines. *American Journal of Physical Anthropology*, 128, 35-56.
- Iinuma, M., Yoshida, S., & Funakoshi, M. (1991). Development of masticatory muscles and oral behavior from suckling to chewing dogs. *Comparative Biochemistry and Physiology Part A: Physiology*, 789-794.
- Jankelson, B., Hoffman, G. M., & Hendron, J. A. (1953). Physiology of the stomatognathic system. *Journal of the American Dental Association*, 375-386.
- Jolly, C. J. (1970). Hadropithecus, a lemuroid small object feeder. *Man*, 525-529.

- Kanazawa, E., & Rosenberger, A. L. (1989). Interspecific allometry of the mandible, dental arch, and molar area in anthropoid primates: Functional morphology of masticatory components. *Primates*, 543-560.
- Kay, R. F. (1975). The functional adaptations of primate molar teeth. *American Journal of Physical Anthropology*, 195-215.
- Kay, R. F., & Hiiemae, K. M. (1974). Jaw movement and tooth use in recent and fossil primates. *American Journal of Physical Anthropology*, 227-256.
- Kay, R. F., Ross, C., & Williams, B. A. (1997). Anthropoid origins. *Science*, 275, 797-804.
- Kendall, D. (1977). The diffusion of shape. *Advances in Applied Probability*, 9, 428-430.
- Kendall, D. G. (1981). The Statistics of Shape. In V. Barnett, *Interpreting Multivariate Data* (pp. 75-80). New York: Wiley.
- Kendall, D. G. (1984). Shape-manifolds, Procrustean metrics and complex projective spaces. *Bulletin of the London Mathematical Society*, 81-121.
- Kendall, D. G. (1985). Exact distributions for shapes of random triangles in convex sets. *Advances in Applied Probability*, 308-329.
- Kendall, D. G. (1989). A survey of the statistical theory of shape. *Statistical Science*, 87-120.
- Kent, J. T. (1994). The complex Bingham distribution and shape analysis. *Journal of the Royal Statistical Society B(56)*, 285-299.
- Kirk, C., & Simons, E. L. (2001). Diets of fossil primates from the Fayum Depression of Egypt: a quantitative analysis of molar shearing. *Journal of Human Evolution*, 203-229.
- Klingenberg, C. P. (1996). Multivariate allometry. In L. F. Marcus, M. Corti, A. Loy, G. Naylor, & D. E. Slice, *Advances in Morphometrics* (pp. 23-49). New York: Plenum Press.
- Klingenberg, C. P. (2009). Morphometric integration and modularity in configurations of landmarks: tools for evaluating a priori hypotheses. *Evolution and Development*, 11(4), 405-421.
- Klingenberg, C. P. (2016). Size, shape, and form: concepts of allometry in geometric morphometrics. *Development Genes and Evolution*, 113-137.

- Klingenberg, C. P. (2016). Size, shape, and form: concepts of allometry in geometric morphometrics. *Development Genes and Evolution*, 113-137.
- Langenbach, G. E., & Weijs, W. A. (1990). Growth patterns of the rabbit masticatory muscles. *Journal of Dental Research*, 20-25.
- Lieberman, D. E. (2011). *The evolution of the human head*. Cambridge: Belknap Press of Harvard University Press.
- Lieberman, D. E., & Crompton, A. W. (2000). Why fuse the mandibular symphysis? A comparative analysis. *American Journal of Physical Anthropology*, 517-540.
- Lieberman, D. E., Hallgrímsson, B., Liu, W., Parsons, T. E., & Jamniczky, H. A. (2008). Spatial packing, cranial base angulation, and craniofacial shape variation in the mammalian skull: testing a new model using mice. *Journal of Anatomy*, 720-735.
- Lieberman, D. E., Ross, C. F., & Ravosa, M. J. (2000). The primate cranial base: ontogeny, function, and integration. *American Journal of Physical Anthropology*, 117-169.
- Lockwood, C. (2007). Adaptation and functional integration in primate phylogenetics. *Journal of Human Evolution*, 52, 490-503.
- Lonnberg, E. (1902). On some remarkable digestive adaptations in diprotodont marsupials. *Proceedings of the Zoological Society of London*, 12-31.
- Marcus, L. F., Hingst-Zaher, E., & Zaher, H. (2000). Applications of landmark morphometrics to skulls representing the orders of living mammals. *Hystrix, Italian Journal of Mammology*, 11, 27-47.
- Martin, R. D. (1990). *Primate Origins and Evolution*. Princeton: Princeton University Press.
- McCarthy, R. C. (2001). Anthropoid cranial base architecture and scaling relationships. *Journal of Human Evolution*, 41-66.
- McCarthy, R. C., & Lieberman, D. E. (2001). Posterior maxillary (PM) plane and anterior cranial architecture in primates. *The Anatomical Record*, 247-260.
- McNamara, J. A. (1974). An electromyographic study of mastication in the rhesus monkey (*Macaca mulatta*). *Archives of Oral Biology*, 821-823.
- McNulty, K. P., & Vinyard, C. J. (2015). Morphometry, Geometry, Function, and the Future. *The Anatomical Record*, 298, 328-333.

- Mitteroecker, P., & Bookstein, F. (2011). Linear discrimination, ordination, and the visualization of selection gradients in modern morphometrics. *Evolutionary Biology*, 38, 100-114.
- Mitteroecker, P., & Gunz, P. (2009). Advances in geometric morphometrics. *Evolutionary Biology*, 36, 235-247.
- Mitteroecker, P., & Huttegger, S. M. (2009). The concept of morphospaces in evolutionary and developmental biology: mathematics and metaphors. *Biological Theory*, 4(1), 54-67.
- Mitteroecker, P., Gunz, P., & Bookstein, F. L. (2005). Heterochrony and geometric morphometrics: a comparison of cranial growth in *Pan paniscus* versus *Pan troglodytes*. *Evolution and Development*, 7(3), 244-258.
- Mitteroecker, P., Gunz, P., Bernhard, M., Schaefer, K., & Bookstein, F. L. (2004a). Comparison of cranial ontogenetic trajectories among great apes and humans. *Journal of Human Evolution*, 46, 679-698.
- Moller, E. (1966). The chewing apparatus: An electromyographic study of the action of the muscles of mastication and its correlation to facial morphology. *Acta Physiologica Scandinavica*, 1-299.
- Monteiro, L. R. (1999). Multivariate regression models and geometric morphometrics: the search for causal factors in the analysis of shape. *Systematic Biology*, 192-199.
- Muchlinski, M. N., Godfrey, L. R., Muldoon, K. M., & Tongaso, L. (2011). Evidence for dietary niche separation based on infraorbital foramen size variation among subfossil lemurs. *Folia Primatologica*, 330-345.
- Perelman, P., Johnson, W. E., Roos, C., Seuanez, H. N., Horvath, J. E., Moreira, M., et al. (2011). A molecular phylogeny of living primates. *Plos Genetics*, 1-17.
- Plavcan, M. J., & Daegling, D. J. (2006). Interspecific and intraspecific relationships between tooth size and jaw size in primates. *Journal of Human Evolution*, 171-184.
- Radinsky, L. (1977). Early primate brains: Facts and fiction. *Journal of Human Evolution*, 6(1), 79-86.
- Rafferty, K. L., Teaford, M. F., & Jungers, W. L. (2002). Molar microwear of subfossil lemurs: improving the resolution of dietary inferences. *Journal of Human Evolution*, 645-657.

- Rasmussen, D. T., & Simons, E. L. (1992). Paleobiology of the oligopithecines, the earliest known anthropoid primates. *International Journal of Primatology*, 477-508.
- Ravosa, M. (1991). Structural allometry of the prosimian corpus and symphysis. *Journal of Human Evolution*, 20, 3-20.
- Ravosa, M. (1996b). Mandibular form and function in North American and European Adapidae and Omomyidae. *Journal of Morphology*, 229, 171-190.
- Ravosa, M. J. (1990). Functional assessment of subfamily variation in maxillomandibular morphology among Old World monkeys. *American Journal of Physical Anthropology*, 199-212.
- Ravosa, M. J. (1998). Cranial allometry and geographic variation in slow lorises (*Nycticebus*). *American Journal of Primatology*, 225-243.
- Ravosa, M. J. (1999). Anthropoid origins and the modern symphysis. *Folia Primatologica*, 70, 65-78.
- Ravosa, M. J., & Daniel, A. N. (2010). Ontogeny and phyletic size change in living and fossil lemurs. *American Journal of Primatology*, 161-172.
- Ravosa, M. J., & Hogue, A. S. (2004). Symphyseal fusion and anthropoid origins. In C. F. Ross, & R. F. Kay, *Anthropoid Origins: New Visions* (pp. 413-462). New York: Kluwer Academic/Plenum Publishers.
- Ravosa, M. J., & Hylander, W. L. (1993). Functional significance of an ossified mandibular symphysis: A reply. *American Journal of Physical Anthropology*, 509-512.
- Ravosa, M. J., & Hylander, W. L. (1994). Function and fusion of the mandibular symphysis in primates: Stiffness or strength? In J. G. Fleagle, & R. F. Kay, *Anthropoid Origins* (pp. 447-468). New York: Plenum Press.
- Ravosa, M. J., & Vinyard, C. J. (2002). On the interface between ontogeny and function. In M. Plavcan, *Reconstructing behavior in the primate fossil record* (pp. 73-111). New York: Kluwer Academic/Plenum Publishers.
- Ravosa, M. J., Stock, S. R., Simons, E. L., & Kunwar, R. (2007). MicroCT analysis of symphyseal ontogeny in *Archaeolemur*. *International Journal of Primatology*, 28, 1385-1396.

- Ravosa, M., & Simons, E. (1994). Mandibular growth and function in *Archaeolemur*. *American Journal of Physical Anthropology*, 95, 63-76.
- Ravosa, M., Vinyard, C., Gagnon, M., & Islam, S. (2000). Evolution of anthropoid jaw loading kinematic patterns. *American Journal of Physical Anthropology*(112), 493-516.
- Richard, A. F. (1985). *Primates in Nature*. New York: W. H. Freeman.
- Rohlf, F. J. (1996). Morphometric spaces, shape components and the effects of linear transformations. In L. F. Marcus, M. Corti, A. Loy, G. J. Naylor, & D. E. Slice, *Advances in Morphometrics* (pp. 117-132). New York: Springer Science+Business Media.
- Rohlf, F. J. (1998). On applications of geometric morphometrics to studies of ontogeny and phylogeny. *Systematic Biology*, 147-158.
- Rohlf, F. J. (1999). Shape statistics: Procrustes superimpositions and tangent spaces. *Journal of Classification*, 16, 197-223.
- Rohlf, F. J. (1999). Shape statistics: Procrustes superimpositions and tangent spaces. *Journal of Classification*, 197-223.
- Rohlf, F. J. (2002). Geometric morphometrics and phylogeny. In N. MacLeod, & P. L. Forey, *Morphology, shape, and phylogeny* (pp. 175-193). London: Taylor and Francis.
- Rohlf, F. J., & Marcus, L. F. (1993). A revolution in morphometrics. *Trends in Ecology and Evolution*, 129-132.
- Rohlf, F. J., & Slice, D. (1990). Extensions of the Procrustes method for the optimal superimposition of landmarks. *Systematic Zoology*, 39(1), 40-59.
- Rohlf, J. F., & Corti, M. (2000). Use of two-block partial least-squares to study covariation in shape. *Systematic Biology*, 49(4), 740-753.
- Rosenberger, A. L. (1986). Platyrrhines, catarrhines and the anthropoid transition. In B. A. Wood, L. Martins, & P. Andrews, *Major topics in primate and human evolution* (pp. 66-88). Cambridge: Cambridge University Press.
- Ross, C. F., & Hylander, W. L. (2000). Electromyography of the anterior temporalis and masseter muscles of owl monkeys (*Aotus trivirgatus*) and the function of the postorbital septum. *American Journal of Physical Anthropology*, 455-468.

- Ross, C. F., & Iriarte-Diaz, J. (2014). What does feeding system morphology tell us about feeding? *Evolutionary Anthropology*, 105-120.
- Ross, C. F., Iriarte-Diaz, J., & Nunn, C. L. (2012). Innovative approaches to the relationship between diet and mandibular morphology in primates. *International Journal of Primatology*, 632-660.
- Ross, C. F., Reed, D. A., Washington, R. L., Eckhardt, A., Anapol, F., & Shahnoor, N. (2008). Scaling of chew cycle duration in primates. *American Journal of Physical Anthropology*, 30-44.
- Ross, C., & Henneberg, M. (1995). Basicranial flexion, relative brain size, and facial kyphosis in *Homo sapiens* and some fossil hominids. *American Journal of Physical Anthropology*, 575-593.
- Ross, C., & Ravosa, M. (1993). Basicranial flexion, relative brain size, and facial kyphosis in nonhuman primates. *American Journal of Physical Anthropology*, 91, 305-324.
- Scapino, R. (1981). Morphological investigation into functions of the jaw symphysis in carnivorans. *Journal of Morphology*, 339-375.
- Scapino, R. P. (1965). The third joint of the canine jaw. *Journal of Morphology*, 23-50.
- Scott, J. E., Hogue, A. S., & Ravosa, M. J. (2012b). The adaptive significance of mandibular symphyseal fusion in mammals. *Journal of Evolutionary Biology*, 661-673.
- Scott, J. R., Godfrey, L. R., Jungers, W. L., Scott, R. S., Simons, E. L., Teaford, M. F., et al. (2009). Dental microwear texture analysis of two families of subfossil lemurs from Madagascar. *Journal of Human Evolution*, 405-416.
- Scott, J., Lack, J., & Ravosa, M. (2012a). On the reversibility of mandibular symphyseal fusion. *Evolution*, 66(9), 2940-2952.
- Sears, K. E., Finarelli, J. J., Flynn, J. J., & Wyss, A. (2008). Morphometric estimators of body mass in New World monkeys (Platyrrhini, Anthropoidea, Primates) with consideration of the Miocene-aged *Chilecebus carrascoensis*. *American Museum Novitates*, 3617, 1-29.
- Seiffert, E. R., & Simons, E. L. (2001). Astragalar morphology of late Eocene anthropoids from the Fayum Depression (Egypt) and the origin of catarrhine primates. *Journal of Human Evolution*, 41, 577-606.

- Seiffert, E. R., Simons, E. L., & Fleagle, J. G. (2000). Anthropoid humeri from the late Eocene of Egypt. *Proceedings of the National Academy of Sciences*, 97, 10062-10067.
- Seiffert, E. R., Simons, E. L., & Simons, C. V. (2004). Phylogenetic, biogeographic, and adaptive implications of new fossil evidence bearing on crown anthropoid origins and early stem catarrhine evolution. In C. F. Ross, & R. F. Kay, *Anthropoid Origins: New Visions* (pp. 157-181). New York: Kluwer Academic/Plenum Publishers.
- Sheppard, I. M. (1964). Incisive and related movements of the mandible. *Journal of Prosthetic Dentistry*, 898-906.
- Simons, E. L. (1992). Diversity in the early Tertiary anthropoid radiation in Africa. *Proceedings of the National Academy of Sciences*, 10743-19747.
- Simons, E. L., & Rasmussen, D. T. (1996). Skull of *Catopithecus browni*, and early Tertiary catarrhine. *American Journal of Physical Anthropology*, 100, 261-292.
- Simons, E. L., Seiffert, E. R., Chatrath, P. S., & Attia, Y. (2001). Earliest record of a parapathecoid anthropoid from the Jebel Qatrani formation, northern Egypt. *Folia Primatologica*, 72, 316-331.
- Simons, E., & Frost, S. (2016). Constructing cranial ontogenetic trajectories: A comparison of growth, development, and chronological age proxies using a known-age sample of *Macaca mulatta*. *American Journal of Physical Anthropology*, 296-308.
- Simons, E., Seiffert, E., Ryan, T., & Attia, Y. (2007). A remarkable female cranium of the early Oligocene anthropoid *Aegyptopithecus zeuxis* (Catarrhini, Propliopithecidae). *Proceedings of the National Academy of Sciences*, 104(21), 8731-8736.
- Slice, D. (2001). Landmark coordinates aligned by Procrustes analysis do not lie in Kendall's shape space. *Systematic Biology*, 50, 141-149.
- Slice, D. E. (1996). Three-dimensional, generalized resistant fitting and the comparison of least-squares and resistant-fit residuals. In L. F. Marcus, M. Corti, A. Loy, G. J. Naylor, & D. E. Slice, *Advances in Morphometrics* (pp. 179-199). New York: Plenum Press.
- Slice, D. E., Bookstein, F. L., Marcus, L. F., & Rohlf, F. J. (1996). A glossary for geometric morphometrics. In L. F. Marcus, M. Corti, A. Loy, G. J. Naylor, & D.

- E. Slice, *Advances in Morphometrics* (pp. 531-552). New York: Springer Science .
- Smith, B. H. (1991). Age of weaning approximates age of emergence of the first permanent molar in nonhuman primates. *American Journal of Physical Anthropology*, 163-164.
- Smith, R. J. (1978). Mandibular biomechanics and temporomandibular joint function in primates. *American Journal of Physical Anthropology*, 341-349.
- Smith, R. J. (1983). The mandibular corpus of female primates: taxonomic, dietary, and allometric correlates of interspecific variations in size and shape. *American Journal of Physical Anthropology*, 315-330.
- Smith, R. J. (1993). Categories of allometry: body size versus biomechanics. *Journal of Human Evolution*, 173-182.
- Smith, R. J., Peterson, C. E., & Gipe, D. P. (1983). Size and shape of the mandibular condyle in primates. *Journal of Morphology*, 59-68.
- Spencer, M. A. (1998). Force production in the primate masticatory system: Electromyography tests of biomechanical hypotheses. *Journal of Human Evolution*, 25-54.
- Spencer, M. A., & Demes, B. (1993). Biomechanical analysis of masticatory function: configuration in Neandertals and Inuits. *American Journal of Physical Anthropology*, 1-20.
- Spencer, M. A., & Hogard, R. (2001). Biomechanics of sexual dimorphism in the anthropoid masticatory system. *American Journal of Physical Anthropology*, 141.
- Spoor, C. F. (1997). Basicranial architecture and relative brain size of Sts 5 (*Australopithecus africanus*) and other Plio-Pleistocene hominids. *South African Journal of Science*, 182-186.
- Strait, D. S. (1999). The scaling of basicranial flexion and length. *Journal of Human Evolution*, 701-719.
- Strait, D. S. (2001). Integration, phylogeny, and the hominid cranial base. *American Journal of Physical Anthropology*, 273-297.
- Szalay, F. S., & Delson, E. (1979). *Evolutionary History of the Primates*. New York: Academic Press.

- Takahashi, L. K., & Pan, R. (1994). Mandibular morphometrics among macaques: the case of *Macaca thibetana*. *International Journal of Primatology*, 597-621.
- Taylor, A. B. (2002a). Masticatory form and function in the African apes. *American Journal of Physical Anthropology*, 133-156.
- Taylor, A. B. (2003). Ontogeny and function of the masticatory complex in Gorilla: Functional, evolutionary, and taxonomic implications. In A. B. Taylor, & M. L. Goldsmith, *Gorilla Biology: A Multidisciplinary Perspective* (pp. 132-193).
- Taylor, A. B. (2005). A comparative analysis of temporomandibular joint morphology in the African apes. *Journal of Human Evolution*, 555-574.
- Taylor, A. B. (2006a). Feeding behavior, diet, and the functional consequences of jaw form in orangutans, with implications for the evolution of Pongo. *Journal of Human Evolution*, 377-393.
- Taylor, A. B. (2006b). Diet and mandibular morphology in African apes. *International Journal of Primatology*, 181-201.
- Taylor, A. B., & Groves, C. P. (2003). Patterns of mandibular variation in Pan and Gorilla and implications for African ape taxonomy. *Journal of Human Evolution*, 529-561.
- Terhune, C. E. (2013). Dietary correlates of temporomandibular joint morphology in the great apes. *American Journal of Physical Anthropology*, 260-272.
- Terhune, C. E., Cooke, S. B., & Otarola-Castillo, E. (2015). Form and function in the platyrrhine skull: A three-dimensional analysis of dental and TMJ morphology. *The Anatomical Record*, 29-47.
- Tullberg, T. (1899). Ueber das System der Nagethiere: eine Phylogenetische Studie. *Nova Acta Soc Sci*.
- Vinyard, C. J. (2008). Putting shape to work: Making functional interpretations of masticatory apparatus shape in primates. In C. J. Vinyard, M. J. Ravosa, & C. Wall, *Primate craniofacial function and biology* (pp. 357-385). Springer.
- Vinyard, C. J., & Ravosa, M. J. (1998). Ontogeny, function, and scaling of the mandibular symphysis in papionin primates. *Journal of Morphology*, 235, 157-175.
- Vinyard, C. J., Ravosa, M. J., & Wall, C. (2008a). *Primate Craniofacial Function and Biology*. New York: Springer Science+Business Media, LLC.

- Vinyard, C. J., Ravosa, M. J., Williams, S. H., Wall, C. E., Johnson, K. R., & Hylander, W. L. (2007). Jaw-muscle function and the origin of primates. In M. J. Ravosa, & M. Dagosto, *Primate origins and adaptations: a multidisciplinary perspective* (pp. 179-220). New York: Kluwer Press.
- Vinyard, C. J., Wall, C. E., Williams, S. H., & Hylander, W. L. (2008b). Patterns of variation across primates in jaw-muscle electromyography during mastication. *Integrative and Comparative Biology*, 48(2), 294-311.
- Vinyard, C. J., Wall, C. E., Williams, S. H., Johnson, K. R., & Hylander, W. L. (2006). Masseter electromyography during chewing in ring-tailed lemurs (*Lemur catta*). *American Journal of Physical Anthropology*, 180, 85-96.
- Vinyard, C. J., Williams, S. H., Wall, C. E., Doherty, A. H., Crompton, A. W., & Hylander, W. L. (2011). A preliminary analysis of correlations between chewing motor patterns and mandibular morphology across mammals. *Integrative and Comparative Biology*, 51(2), 260-270.
- Vogel, C. (1964). Über eine Schadelbasisanomalie bei einem in freier Wildbahn geschossen *Cercopithecus torquatus atys*. *Zeitschrift für Morphologie und Anthropologie*, 262-276.
- Wagner, G. P., & Schwenk, K. (2000). Evolutionarily stable configurations: Functional integration and the evolution of phenotypic stability. *Evolutionary Biology*, 155-217.
- Walker, P., & Murray, P. (1975). An assessment of masticatory efficiency in a series of anthropoid primates with special reference to the Colobinae and Cercopithecinae. In R. H. Tuttle, *Primate Functional Morphology and Evolution* (pp. 135-150). Paris: Mouton Publishers.
- Ward, S. C., & Molnar, S. (1980). Experimental stress analysis of topographic diversity in early hominid gnathic morphology. *American Journal of Physical Anthropology*, 383-395.
- Weber, M. (1928). *Einführung in die Anatomie und Systematik der recenten un fossilen Mammalia. Bd. 2, Systematischer Teil*. Gustav Fisher.
- Weijs, W. A. (1994). Evolutionary approach of masticatory motor patterns in mammals. In V. I. Bels, M. Chardon, & P. Vandewalle, *Biomechanics of feeding in vertebrates* (pp. 282-320). Berlin: Springer-Verlag.

- Weijs, W. A., & Dantuma, R. (1981). Functional anatomy of the masticatory apparatus in the rabbit (*Oryctolagus cuniculus* L.). *Netherlands Journal of Zoology*, 99-147.
- Weijs, W. A., Brugman, P., & Grimbergen, C. A. (1989). Jaw movements and muscle activity during mastication in growing rabbits. *Anatomical Record*, 407-416.
- Williams, S. H., Vinyard, C. J., Wall, C. E., & Hylander, W. L. (2007). Masticatory motor patterns in ungulates: a quantitative assessment of the Triplet model. *Journal of Experimental Zoology A: Comparative Experimental Biology*, 226-240.
- Williams, S. H., Vinyard, C. J., Wall, C. E., & Hylander, W. L. (2009). An in vivo analysis of mandibular corpus bone strain in goats and alpacas: implications for understanding the biomechanics of mandibular form in selenodont artiodactyls. *Journal of Anatomy*, 65-78.
- Williams, S. H., Wall, C. E., Vinyard, C. J., & Hylander, W. L. (2008). Symphyseal fusion in selenodont artiodactyls: new insight from in vivo and comparative data. In C. J. Vinyard, M. J. Ravosa, & C. E. Wall, *Primate Craniofacial Function and Biology* (pp. 39-61). New York: Springer.
- Wood, B. A. (1978). Allometry and hominid studies. *Geological Society, London, Special Publications*, 125-138.
- Wood, B. A., & Collard, M. (1999a). The human genus. *Science*, 65-71.
- Wood, B. A., & Collard, M. (1999b). The changing face of genus *Homo*. *Evolutionary Anthropology*, 195-207.
- Wrangham, R. @., Jones, J. H., Laden, G., Pilbeam, D., & Conklin-Brittan, N. L. (1999). The raw and the stolen: Cooking and the ecology of human origins. *Current Anthropology*, 567-594.
- Wrangham, R. W. (2009). *Catching fire: How cooking made us human*. New York: Basic Books.